

MECHANISTIC INVESTIGATIONS OF TRANSITION METAL CATALYZED REACTIONS

JONATAN KLEIMARK



Department of Chemistry
University of Gothenburg
2012

DOCTORAL THESIS

Submitted for partial fulfillment of the requirements for the degree of
Doctor of Philosophy in Chemistry

Mechanistic Investigations of Transition Metal Catalyzed Reactions

JONATAN KLEIMARK

© Jonatan Kleimark

ISBN: 978-91-628-8394-2

Available online at: <http://dhl.handle.net/2077/27967>

Department of Chemistry

University of Gothenburg

SE-412 96 Göteborg

Sweden

Printed by Ineko AB

Göteborg 2011

Nature never deceives us; it is always we who deceive ourselves

Jean-Jaques Rousseau

Abstract

Transition metal catalyzed reactions have had a large impact on the human progress for the last century. Several extremely important areas, such as the agricultural industry and the plastic industry, have benefited from this development. The evolution of different transition metal catalysts has also been very important for the pharmaceutical industry. One vital factor when developing new and more effective catalysts is to obtain mechanistic insights. In this thesis, several different methods to investigate mechanisms for transition metal catalyzed reactions are presented.

The factors controlling regioselectivity for a palladium catalyzed allylic alkylation has been studied. Pre-formed (η^3 -allyl)Pd complexes were used to minimize dynamic processes. In the study it was found that the regioselectivity depends mainly on steric interactions, rather than electronic effects. For complexes with less steric hindrance, the *trans* effect controls the selectivity. Furthermore, the mechanism for a sulfinyl nucleophile, employed in the same type of reaction, has been studied and the mode of attack has been revealed. The importance of a fast palladium catalyzed Mislow-Braverman-Evans rearrangement to ensure that the correct product was formed, was also disclosed.

The important Mizoroki-Heck reaction has been investigated in two different studies. The first study revealed the mechanistic pathway for a Pd(II) catalyzed domino Mizoroki-Heck-Suzuki diarylation reaction. The dependence of benzoquinone as the re-oxidant, in order to achieve the diarylation product, was explained by its ability to coordinate to the palladium moiety, thereby allowing access to a new low-energy pathway to the product. In the second study, a new and mild nickel catalyzed variant of the Mizoroki-Heck reaction was presented and the mechanistic pathway for the reaction was introduced. In addition to this, the reasons for several unsuccessful conditions and additives were uncovered.

The development of new, environmentally more benign, catalysts for cross coupling reactions is important. Iron is one of the most promising metals for this purpose, but the mechanistic knowledge of this reaction is still not comprehensive. In this thesis, several mechanistic and computational studies reveal new insights into this reaction, paving the way to develop new and more effective catalysts and conditions for the reaction.

Keywords: alkene insertion, allylic alkylation, catalysis, cross coupling, density functional theory, free energy surface, iron, kinetic investigation, Mizoroki-Heck reaction, nickel, palladium, reaction mechanism, sulfinylation, transition metal.

ISBN: 978-91-628-8394-2

List of publications

This thesis is based on the following papers, which are referred to in the text by their Roman numerals. Reprints were made with permission from the publishers.

- Paper I: *Sterically Governed Selectivity in Palladium-Assisted Allylic Alkylation*
J. Kleimark, C. Johansson, S. Olsson, M. Håkansson, S. Hansson, B. Åkermark, P.-O. Norrby, *Organometallics*, **2011**, *30*, 230-238.
- Paper II: *Palladium-Catalyzed Allylic Sulfinylation and the Mislow-Braverman-Evans Rearrangement*
J. Kleimark, G. Prestat, G. Poli, P.-O. Norrby, *Chem. –Eur. J.* **2011**, *17*, 13963-13965
- Paper III: *Transmetalation versus β -Hydride Elimination: The Role of 1,4-Benzoquinone in Chelation-Controlled Arylations using Arylboronic Acids*
C. Sköld, J. Kleimark, A. Trejos, L. R. Odell, S. O. Nilsson Lill, P.-O. Norrby, M. Larhed
Accepted for publication in *Chemistry – a European Journal*
- Paper IV: *Mild and Efficient Nickel-Catalyzed Heck Reactions with Electron Rich Olefins*
T. Gøgsig, J. Kleimark, S. O. Nilsson Lill, S. Korsager, A. Lindhart, P.-O. Norrby, T. Skrydstrup
Submitted to *Journal of the American Chemical Society*
- Paper V: *Mechanistic Investigation of Iron-Catalyzed Coupling Reactions*
J. Kleimark, A. Hedström, P.-F. Larsson, C. Johansson, P.-O. Norrby, *ChemCatChem*, **2009**, *1*, 152-161
- Paper VI: *Low Temperature Studies of Iron Catalyzed Cross Coupling of Alkyl Grignards with Aryl Electrophiles*
J. Kleimark, P.-F. Larsson, P. Emamy, A. Hedström, P.-O. Norrby
Accepted for publication in *Advanced Synthesis and Catalysis*

Publication not included in this thesis:

Computational Insights into Palladium-Mediated Allylic Substitution
Jonatan Kleimark and Per-Ola Norrby in *Transition Metal Catalyzed Enantioselective Allylic Substitution in Organic Synthesis*, Ed: U. Kazmaier; *Top. Organomet. Chem.* **2011**, *38*, 65-94
DOI: 10.1007/3418_2011_8

Contribution to the papers

- I. Performed all the computational work. Contributed to the interpretation of the results. Wrote a large part of the manuscript.
- II. Outlined the study. Planned and performed all the computational work. Contributed to the interpretation of the results. Wrote the major part of the manuscript.
- III. The computational study was performed in collaboration with Dr. Christian Sköld at Uppsala University. Performed part of the computational work for each of the steps in the catalytic cycle. Contributed to the interpretation of the results and the writing of the paper.
- IV. Planned and performed all the computational work and analyzed the results. Wrote the part of the manuscript concerning the computational work.
- V. Contributed to the outline of the study. Performed a large part of the experimental work and all of the computational work. Contributed to the interpretation of the results. Wrote a large part of the manuscript.
- VI. Outlined the study. Planned and performed the kinetic study and the computational work. Contributed to the interpretation of the results. Wrote a large part of the manuscript.

Abbreviations

1D	1-dimensional
2D	2-dimensional
Ac	acetate
acac	acetylacetone
BINAP	2,2'-bis(diphenylphosphino)-1,1'-binaphthyl
BQ	benzoquinone
COD	1,5-cyclooctadiene
DCM	dichloromethane
DBU	1,8-diazabicyclo[5.4.0]undec-7-ene
DFT	density functional theory
DIPEA	diisopropyl ethyl amine
DMF	dimethyl formamide
dpe	diphosphinoethane
dppe	1,2-bis(diphenylphosphino)ethane
dppf	1,1'-bis(diphenylphosphino)ferrocene
dppp	1,3-bis(diphenylphosphino)propane
ECP	effective core potential
FES	free energy surface
GC	gas chromatography
GC-MS	gas chromatography - mass spectrometry
GGA	generalized gradient approximation
HF	Hartree-Fock
Hz	Hertz
L	ligand
LCAO	linear combination of atomic orbitals
LDA	local-density approximation
LG	leaving group
MBE	Mislow-Braverman-Evans
MBPT	many-body perturbation theory
MP	Møller-Plesset
NBO	natural bond orbital
NLDA	nonlocal-density approximation
NMP	N-methyl pyrrolidine
NMR	nuclear magnetic resonance
NPA	natural population analysis
Nu	nucleophile
OA	oxidative addition
Tf	trifluoromethanesulfonate (triflate)
PBF	Poisson-Boltzmann finite element
PCM	polarizable continuum model
PHOX	diphenylphosphinophenylloxazoline
Sol	solvent
RE	reductive elimination
TBAB	tetrabutylammonium bromide
TESOTf	triethylsilyl trifluoromethanesulfonate
THF	tetrahydrofuran
TM	transmetalation
TMEDA	tetramethyl ethylenediamine
TS	transition state

Table of contents

Abstract.....	i
List of publications.....	iii
Contribution to the papers.....	iv
Abbreviations	v
1. Introduction.....	1
1.1 Transition metal catalysis	1
1.2 Palladium assisted allylic alkylation.....	1
1.3 Alkene insertion reactions.....	2
1.4 Cross coupling reactions.....	4
1.5 Kinetic experiments.....	5
1.6 Theoretical methods.....	6
1.7 Aims of the thesis.....	11
2. Palladium assisted allylic substitution (Papers I-II)	12
2.1 Background	12
2.2 A tethered ligand – a way to investigate regioselectivity (Paper I).....	18
2.3 Allylic sulfinylation – mechanism and the MBE rearrangement (Paper II).....	28
3. Alkene insertion reactions (Papers III-IV).....	35
3.1 The Mizoroki-Heck reaction.....	35
3.2 Chelation controlled atypical diarylation reaction (Paper III).....	38
3.3 Nickel catalyzed Mizoroki-Heck reaction (Paper IV)	50
4. Iron catalyzed cross coupling reactions (Papers V-VI)	59
4.1 Background	59
4.2 Possibilities for iron catalyzed cross coupling.....	61
4.3 Mechanistic investigation of iron catalyzed cross coupling (Papers V and VI)	64
5. Summary and concluding remarks.....	86
6. Outlook.....	88
7. Acknowledgements	90
7. References.....	92

1. Introduction

1.1 Transition metal catalysis

Catalysis is the phenomenon where an additive can increase the rate of a reaction without being consumed. This is accomplished through a lowering of the activation barrier of the reaction. All life on earth is dependent on the catalytic ability of our enzymes, which carry out most of the chemical transformations in our bodies. Humans have tried to harness the tremendous potential of catalysts for many years.

There are two different kinds of catalysis, *heterogenous* and *homogenous*. In the former the catalyst acts in a different phase than the reactants, the most well known examples are the catalytic converters in cars, which are solid-state catalyst that convert NO_x-gases, carbon monoxide and hydrocarbons to N₂, water and carbon dioxide, or the Haber-Bosch process, responsible for the production of fertilizers for the agricultural industry. *Homogenous catalysis*, where the catalyst acts in the same phase as the reactants, is the process which this thesis will focus on, and this is where most of the transition metal catalysis occurs. The versatility of the transition metals as catalysts has ensured that they have been employed for a long time in chemistry. Applications such as the Ziegler-Natta^[1] or the Wacker^[2] processes have been used for several decades in large scale.

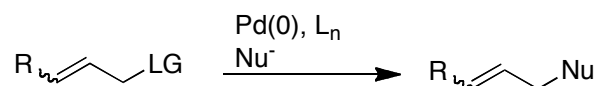
Today, reactions catalyzed by transition metals constitute a large part of the tools used in organic synthesis. The rich chemistry provided by the accessible d-orbitals make complexes of transition metals favorite aides in the never-ending quest for ways to build new molecules. As a testament to the importance of the field, several Nobel prizes have been awarded to transition metal catalyzed reactions in the last decade.^[3]

The research presented in this thesis has been focused on three different classes of catalyzed reactions, which each constitutes an important part of modern organic chemistry. The mechanistic investigations performed and introduced here give further insight into the complex nature of catalytic reactions, and can be of importance in the ongoing work to improve the existing reactions as well as to facilitate the development of new and more efficient reactions.

1.2 Palladium assisted allylic alkylation

The palladium assisted allylic alkylation has a long history within organic chemistry.^[4] The most common version of this reaction is the Tsuji-Trost reaction (Scheme 1), where the nucleophilic carbon in a stabilized carbanion, for example in a malonate, attacks a palladium allyl moiety.

Tsuji and co-workers, who reacted pre-formed palladium allyls with malonates, reported the reaction in the mid 1960s.^[5] Further development of the reaction by Trost and co-workers in the following years, using allylic acetates and palladium complexes with phosphine ligands, resulted in both catalytic activity and asymmetric versions of the reaction.^[6]



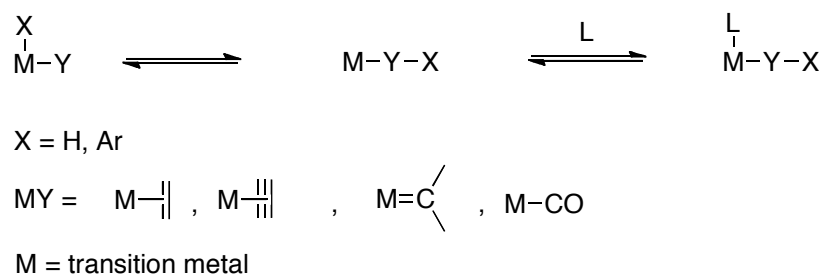
Scheme 1. The classic Tsuji-Trost reaction

The continued efforts over the last 50 years have resulted in a reaction that can be performed under mild conditions, with many different leaving groups, such as acetates, benzoates, epoxides, carbonates, carbamates and halides.^[7] A multitude of nucleophiles have also been shown to be feasible for the reaction, for example alkali metal enolates^[8] or heteroatom nucleophiles such as amines or anions of imides, but the most common are the above-mentioned stabilized carbon nucleophiles, the malonates.^[7]

Knowledge about the mechanism of the palladium catalyzed allylic alkylation reaction has been a crucial factor in the development of improvements for this reaction. Even if much information is known, there is still a need for mechanistic investigations. New data are imperative for further knowledge of important factors governing regio- and enantioselectivity, as well as development of new and more efficient conditions. In this thesis, some ways to get insights into the mechanism of the allylic alkylation reaction are presented.

1.3 Alkene insertion reactions

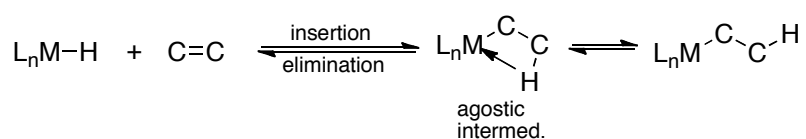
The insertion of an unsaturated ligand, such as an alkene, into an adjacent metal-ligand bond, is a very common reaction for many organometallic complexes. A schematic representation of this reaction class, known as migratory insertion, is depicted in Scheme 2. As the insertion generates a vacant coordination site, a ligand, L, is used in this example to bind to this site. Some of the most famous of the insertions are *carbonylation*, *hydroformylation*, *hydrogenation*, or *alkene insertion* reactions. The reverse reaction is also a feature of many of the same organometallic complexes, and is referred to as *decarbonylation*, if $Y = \text{CO}$, or a β -*elimination* if $X = \text{H}$ or alkyl.



Scheme 2. Migratory insertion and different ligands able to participate in this reaction

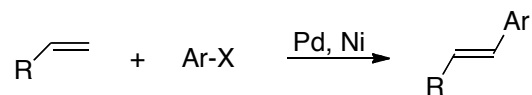
This thesis will deal with one of the mentioned insertion reactions, namely the insertion of an alkene into a M-C bond. Some important applications of this reaction type are the dimerization, oligomerization and polymerization of alkenes, which are extremely important industrial reactions. The polymerization reaction generates millions of tons of polypropylene and polyethylene annually through the Ziegler-Natta process.^[1] Furthermore, the Shell higher olefins process, utilizing a Ni-catalyst, produces large amounts of 1-alkenes of various lengths.^[9]

The insertion of an alkene into a metal-alkyl bond has a higher thermodynamic driving force than the insertion into a metal-hydride bond, but the former reaction has a larger kinetic barrier, primarily for steric reasons.^[10] The hydride version of the reaction takes place via an agostic intermediate as shown in Scheme 3. The reverse reaction, the β -hydride elimination, is important for the product-forming step in the alkene reactions discussed in this thesis. For some metals, for example the *f*-block metals, the M-H and M-alkyl bonds are comparable in strength, and for these, both β -hydride and β -alkyl elimination can be seen.^[11]



Scheme 3. Insertion/ β -hydride elimination equilibrium with agostic intermediate

A common alkene insertion reaction in synthetic organic chemistry is the *Mizoroki-Heck reaction*, which is a versatile and flexible reaction, usually catalyzed by palladium, but some nickel versions also exist (Scheme 4).^[12] Even though it was discovered in the 1970's, new variants and ways to control selectivities are still discovered. In this thesis, two different Mizoroki-Heck reactions are studied, the first a chelation-controlled version employed in a tandem reaction, the second a nickel catalyzed version.

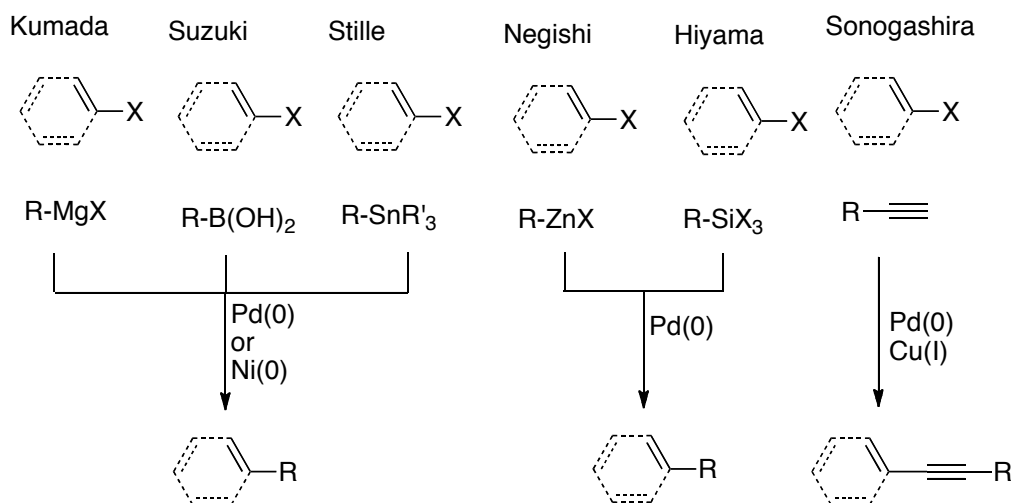


Scheme 4. The Mizoroki-Heck reaction

1.4 Cross coupling reactions

The cross coupling reaction emerged in the field of organic chemistry in the beginning of the 1970s and has since evolved to one of the most important reactions, as indicated by the awarding of the Nobel prize in 2010 to three of the most influential people in this field.^[3c]

The endeavor began with the pioneering work of Kumada^[13] and Corriu^[14] who discovered the possibility to couple an aryl halide with a Grignard reagent in the presence of a nickel catalyst. In the following years the development of other carbon nucleophiles has resulted in the use of organozinc, organotin, organoboron, and organosilicon reagents. These are all more tolerant toward functional groups than the original Grignard reagent. The development of the palladium catalyst, which is less toxic and more stable towards oxygen, has in most cases replaced the original nickel catalyst.^[15] This improvement has given many new and versatile couplings, among the most famous are Suzuki,^[16] Kumada,^[13] Negishi,^[17] Hiyama,^[18] Stille,^[19] and Sonogashira^[15c] coupling reactions (Scheme 5).



Scheme 5. The most common named carbon-carbon bond forming cross coupling reactions

Further development of the cross coupling reaction includes new ways of performing the reaction, such as employing new ligands or substrates. One other important improvement is the

use of other metals as catalysts. One of the most promising metals for this purpose, *iron*, will be presented in this thesis.

1.5 Kinetic experiments

In kinetic investigations one measures the rate of product formation or reactant disappearance for a specific reaction. From this, insight into several aspects of the reaction mechanism can be acquired.

1.5.1 Absolute and relative kinetics

Absolute kinetic studies measures the rate of formation of products or disappearance of starting materials, where one parameter is varied, and the others are kept constant. The parameter could be the concentration of one of the reactants or the catalyst. Equation 1 shows the rate of disappearance for reactant A in a bimolecular reaction between A and B, k is the rate constant and m and n is the reaction order of each reactant.

$$-\frac{d[A]}{dt} = k[A]^m[B]^n \quad (1)$$

The reaction order of the involved species can be deduced from the kinetic experiments. A first order dependence means that one molecule is engaged in the rate-determining step, a second order dependence that two molecules are involved. In Equation 1, m and n represent the reaction order for the two involved reactants. By varying each parameter all the reaction orders for the involved species can be determined and information about the rate-limiting step can be established. One can also vary the temperature of a reaction to gain information about the enthalpy and entropy of activation. It is imperative to take great care when carrying out absolute kinetic experiments, since the methods are highly sensitive to small alterations in the reaction conditions.

In relative kinetic experiments two different substrates for a specific reaction are subjected to the reaction at the same time. The relative rates of formation of the products or disappearance of starting material are then measured. This kind of competition experiment is much less sensitive to variations and the analysis of the data is easier. From this, knowledge about the selectivity-determining step can be gained.

1.6 Theoretical methods

Because of the rapid progress of computers and processing speed, the area of computational chemistry has developed extremely fast in the last decades. From the small systems, consisting of only few atoms that were possible to manage in the end of the 1980s, the computational chemists of today can handle enzymatic systems with several thousand atoms.

1.6.1 Wavefunction methods

One of the important developments for calculations in organic chemistry was the *Hartree-Fock* (HF) method, in which the Schrödinger equation (Equation 2) can be solved iteratively.^[20]

$$H\Psi = E\Psi \quad (2)$$

However, HF calculations use the approximation that each electron interacts with the average of all the other electrons, and ignores the important *electron correlation*, which postulates that when one electron moves to a certain point in space, all the other electrons must move away from that point. In spite of this simplification, the HF method is able to give fairly accurate total energies for molecules, as well as molecular geometries and reaction barriers. In cases with higher electron densities, such as transition metals, the electron correlation is large enough to give significant errors for HF results. Therefore, other more accurate methods are needed in these occasions.

Small perturbations can be introduced to the HF wavefunction, in order to obtain a more accurate solution. An easy way to do this is to mix the ground state with other low-energy states. In the *many-body perturbation theory* (MBPT), or *Møller-Plesset theory* (MP), the HF excited states are used in this way.^[20] MP2 uses the single and double excitations. Three or more electrons can be excited simultaneously in MP3, MP4 and MP5 methods, of course at a much greater computational cost. A development of this technique is the *coupled-cluster theory*, the variant termed CCSD(T) is used today as a “gold standard” for computational benchmarking, but this method is very costly, and is practical only for up to around a dozen atoms.

1.6.2 Density functional theory

An alternative to the wavefunction methods is density functional theory (DFT),^[20] which, unlike the above-mentioned methods, does not solve the Schrödinger equation; instead it solves a corresponding equation for the electron density.

Initially, DFT was used to calculate the total energy of a system by considering the electron density at each point in space, the *local density approximation* (LDA). The further development of this technique resulted in the *non-local density approximation* (NLDA or GGA) where the variation in density, the gradient, was taken into account. This approach was at least as accurate as HF methods, and at a lower computational cost.^[20-21] In more recent years, new improvements have resulted in a method that is as fast as HF calculations and has the accuracy of the MP methods. Particularly the work from Becke providing the hybrid theory, a merge between HF and DFT has been instrumental in the development of DFT as the standard method of today.^[22] The hybrid theory uses a combination of a partially exact treatment of the exchange term and an approximation of the electron correlation term to generate a more accurate and generalized DFT method. Most of the published computational studies today employ Becke's hybridization methods,^[23] especially the B3LYP variant.^[22, 24] Even more recent improvements of these methods involve accounting for van der Waals dispersion forces, for example by a parameterized functional, such as M06-2X,^[25] or by calculation of a correction term.^[26]

1.6.3 Basis sets

All of the aforementioned methods require a mathematical description of the distribution of electrons in space. In an atom, the electrons are distributed in *orbitals*, with each orbital able to confine two electrons. The atomic orbitals are the well-known 1s, 2p and so on, orbitals. Usually the molecular orbitals are constructed from the atomic orbitals, this is called *linear combination of atomic orbitals* (LCAO). In trivial cases the simple atomic orbitals are employed, but in more complex examples, the requirement of accurate results demands the need of the orbitals to be able to change size and shape. Giving each orbital two different sizes is denoted double- ζ (DZ), whereas using three different sizes is termed triple- ζ (TZ). Sometimes very large orbitals are used, especially when anions need to be accounted for, these are called diffuse orbitals and are indicated by a "+" or "aug-" in the name of the basis set.

The shape of the orbitals can be adjusted by adding orbitals of a higher quantum number. The mixing of these different orbitals result in new orbitals that better describe chemical bonds, such as π -bonds. The use of the extra orbitals is called polarization and is denoted with a "*" or "**" describing the use of an extra set of d-orbitals on heavy atoms and p-orbitals on hydrogens, respectively. Another way to indicate this is by adding (d) or (d,p) to the name of the basis set.

The large number of electrons in the heavier elements is a problem in calculations since they increase the required time for each calculation, without significantly changing the result. Because it is the valence electrons that constitute the part of the atom that contribute to bonds and other

interactions, it is these that will give changes to the total energy. Therefore, the core electrons of heavy atoms are sometimes treated with an *effective core potential*^[27] (ECP) that is as a total charge from these electrons. This greatly reduces the basis set size.

1.6.4 Solvent

Since most organic reactions are carried out in a solvent, and not in the ideal “gas phase” that makes up the best arena for calculations, some consideration must be spent to account for the implementations of the solvent. Most structures will be reasonably accurate when optimized in gas phase, as long as they do not carry opposite charges. This problem occurs when dealing with, for example, two ionic species of opposite charge. The reaction between these will generally be barrier-less in gas phase, something that can be far from the reality in solution. The most popular way to answer this problem is to use a continuum solvent model. Several are available and one of the most common is the *polarizable continuum model*^[28] (PCM). It encloses the molecule with a cavity dotted by parameterized point charges, which has been modeled to simulate the average influence of the solvent. The method employed in this thesis is a variant of the PCM method, the *Poisson-Boltzmann finite continuum model* (PBF).^[29] This method uses two parameters to describe different solvents, the *probe radius*, derived from the size of the solvent molecule and used to construct the solvent accessible surface area, and the *dielectric constant* of the solvent.

1.6.5 Calculating energies and analyzing results

A simple DFT optimization of an organic molecule in gas phase results in a large amount of information. The most important property is the energy of the molecule. It is provided in the unit Hartree and can only be used as a relative value. The energy can only be compared to other calculated energies with the same setup as the first one. This is the *potential energy* of the molecule. A more accurate energy for the molecule is the *Gibbs free energy*, denoted G , which can be calculated by adding the thermodynamic and solvation effects. The method employed in this thesis approximates this by adding the vibrational contributions to the single-point energy with solvation of an optimized gas-phase structure.

When comparing energies there are a few rules of thumb that can be important to remember when the energy is used to indicate ratios, enantiomeric excesses or selectivities. A difference of 2 kJ/mol is equivalent to a 2:1 ratio, and a difference of 6 kJ/mol corresponds to a 10:1 ratio, this of course means that a 12 kJ/mol difference is equivalent to a 100:1 ratio. All of these ratios are valid at room temperature.

The easiest way to analyze a chemical reaction computationally is to construct a reaction profile, a *free energy surface* (FES), where the starting point is the sum of all starting reactants, and

consequently, the end point is the sum of all products. All intermediate points are the sum of the relevant intermediates, not yet consumed reactants and already formed products. In catalytic systems it is important to note that the starting point is arbitrary. The relationship between all steps are easiest seen when drawing two full catalytic cycles after each other, as depicted in Figure 1.^[30]

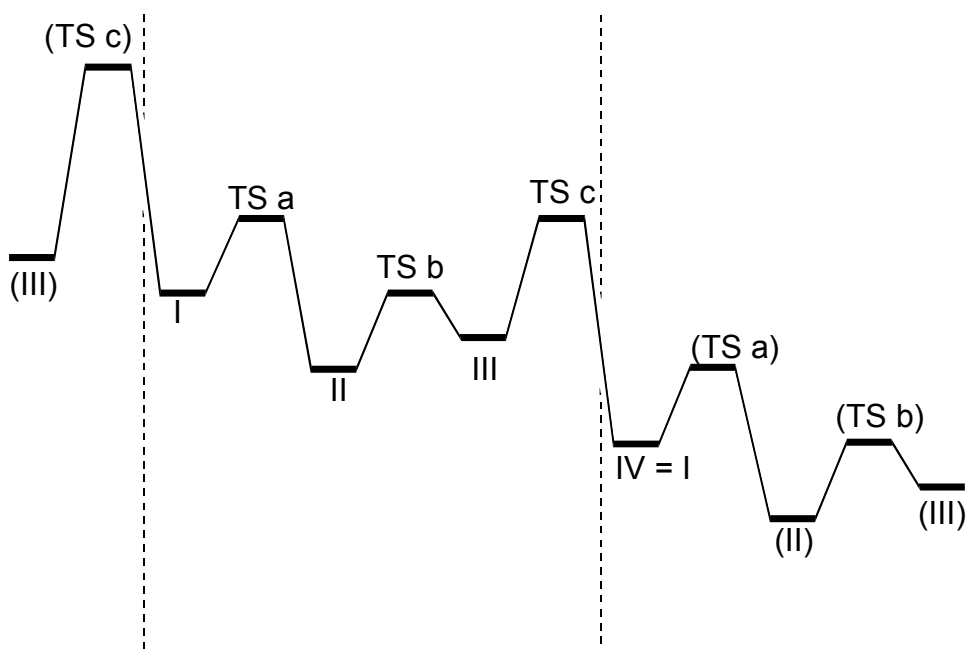


Figure 1. Free energy surface (FES) for a catalytic reaction

The overall exergonicity of the reaction can be seen as the difference between the same point in two subsequent catalytic cycles (e.g. between I and IV in Figure 1). The interpretation of the surface reveals several interesting points. Firstly, all transition states that are higher than all the subsequent points can be identified as *effectively irreversible*. In Figure 1 this is true for **TS c**, maybe also for **TS a**, even if the difference between these points is hard to determine, and can be within the accuracy limit of the method employed. However, these transition states are selectivity determining for the bonds formed in the corresponding step. **TS b**, on the other hand, is a completely reversible step, and will not have any influence on the reaction. This is a classic Curtin-Hammett situation where **II** and **III** are in rapid equilibrium.^[31] With the important **TS a** and **TS c** established, the activation free energy can be calculated as the difference between the TS and the lowest preceding point. In Figure 1 the barriers corresponds to $G(\text{TS a}) - G(\text{I})$ and $G(\text{TS c}) - G(\text{II})$. The rate determining step is the one with the highest barrier (**TS c** in Figure 1) and the resting state is the lowest preceding point (**II** in Figure 1). Other ways to analyze free

energy surfaces are present in the literature, one example is the *energetic span model* by Shaik and co-workers.^[30]

The barriers calculated must be compared to the reaction conditions, especially the temperature, which of course is the factor that most greatly influences the possibility for the reaction to progress. At room temperature, a good estimate is that a barrier should not be above 100 kJ mol^{-1} in order to proceed at an acceptable rate.

1.7 Aims of the thesis

The overall goal of this work was to provide information about new and existing tools for synthetic organic chemistry. The studies were done through mechanistic investigations of transition metal catalyzed reactions, using a combination of kinetic experiments and computational studies.

In this thesis, the aims have been to investigate several different transition metal catalyzed reactions:

1. For the palladium catalyzed allylic alkylation reaction, the factors that are determining the observed regioselectivity and the mechanistic pathways for a sulfinylation version of the reaction were examined.
2. In two different versions of the Mizoroki-Heck reaction, understanding of the critical role of benzoquinone in a chelation-controlled *domino* Mizoroki-Heck-Suzuki reaction and the catalytic cycle for a new and mild nickel catalyzed version of the reaction were investigated.
3. The mechanism and the nature of the active catalyst for the environmentally friendly iron catalyzed cross coupling reaction was thoroughly studied.

2. Palladium assisted allylic substitution (Papers I-II)

The palladium assisted allylic alkylation reaction is under constant development, with new features added to the reaction continuously. Some of the most important fields for progress are enantioselectivity, regioselectivity and development of new nucleophiles. The selectivity is important since there is always a need for new ways to control the stereochemical outcome of a reaction. Development of novel nucleophiles can open new pathways to the formation of new bonds, such as carbon-heteroatom bonds, but can also provide milder and more efficient ways to form chemical bonds.

2.1 Background

2.1.1 Ligands for palladium assisted allylic alkylation

Ligands have a profound effect on the allylic alkylation reaction; it is therefore an area that has been intensely studied. There are two different purposes for the ligands in the reaction. Firstly to enhance the reactivity of the palladium allyl complex towards nucleophilic attack, and secondly, they are responsible for controlling the stereo- and regioselectivity of the reaction. The π -accepting ligands will remove electron density from the metal; a feature known as *back bonding*,^[32] and thereby making the allyl moiety more positively charged and more prone to be attacked by a nucleophile. The most frequently used π -accepting ligands are the phosphorous-containing ones, such as PPh_3 or 1,3-bis(diphenylphosphino)propane (dppp) (Figure 2).

Chiral versions of the ligands are used to induce stereoselectivity, and there is an enormous amount of different ligands at hand.^[7a] Many of these are bidentate so called P,P-ligands with two phosphorous atoms coordinating to the palladium center, but there are many P,X-ligands, where X represents a heteroatom, such as N, S or O. Some of the most frequently used chiral ligands are the BINAP-ligands,^[33] but others, such as the Trost modular ligand,^[34] and the PHOX-ligands^[35] are regularly used in asymmetric allylic alkylation (Figure 2).

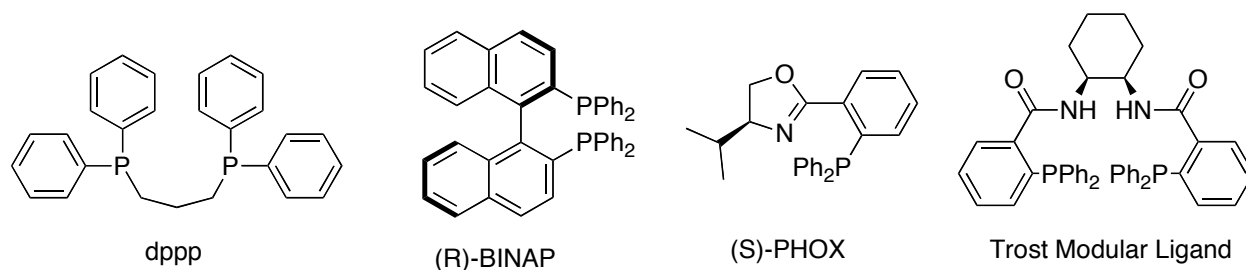
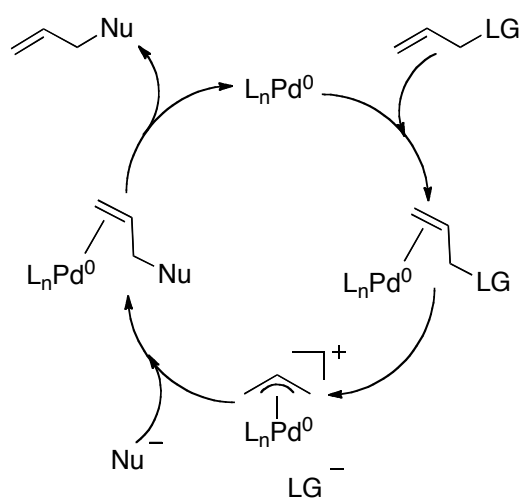


Figure 2. Some important ligands in palladium catalyzed allylic substitution reactions

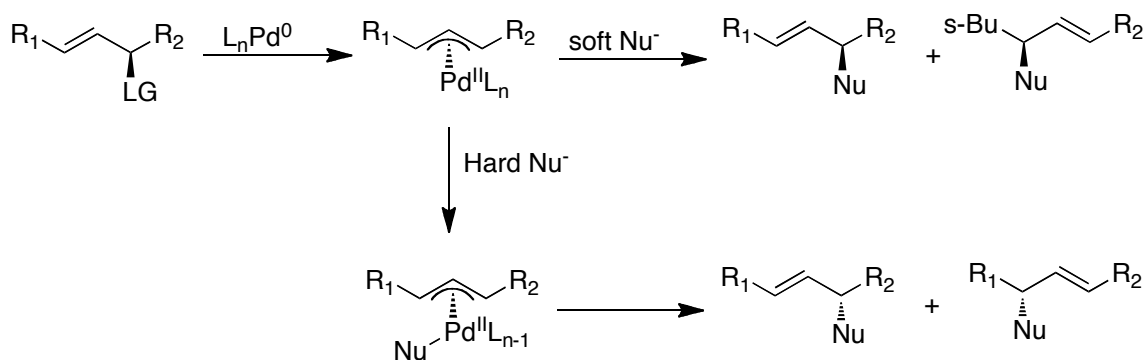
2.1.2 Catalytic cycle and mechanism

The catalytic cycle of the reaction starts with coordination of the alkene to the Pd⁰ complex in an η^2 -fashion, followed by an ionization and expulsion of the leaving group to form the η^3 -complex, with the leaving group as the counter ion. This Pd^{II} complex can undergo a nucleophilic attack to again give an η^2 -complex with the product coordinated. In the final step, the product is released from the palladium complex. The cycle has been closed, and the reformed Pd⁰ can perform another cycle (Scheme 6).



Scheme 6. Catalytic cycle for the Tsuji-Trost reaction

Both the ionization and the nucleophilic attack go through an inversion of the stereochemistry when soft nucleophiles such as malonates are used. This results in an overall retention of the stereochemistry in the reaction.^[36] On the other hand, when using hard, unstabilized carbon nucleophiles, such as Grignard or other organometallic reagents, the reaction pathway is different. The nucleophile will coordinate to palladium in the η^3 -allylic complex, and form the product via a reductive elimination (Scheme 7). This will result in an overall inversion of the stereochemistry.^[36b] Heteroatom nucleophiles, such as amines and alcohols usually follow the same pathway as the stabilized carbon nucleophiles, giving retention of stereochemistry.^[37]



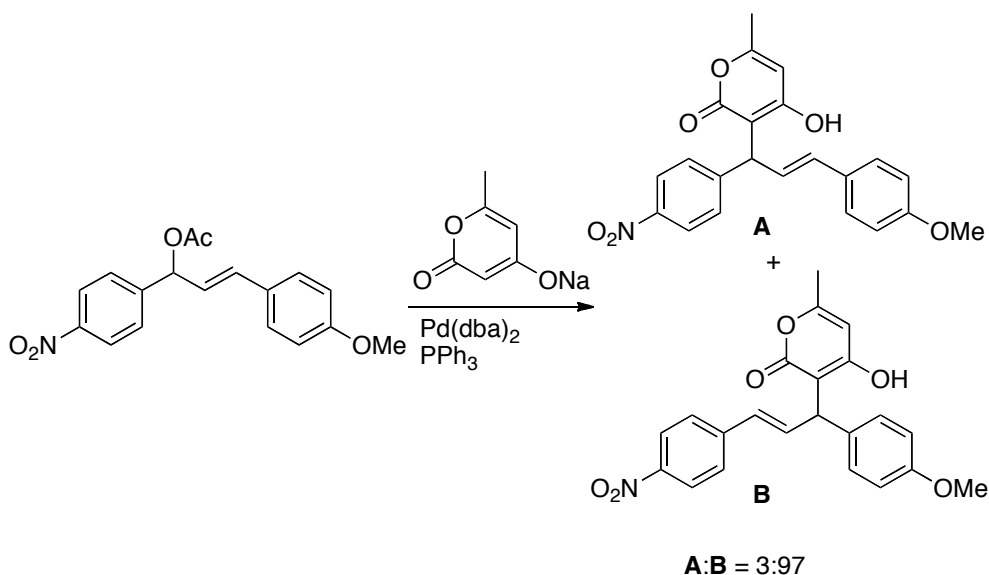
Scheme 7. The different stereochemical outcomes when using soft or hard nucleophiles

2.1.3 Regioselectivity

(η^3 -Allyl)palladium complexes react almost exclusively at the terminal carbons of the allylic moiety. The factors governing the regioselectivity for the nucleophilic attack are both electronic and steric. When the electronic properties of the termini are similar, nucleophiles tend to attack at the least hindered site. For example, the linear product is the major outcome when an allylic substrate that proceeds via a mono-substituted (η^3 -allyl)palladium intermediate, is subjected to the reaction.^[7a]

Since the branched product can be chiral, much effort has been put into directing the attack to this position. It has been shown that the electronic properties of the ligand and the allylic moiety are important in controlling regioselectivity, the nucleophilic attack of a nucleophile occurs at the more electron-rich position of the allyl. This can be seen as somewhat counterintuitive but one must remember that this must also be regarded as the site where a cation is most stable.

Åkermark and co-workers demonstrated that more π -accepting ligands lead to attack at the more substituted position, due to the greater degree of positive charge residing at the more substituted carbon.^[38] Special ligands have been designed to promote attack at the more substituted terminus. These are unsymmetrical ancillary ligands that facilitate an attack at the most hindered site, either by orienting the nucleophile to this position or by making the position more electrophilic.^[39] Scheme 8 shows two examples where electronic properties determine the regiochemical outcome of an allylic substitution reaction.^[40]



Scheme 8. Two examples of electronically controlled regioselectivity

2.1.4 Nucleophiles

A wide range of nucleophiles have been utilized in allylic alkylations and, as already mentioned, the most important of these are the stabilized carbon nucleophiles, which come in many different forms. The common motif for these reagents is the methylene or methine group, surrounded by electron-withdrawing groups, such as carbonyl, cyano, nitro and sulfonyl groups (Figure 3).^[7a] The active nucleophile is formed upon deprotonation. Also neutral nucleophiles, such as enamines, are reactive in this kind of reaction.^[41]

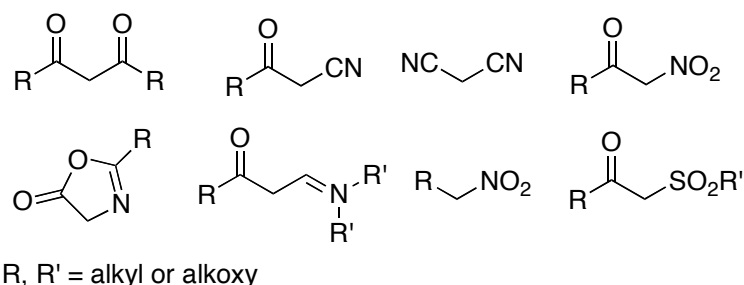


Figure 3. Some pronucleophiles used in allylic substitution

Alkali metal enolates have been employed, although with mixed outcome,^[42] and other milder enolates, such as boron,^[43] silicon^[44] and zinc enolates^[45] show better results.

Heteroatom nucleophiles have been shown to be more prone to attack at the more hindered site than the carbon nucleophiles. Oxygen nucleophiles, such as O-aryl species, follow this pattern,^[46] and so does nitrogen nucleophiles, such as amines, aziridines, hydroxylamines and hydrazines.^[47]

2.1.5 *Trans effect and trans influence*

Since allylic alkylations are carried out with the aid of a palladium catalyst, in the shape of a square-planar metal-ligand complex, it is important to take special notice of this kind of structure. Very important features of these complexes are the *trans influence* and the *trans effect*. These two concepts provide a strong control of the reactivity and structure of the complexes.

The *trans influence* is a purely thermodynamic phenomenon, and is used to describe effects on the ground state of the complexes. It can be described as “to which extent a ligand weakens the bond *trans* to itself”. For example, a certain ligand can extend the metal-ligand bond or influence the magnitude of the M-P coupling constant *trans* to it.

The *trans effect*, on the other hand, is a kinetic effect on the rate of dissociation or on the reactivity of the ligand *trans* position. The effect can be very large, as much as several orders of magnitude on the rate constants. There is a close relationship between the *trans effect* and *trans influence*, even if some exceptions exist.

In general, a *trans influence* series can be described as in Figure 4.^[7a] As can be seen from the series, strong σ -donors, such as hydrides, result in large *trans influence*, but π -acceptor ligands, such as olefins, can also lead to a fairly strong *trans influence*.

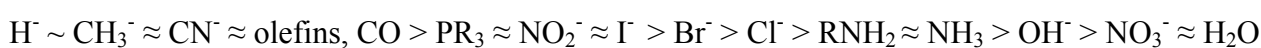


Figure 4. An approximate *trans influence* series^[7a]

2.1.6 *Factors influencing selectivity*

Asymmetric versions of the Tsuji-Trost reaction have been applied to complexes that give symmetrically substituted (η^3 -allyl)Pd intermediates, such as cycloalkenyl or 1,3-diphenylallyl,^[48] and unsymmetric (η^3 -allyl)Pd intermediates, such as monosubstituted allyls. In the former case, the enantioselectivity is governed by the regioselectivity of the nucleophilic attack,^[46] which is governed by the stereochemical control from the ligand.^[4c, 48-49] In the latter case, however, several factors can influence the outcome, for example steric and electronic influences from the substrate,^[50] regiochemical memory of the position of the leaving group,^[51] the preferred configuration being *anti* or *syn*^[52] (see Figure 5 for an explanation of the *anti/syn* nomenclature) and dynamic exchange in the intermediate,^[53] the nucleophile,^[54] and the nature of

the ligands.^[46, 55] As one example of one of these factors, the *syn* configuration of a monosubstituted allylic substrate has a strong preference for terminal attack, whereas the *anti* configuration results in product mixtures, with considerable quantities of internal attack.^[52] Since the consequence of an internal attack is a new stereocenter, there is a great interest in learning how to control this selectivity and it is worth mentioning that other metals, such as molybdenum, tungsten, rhodium, ruthenium and iridium, have been extensively employed to achieve the branched product.^[7a]

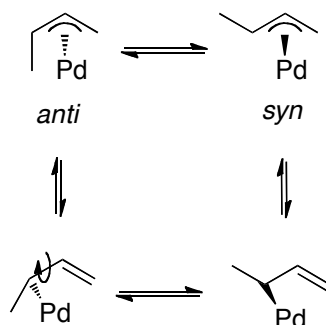


Figure 5. *Anti* and *syn* configuration of a $(\eta^3\text{-allyl})\text{Pd}$ complexes

However, by manipulating the ligands of the palladium complex they can be able to direct the attack to the more substituted carbon of the allylic moiety. Ligands that induce distortions in the intermediate have proven to have a strong effect on the regioselectivity of the nucleophilic attack.^[56] Ligands containing phosphorous have been widely employed because of the large *trans* effect of the phosphorous will increase reaction at the carbon *trans* to any phosphine.^[38b] Other heteratoms have also been used in the ligand synthesis, such as oxygen, nitrogen and in some cases sulfur.^[7a] As mentioned before, several different classes of ligands have been developed and provide great opportunities to achieve selectivity. Although high selectivities can be accomplished in many cases, still there does not exist a general approach to control selectivity and a lack of knowledge of the balance between the different effects, steric and electronic, is apparent.

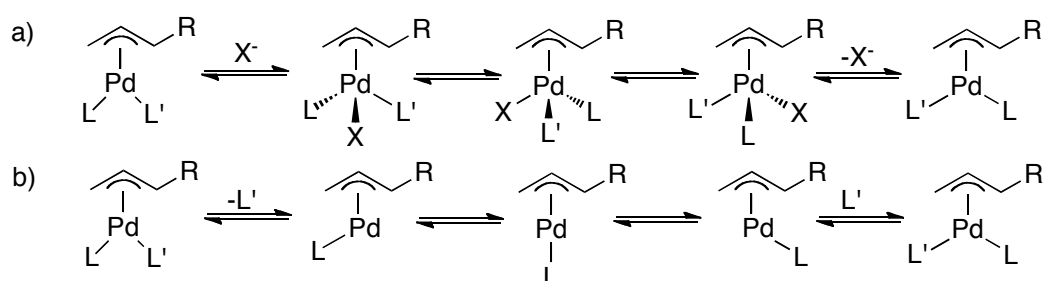
2.1.7 Computational work on the palladium mediated allylic alkylation

Several important issues regarding palladium mediated allylic alkylation reaction have been studied computationally.^[57] The structure and geometry of the $(\eta^3\text{-allyl})\text{Pd}$ complex have been rationalized, and can be accurately reproduced with many different methods.^[58] Other important features, including ligand effects, such as the *trans* effect, and dynamic processes can also be understood and rationalized through computational methods. Most importantly, the reactivity and

selectivity can be explained and predicted. The important contributions in this field have been summarized recently.^[57b]

2.2 A tethered ligand – a way to investigate regioselectivity (Paper I)

Trying to distinguish and measure the different factors controlling regioselectivity in the title reaction is a challenging task. Some examples exist in the literature, for example has the difference in *trans* effect between phosphorous and chloride been measured,^[59] but the results are hard to interpret due to the influence of dynamic processes in the system. It has also been established that the efficient apparent rotation (Scheme 9) of the cationic (η^3 -allyl)Pd complexes can diminish the apparent *trans* effect.^[60] It should be noted that some doubt about the influence of the dissociative mechanism for apparent rotation has been presented.^[60]



Scheme 9. Apparent rotation via a) pseudorotation b) a dissociative mechanism

In an attempt to quantify the *trans* effect, and separate it from steric effects, a tethered ligand system was devised (Figure 6). The tethered system hinders the apparent rotation and ensures that the sulfur atom always is positioned *trans* to the terminal position of the allylic moiety and that the auxiliary ligand is positioned *trans* to the internal position.

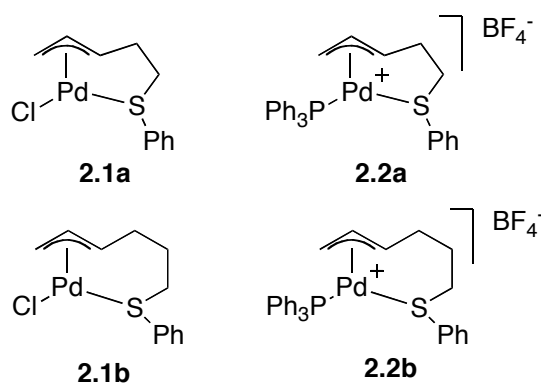


Figure 6. (η^3 -allyl)Pd complexes with a tethered sulfide ligand

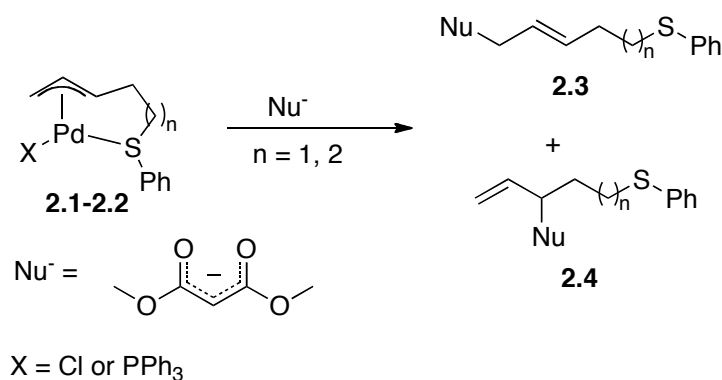
This system has been utilized earlier but at that time there were no means to elucidate the preferred configuration of the complex.^[61] Krafft and co-workers performed studies on a range of

tethered ligands in a catalytic system, including alkenes^[62] and sulfides,^[63] and postulated that the tethered ligand interacted with the incoming nucleophile instead of the Pd, thereby ruling out the *trans* effect as a factor influencing the selectivity. A similar study has been conducted by Yoshida and co-workers on the effect of a removable pyridine tether, but no analysis of the reasons for the regioselectivity was presented.^[64]

To investigate this area further and to ensure the coordination of the tethered ligand, our study was performed with preformed Pd-complexes, and by running the reaction with stoichiometric amounts of the tethered complex, any interference from exchangeable ligands in the reaction mixture was minimized.

2.2.1 Experimental results[†]

The above-mentioned Pd complexes were employed in an allylic alkylation reaction with sodium malonate as the nucleophile (Scheme 10).



Scheme 10. Allylic alkylation reaction and potential regioisomeric outcome for the Pd complexes

The regioisomeric outcome of the reactions was analyzed by GC-MS and NMR spectroscopy. The product distribution between the terminal and internal attack is found in Table 1.

Table 1. Product distribution from reactions in Scheme 10

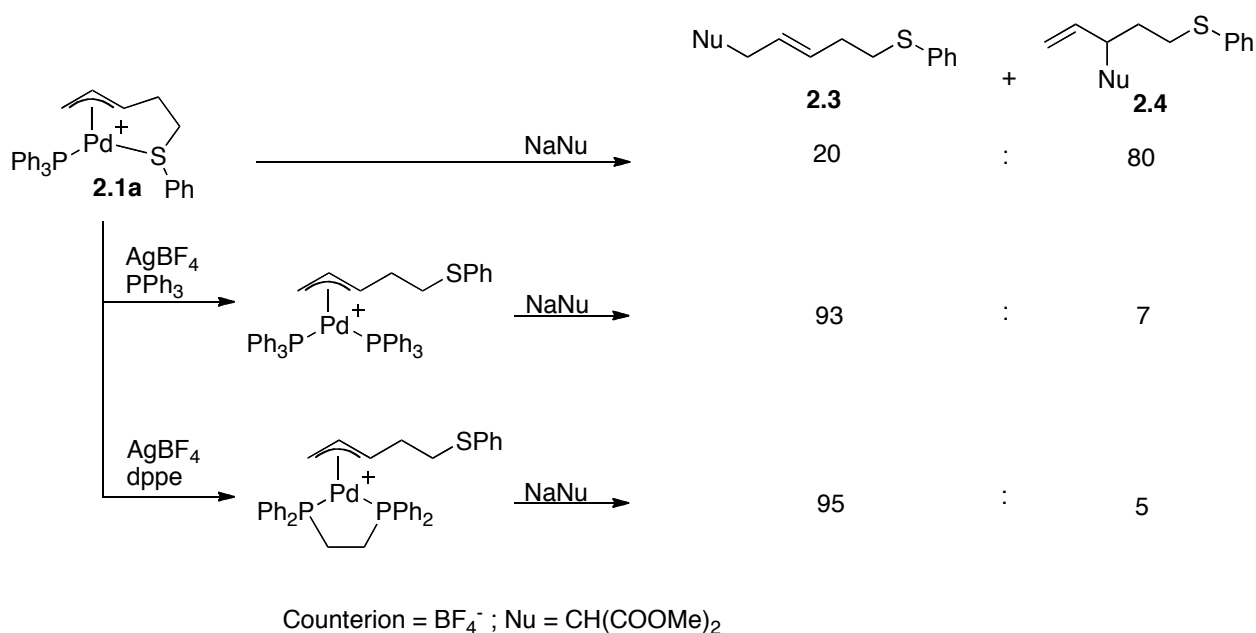
complex	ligand X	tether length	linear 3 (%)	Branched 4 (%)
2.1a	Cl	2	40	60
2.1b	Cl	3	80	20
2.2a	PPh ₃	2	20	80
2.2b	PPh ₃	3	80	20

The results for the phosphorous containing complexes show a dependence on the nature of the allyl part and very little influence from the auxiliary ligand. The shift in preference from

[†] Experimental study performed by Dr. Charlotte Johansson

branched to linear when going from the shorter tether to the longer indicates that the important factor for the regioselectivity is the steric influence from the tethered ligand, and not the *trans* effect. However, when comparing the result between the chloride and the phosphine complexes an increase in the amount of branched product is seen when employing the shorter tether. This indicates that attack *trans* to phosphorous is favored, which is in agreement with the difference in *trans* effect arising from these ligands. The result from our study is in agreement with the previously mentioned investigation by Krafft and co-workers,^[63] implying that the tethered ligand indeed is coordinated to Pd during the reaction.

Furthermore, complex **2.1a** was subjected to another reaction where the tethered ligand complex first was treated with an excess of two different phosphorous ligands, PPh₃ and 1,2-bis(diphenylphosphino)ethane (dppe), followed by the same nucleophile as in the previous reaction, sodium malonate (Scheme 11). These experiments gave mainly terminal attack in both cases, mirroring the result from isolated *syn* complexes^[52a, 65] and similar experiments conducted by Krafft and co-workers.^[63] These results definitely disprove the proposal by Krafft and co-workers that uncoordinated ligands direct the nucleophilic attack.^[63]



Scheme 11. Selectivities with and without coordination of the tethered sulfide ligand

The obtained results could be explained by a difference in configuration for the two tether lengths, where the longer tether could prefer the *syn* configuration and the shorter the *anti* configuration, which would result in different product distribution according to earlier work.^[52] However, preliminary results from calculations employing a molecular mechanics force field adjusted to (η^3 -allyl)Pd complexes, indicated that both tethers preferred the *syn* configuration.^[61]

To be certain of which of the configurations that was preferred, further structural determination was needed.

2.2.2 Structural determination of complexes

All four complexes were fully characterized by 1D- and 2D- ^1H NMR spectroscopy. The coupling constants were measured and special care was taken to investigate the coupling constant between the proton in the allylic moiety that can be in *anti* or *syn* position, and the proton on the center carbon in the allylic moiety (Figure 7). This coupling constant, for all the involved structures, was found to be in the range of 11-13 Hz, corresponding to *syn* complexes in solution.^[66]

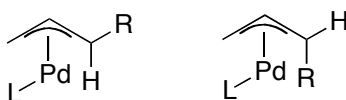


Figure 7. Schematic figure of the proton *anti* and *syn*

The solid state of the complexes was analyzed with X-ray crystallography,[†] which revealed that all four structures feature Pd in a distorted square-planar geometry and with *syn*-geometry. One aspect, which was noted as a difference between the different tethers, was that the shorter tether displays slightly more strain, indicated by the internal carbon being somewhat out of the allylic plane.

The unanimous result from the structural data regarding the *syn* configuration of the Pd complexes disproves the theory that different configurations can lead to the dissimilar product distribution in the studied allylic alkylation. In order to understand the reason behind this tantalizing problem, a DFT study was initialized.

2.2.3 Computational approaches and results

A molecular mechanics force field, especially constructed for this system,^[61] was used to examine the conformational and configurational space of the complexes. The generated structures were re-optimized using DFT calculations and from these the transition states were located.

The results from the DFT calculations were verified by testing against the known X-ray structure **2.5** (Figure 8).^[67] An overlay of the optimized DFT structures and the X-ray structures revealed an overall rms deviation of 0.0531 Å, where almost all of the error originates from the slightly elongated Pd-S bond in the DFT structures. Since this is a systematic error that will occur in all of the calculations, we can expect error cancellation when comparing related structures.

[†] X-ray crystallography performed by Susanne Olsson

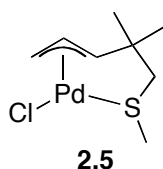


Figure 8. X-ray structure **2.5** that was used to verify the DFT method

The molecular mechanics conformational search generated 8 geometries for the short tether and 12 for the longer tether, including both *anti*- and *syn*-isomers, for the chloride complexes. The re-optimization at the DFT level could exclude the *anti*-isomers, due to their much higher energy, at least 18 kJ mol⁻¹ higher than the most stable *syn*-complex. For each tether-length, two low-energy complexes were selected and used in the further studies. These four structures were used as starting points for the optimization of the corresponding phosphine complexes, for which no molecular mechanics data could be obtained.

The transition state searches were conducted with sodium dimethylmalonate as the nucleophile. The sodium moiety was coordinatively saturated with two explicit dimethyl ether molecules, to minimize non-physical interactions with the substrate. For every complex, at least three different rotamers of the malonate were tested. A typical transition state structure is shown in Figure 9.

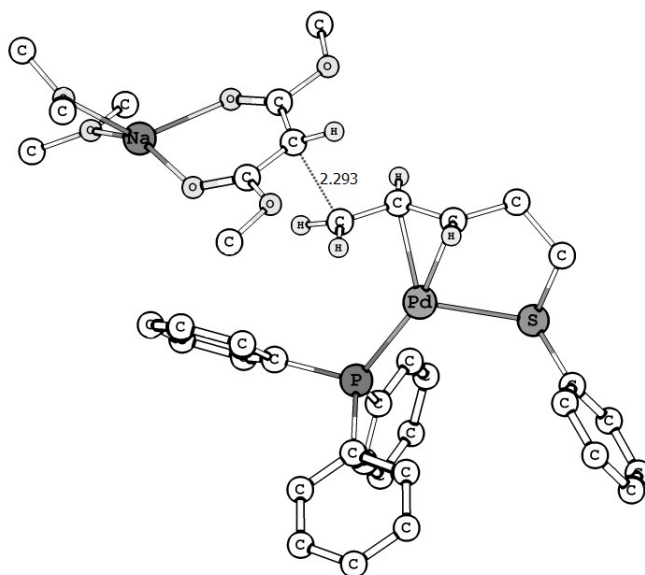


Figure 9. Transition state for terminal attack on complex **2.2a** (hydrogens omitted for clarity)

The preference for internal attack was calculated as the difference in free energy between the most stable complexes for the nucleophilic attack on the terminal and internal position, respectively. When comparing to the experimental results, it is important to remember that the ratios in Table 1 corresponds to a $\Delta\Delta G_{\text{exp}}^{\ddagger} = 4$ kJ mol⁻¹ for **2.2a** and -4 kJ mol⁻¹ for **2.2b** (preference for terminal attack). The first computational approach used a standard basis set,

lacvp*, which gave a preference for terminal attack for both complexes with $\Delta\Delta G^\ddagger = -2 \text{ kJ mol}^{-1}$ for **2.2a** and -23 kJ mol^{-1} for **2.2b**. Single point calculations with a larger basis set, LACVP**+, gave considerably better results for the shorter tether with $\Delta\Delta G^\ddagger = 5 \text{ kJ mol}^{-1}$, reproducing the preference for the internal attack. For the longer tether, results were still showing a favored terminal attack but it is strongly exaggerated, 31 kJ mol^{-1} . When applying a vdW correction^[26] to the transition state structures the calculated energy differences closely resembles the experimental values with $\Delta\Delta G^\ddagger = 6 \text{ kJ mol}^{-1}$ for **2.2a** and -10 kJ mol^{-1} for **2.2b**. It is worth mentioning that independent of the level of calculation, the amount of internal attack decreases when going from the short to longer tether.

2.2.4 Factors influencing the stereochemical outcome of the reaction

The computational study could fairly accurately reproduce the experimental results, but the energies do not provide any clues regarding the reason for the surprising shift in selectivity. To rationalize this anomaly we decided to subject the structures of **2.2a-b** to further investigation.

As already mentioned, many different factors can affect the regioselectivity in an allylic alkylation reaction. The difference in selectivity between the *syn/anti* configurations has already been ruled out due to high-energy ground states. To further strengthen this, the *anti* transition states were located and similarly found to be too high in energy.

The reactivity has also been shown to be dependent on the length of the breaking Pd-C bond, the preferred rotation of the η^3 -allyl moiety, and steric hindrance.^[56] Since previous research^[56] had shown that a difference in only 0.01 Å provided twice as high reactivity, the solid-state structures in our study were scrutinized (Figure 10).

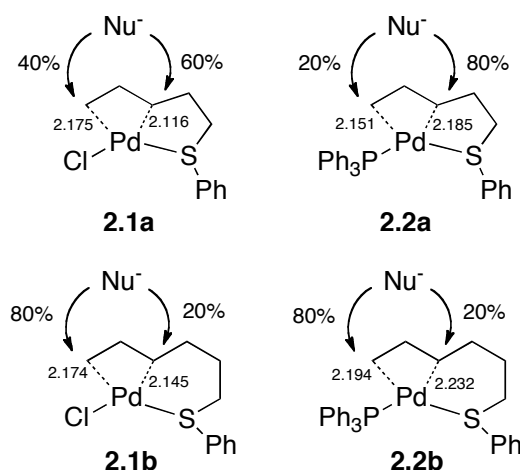


Figure 10. Length of the bonds in the X-ray structures versus the regioselectivity in the nucleophilic attack

The calculated structures from the DFT study showed similar trends as the solid state ones and are therefore omitted for clarity.

As can be seen from Figure 10, there is no relationship between the Pd-C bond length and the position where the nucleophilic attack takes place. For example, in complex **2.1a** the shortest Pd-C bond length is the most reactive, something that also is true for complex **2.2b**. On the other hand, in the remaining two complexes, **2.2a** and **2.1b**, the nucleophilic attack takes place at the carbon with the longest Pd-C bond. A *trans* influence can be observed within the system, the Pd-C bonds *trans* to phosphorous are slightly longer than those *trans* to chloride. In spite of this, no kinetic *trans* effect can be perceived.

Another factor that has proven to influence the reactivity of the allylic carbons is the enforced product-like rotation of the (η^3 -allyl)Pd moiety in the ground state. To investigate this, we measured the displacement of the terminal and internal allylic carbons, with respect to the S-Pd-P(or Cl) plane (Figure 11).

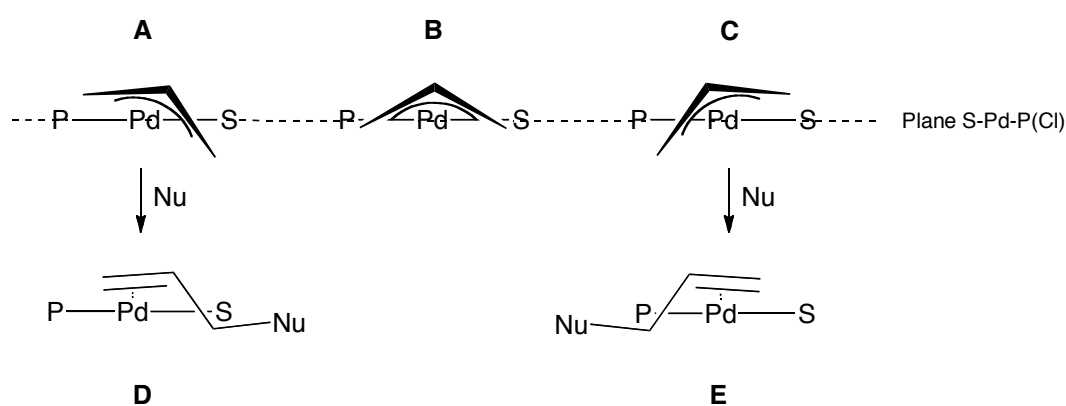


Figure 11. Different orientations of the η^3 -allyl with respect to the S-Pd-P(or Cl) plane

The three different situations, **A**, **B**, and **C** represent the different orientations the allylic moiety can exhibit. Situation **B** is the simple symmetric form. **A** and **C** are the unsymmetric versions, where **A** represents the orientation where the ground state resembles the product from the internal attack (structure **D**) and therefore should favor this attack, and **C** instead shows a resemblance to the product from the terminal attack (structure **E**) leading to a preferential terminal attack. The measured distances from both X-ray structures and calculated DFT structures have been compiled in Table 2.

Table 2. Torsion angles (°) of the allylic moiety for 1a-b and 2a-b, in the X-ray structures and two lowest energy DFT structures for each complex

Structure	C1 to plane [P(or Cl)-Pd-S] ^a	C3 to plane [P(or Cl)-Pd-S] ^a	Structure	C1 to plane [P(or Cl)-Pd-S] ^a	C3 to plane [P(or Cl)-Pd-S] ^a
2.1a (x-ray)	0.309	-0.199	2.2a (x-ray)	0.072	-0.317
2.1a (DFT_1)	0.144	-0.311	2.2a (DFT_1)	0.098	-0.268
2.1a (DFT_2)	0.087	-0.121	2.2a (DFT_2)	0.106	-0.162
2.1b (x-ray)	-0.107	-0.419	2.2b (x-ray)	-0.116	-0.185
2.1b (DFT_1)	-0.067	-0.330	2.2b (DFT_1)	-0.055	-0.078
2.1b (DFT_2)	-0.294	-0.275	2.2b (DFT_2)	-0.328	-0.607

^a Positive value if situated on the same side of the plane as H2.

In both the X-ray structures and the calculated structures the shorter tether displays an orientation similar to situation **A** that corresponds to a preference for internal attack, something that satisfactorily correlates to experimental results. However, the longer tether is almost symmetrical and it is therefore difficult to rationalize the regioselective results from this structure with an enforced rotation.

Steric interactions have also been shown to be of great importance on the selectivity in allylic alkylations,^[56] and a strong indication of this was the necessity to include vdW interactions^[26] in the calculations to accurately reproduce the experimental results. In an attempt to reveal the important steric interactions in the studied nucleophilic attack, the four lowest energy transition states, including both the long and short tether, were overlaid (Figure 12). When doing this, a great difference can be noticed between the two sets of structures, where the longer tether adopts an orientation similar to an unstrained *syn*-configuration.^[37b, 68] In contrast to this, the first non-allylic methylene group in the shorter tether is bent down from the allylic plain, due to the higher strain in the smaller ring, giving more space for the incoming nucleophile to attack at the internal position.

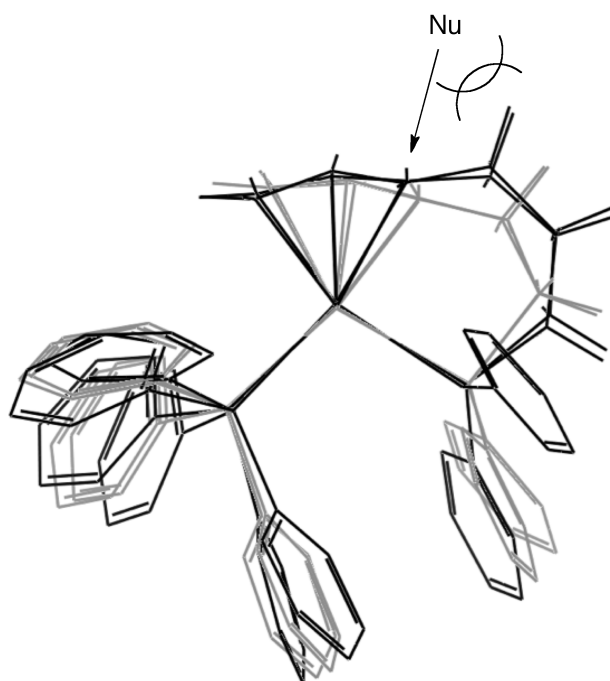


Figure 12. Overlay of the two lowest energy conformers of the short **2.2a** (grey) and long **2.2b** (black) tether, showing steric interactions with a nucleophile attacking the internal position. Some hydrogens omitted for clarity

To further investigate the apparently vital steric interactions, we measured the distance of the forming bond lengths in the transition states for the nucleophilic attack (Table 3). As has been shown, the Bell-Evans-Polanyi theory,^[69] as well as the Hammond postulate,^[70] implies that increased steric hindrance should result in a “later” transition state.^[71] In agreement with this, our data suggest that the “earliest” attack takes place for the internal position in the shorter tether complex, with a 0.02 Å shorter forming bond of the terminal position. In the longer tether, the opposite is true, with the forming bond of the internal position being shorter by 0.03 Å, indicating steric hindrance at this position.

Table 3. Average length of the forming C-C bond in nucleophilic attack on **2.2a-b**

Complex	Internal attack distance (Å)	Terminal attack distance (Å)
2.2a	2.31	2.29*
2.2b	2.23*	2.26

*Preferred site of nucleophilic attack

2.2.5 Conclusions

The experimental results from an allylic alkylation reaction between four different preformed (η^3 -allyl)Pd complexes and a malonate nucleophile showed large dependence on the geometry of

the allyl. Surprisingly, the electronic effects seemed to be of lesser importance, even if a small *trans* effect could be detected. Structural investigation, both in solution phase and solid state X-ray crystallography, revealed similar *syn*-configuration of all palladium complexes.

The subsequent DFT study could reproduce the results from the experimental examination, but a vdW correction was necessary to achieve a good agreement.

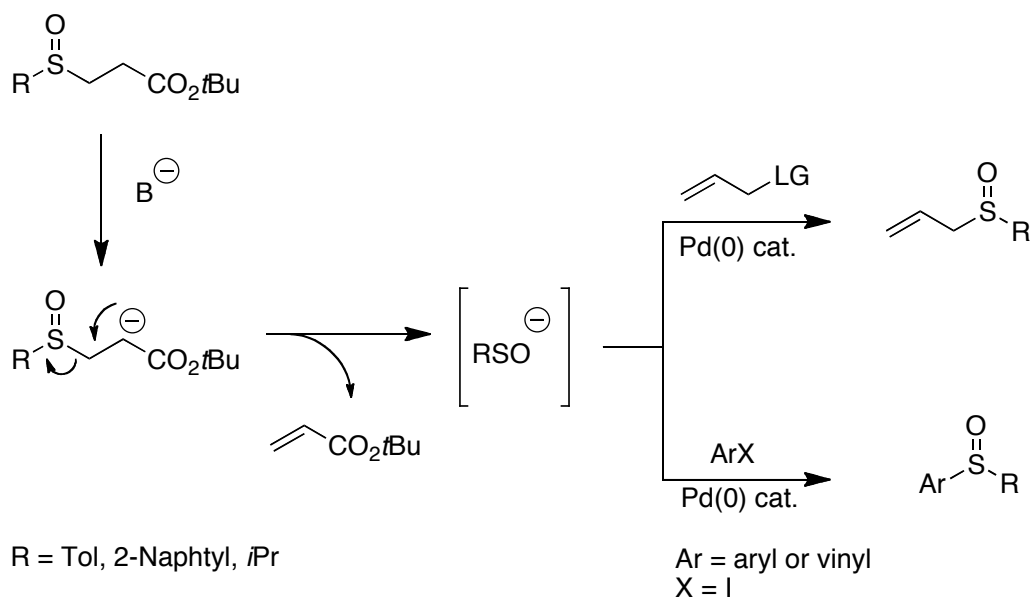
To inspect the reasons for the change in selectivity, various factors for controlling selectivity were investigated, including length of the reacting Pd-C bond, enforced rotation of the allyl moiety in the ground state, interactions between the nucleophile and the (η^3 -allyl)Pd complex as well as *trans* effects from the ligands on Pd. The decisive regioselective factors were found to be a combination of important steric hindrance from hydrogens in the adjacent methylene group and the rotation of the allylic moiety.

2.3 Allylic sulfinylation – mechanism and the MBE rearrangement (Paper II)

2.3.1 Background

The sulfoxide is an important functional group in organic chemistry. Sulfoxides can act as chiral ligands^[72] or auxiliaries^[73] in organic reactions, as well as being key groups in the pharmaceutical industry.^[74] The standard way of synthesizing sulfoxides today is through controlled sulfide oxidation.^[75] In a study aimed at finding new ways to synthesize sulfoxides, Poli and co-workers used the sulfenate anion as nucleophile in a palladium catalyzed allylic sulfinylation reaction to produce sulfoxides under mild conditions (Scheme 12).^[76]

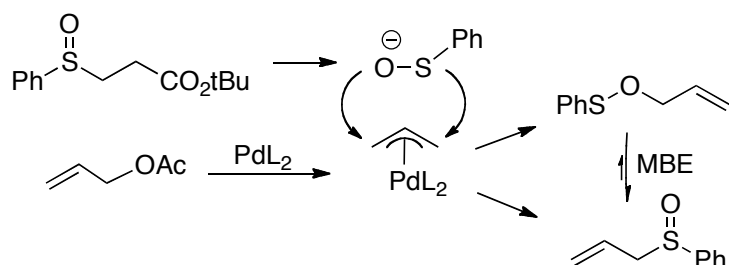
The sulfenate anions were generated in situ from β -sulfinyl esters via a base promoted elimination (Scheme 12).^[77] This nucleophile was then reacted in both palladium catalyzed allylation^[76] and arylation^[78] reactions. Both cyclic and acyclic allyls were coupled to aryl or alkyl sulfoxides in the allylation, and the arylation was possible to perform with aryl and vinyl iodides. An enantioselective version of the latter reaction was also developed.^[79] Furthermore, the versatile nucleophile was employed in different *pseudo-domino* palladium catalyzed processes.^[80]



Scheme 12. Generation and reaction of sulfenate anions as nucleophiles in allylic sulfinylations and arylations

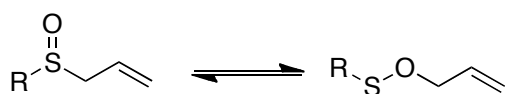
2.3.2 The Mislow-Braverman-Evans rearrangement

The conversion of sulfenate esters to sulfoxides is of interest to the mechanism of the sulfenylation. The nucleophilic attack of the anion could be achieved through either an attack from the sulfur or the oxygen of the sulfenate anion (Scheme 13). A fast conversion between the two possible products can thereafter give the thermodynamically most stable product.



Scheme 13. Sulfenate allylation via either nucleophilic S- or O-attack

The possible involvement of the Mislow-Braverman-Evans^[81] (MBE) rearrangement was therefore considered (Scheme 14). The only isolated product was the sulfoxides and therefore the attack was either restricted to *only* sulfur-attack, or the MBE rearrangement was responsible for the rapid conversion of the sulfenate ester to the sulfoxide.



Scheme 14. The Mislow-Braverman-Evans rearrangement

Some previous computational investigations regarding the MBE rearrangement have been conducted. Jones-Hertzog and Jorgensen studied the transition state of the reaction.^[82] They found that the *endo*-transition state was favored over the *exo* by ca 8 kJ/mol, but they also erroneously concluded that the sulfenate ester was more stable by at least 12 kJ/mol. The latter conclusion was a bit surprising since the experimental evidence points at the sulfoxide as the more stable structure. In a later study, the same group could also rationalize the regioselectivity of the rearrangement when using substituted allyls.^[83]

2.3.3 Computational study of the Mislow-Braverman-Evans rearrangement

Our standard setup for computational investigations of mechanistic problems is DFT at the B3LYP level^[22, 24a] with a polarized double- ζ basis set (6-31G*), augmented by vibrational corrections, ECP basis sets for heavy elements,^[27] continuum solvation,^[28-29] and dispersion

correction.^[26] However, previous work by Jorgensen and coworkers, employing similar methods, predicted an equilibrium shifted towards the sulfenate product in the MBE rearrangement.^[82] We could verify this problem when employing our standard setup on the same system. The solution to this problem was to employ larger basis sets. At the cc-PVDZ level, the results were fairly converged, but since a slight shift in energy occurred when using cc-PVTZ,^[84] the latter basis set was chosen for further studies. The geometries were well converged at the 6-31G* level, something that was confirmed by small differences in energy between cc-PVTZ and cc-PVTZ//6-31G* calculations. Single point cc-PVTZ calculations at 6-31G*-derived IRC points also revealed that the transition state of the rearrangement shifted with less than 0.1 Å with the larger basis set (Figure 13). Applying a solvent model of dichloromethane (DCM) did not give any large effects either.

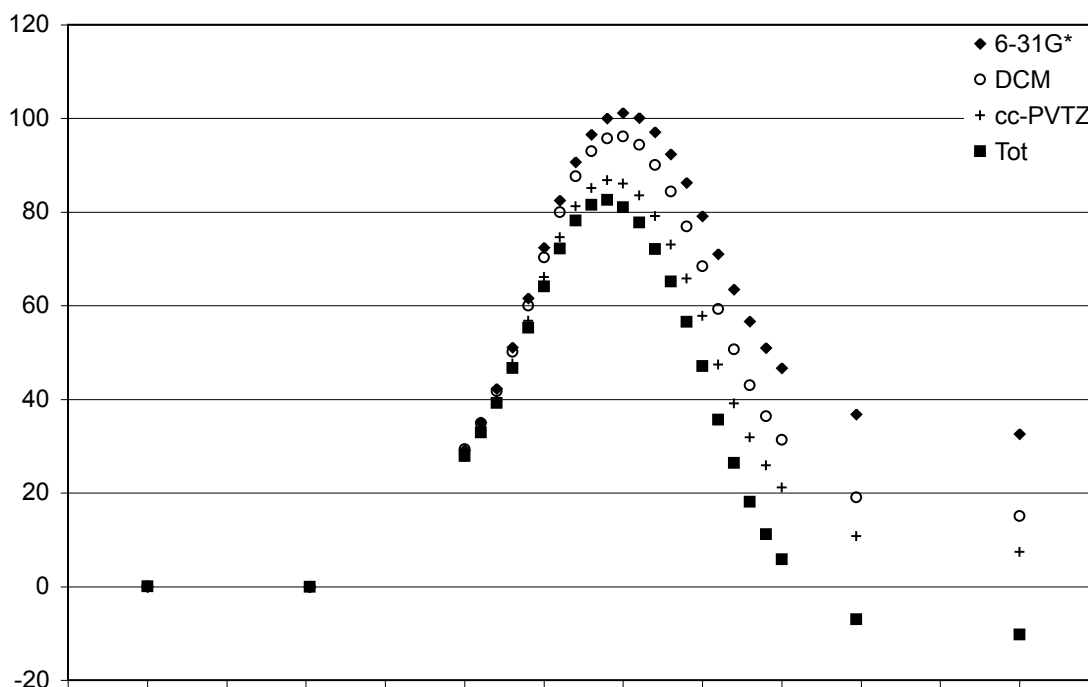


Figure 13. IRC points for the Mislow-Braverman-Evans rearrangement at different levels of theory

In summary, to guarantee proper energetics in the study of this rearrangement, we employ geometry optimizations at the B3LYP level with a lacvp* basis set, validate all stationary points with vibrational calculations, and calculate the final free energies by adding contributions from vibrations, solvation and basis set correction using cc-PVTZ basis set for the organic moieties and lacv3p*+ for Pd.

This method was utilized for three model systems, the methyl allyl sulfoxide, **2.6a**, and the experimentally more relevant phenyl allyl sulfoxide, **2.6b**, and phenyl cinnamyl sulfoxide, **2.6c**. For all the MBE pairs the devised method correctly predicted the sulfoxide **2.6a-c** as being

preferred over the corresponding sulfenate **2.7a-c**, by 7-25 kJ mol⁻¹. In addition to this, the transition states for the rearrangements were identified^[85] and the barriers were calculated to 82-104 kJ mol⁻¹.

To further extend the method to the above-mentioned sulfonylation conditions we also investigated the palladium catalyzed MBE rearrangement, using palladium with a diphosphinoethane (DPE, H₂PCH₂CH₂PH₂) ligand, as the model for the experimentally competent DPPE-ligand. The transition states for the same rearrangements were localized; a typical transition state for the Pd-catalyzed MBE rearrangement is shown in Figure 14. The metal fragment is similar to an (η^3 -allyl)Pd complex, but the distances between Pd and the terminal carbons are considerably longer.

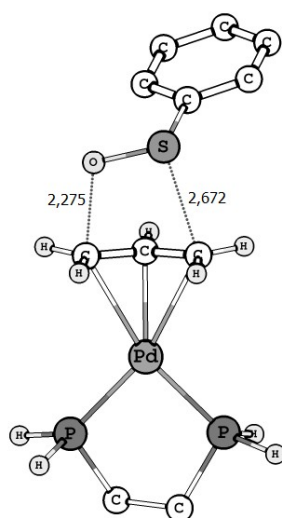
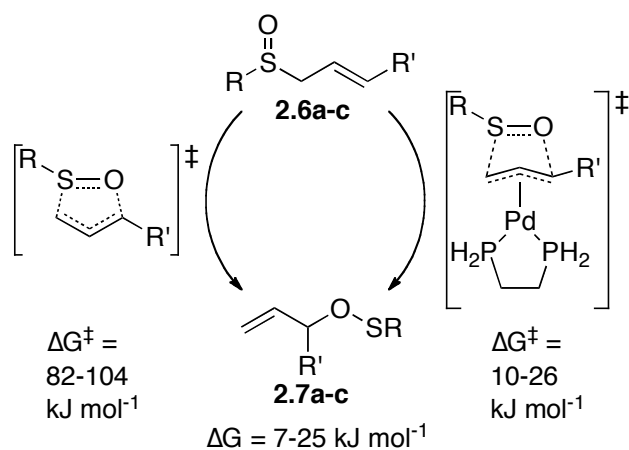


Figure 14. Typical transition state for the Pd-catalyzed MBE rearrangement

The barriers for the rearrangement were found to be only 10-26 kJ mol⁻¹ in the presence of the Pd⁰ DPE complex. Consequently, the rate of the rearrangement can be increased by palladium complexes, something that previously not has been shown, but Pd-catalysis of the similar Overman rearrangement has been demonstrated.^[86] Scheme 15 summarizes the results from the computational study on the MBE rearrangement.



Scheme 15. Uncatalyzed vs. Pd-catalyzed MBE rearrangement

2.3.4 Investigation of the allylic sulfonylation reaction

The method was then employed in the previously described allylic sulfonylation reaction. An NPA analysis^[87] of the sulfonate anion revealed a full negative charge on the oxygen, but the HOMO still has a significant component on the sulfur, therefore we assumed that both S and O could act as competent nucleophiles (Scheme 13). As has been shown before, nucleophilic attack in gas phase on η^3 -allyl Pd complexes is monotonous, without a transition state on the potential energy surface.^[88] Location of TSs therefore required optimization in solvent, and consequently excluded accurate calculation of the vibrational free energy component with our currently available software. However, for *relative* energies of similar competing transition states, the influence of this factor should be negligible.

For the unsubstituted allyl, attacks by S or O were found to be almost isoenergetic, differing only by 1 kJ mol⁻¹. Nevertheless, the product will undergo rapid MBE rearrangement and only the sulfoxide will be isolated (Scheme 13). The energy surface for the reaction is somewhat irregular; the addition TS does not lead directly to the product, but to another, lower saddle point that is also a TS for the MBE rearrangement (Figure 15). It is important to note that care must be taken in search of the TS for the nucleophilic attack, since the automatic search procedures easily can identify the lower energy TS for the rearrangement. The latter TS can also be located *in vacuo*.

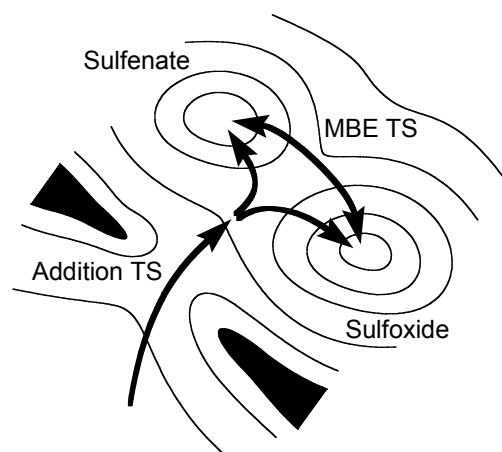
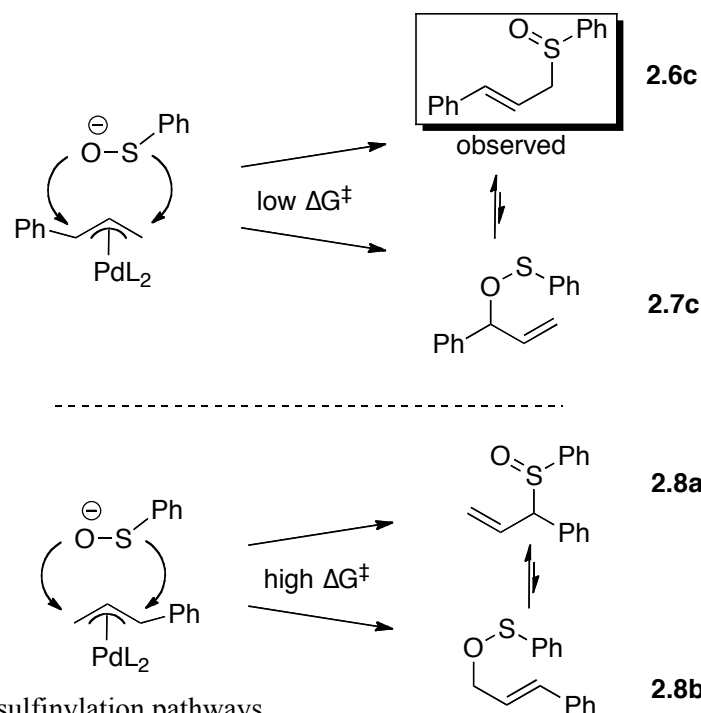


Figure 15. Potential energy surface for the sulfenate attack on (η^3 -allyl)Pd

For the cinnamyl substrate, the reaction is more complex with four different types of attack possible, each with several rotameric vectors. This will lead to two manifolds of rapidly equilibrating products, where only one of the sulfoxides was experimentally observed (Scheme 16). When investigating this reaction, the manifold containing the observed product was indeed found to be lowest in energy. Several different approach vectors were examined, and the one leading to the observed sulfoxide, **2.6c**, was favored, however only by 2 kJ mol⁻¹ in comparison to the oxygen attack in the internal position (**2.7c**). The paths leading to the internal sulfoxide (**2.8a**) or terminal sulfenate (**2.8b**) were at least 12 kJ mol⁻¹ higher in energy. Since the lowest energy paths will lead to the same product, either directly or through a MBE rearrangement, these results were in excellent agreement with the experimental observation for the *p*-tolyl sulfenate. Steric effects and charge distribution can rationalize the results. The cationic charge is most highly concentrated at the benzylic position, the preferred reaction site for the formally anionic oxygen. On the other hand, the formally neutral and larger sulfur atom preferentially attacks the sterically least hindered position.



Scheme 16. Cinnamyl sulfonylation pathways

2.3.5 Conclusions

In conclusion, a viable method for treating the intricate sulfoxide-sulfenate equilibrium has been presented, and showed excellent results for several different rearrangement pairs. Furthermore, the catalytic effect of palladium complexes on the MBE rearrangement has been shown.

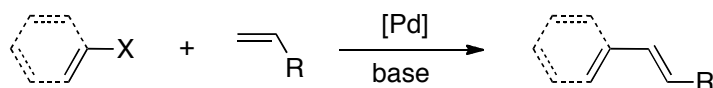
The new method was employed in an investigation of the synthetically interesting allylic sulfonylation, and revealed that there is little difference in reactivity between the two potential nucleophilic sites. The difference in regiochemical preference for these sites, and the rapid, catalyzed equilibrium between the products, ensures that the reaction shows a very strong preference for one of the two possible sulfoxide products.

3. Alkene insertion reactions (Papers III-IV)

There are several different important reactions where an alkene insertion constitutes an important step. One example of this is the Mizoroki-Heck reaction, which since its discovery has proved to be an effective and useful way to generate substituted alkenes.^[12]

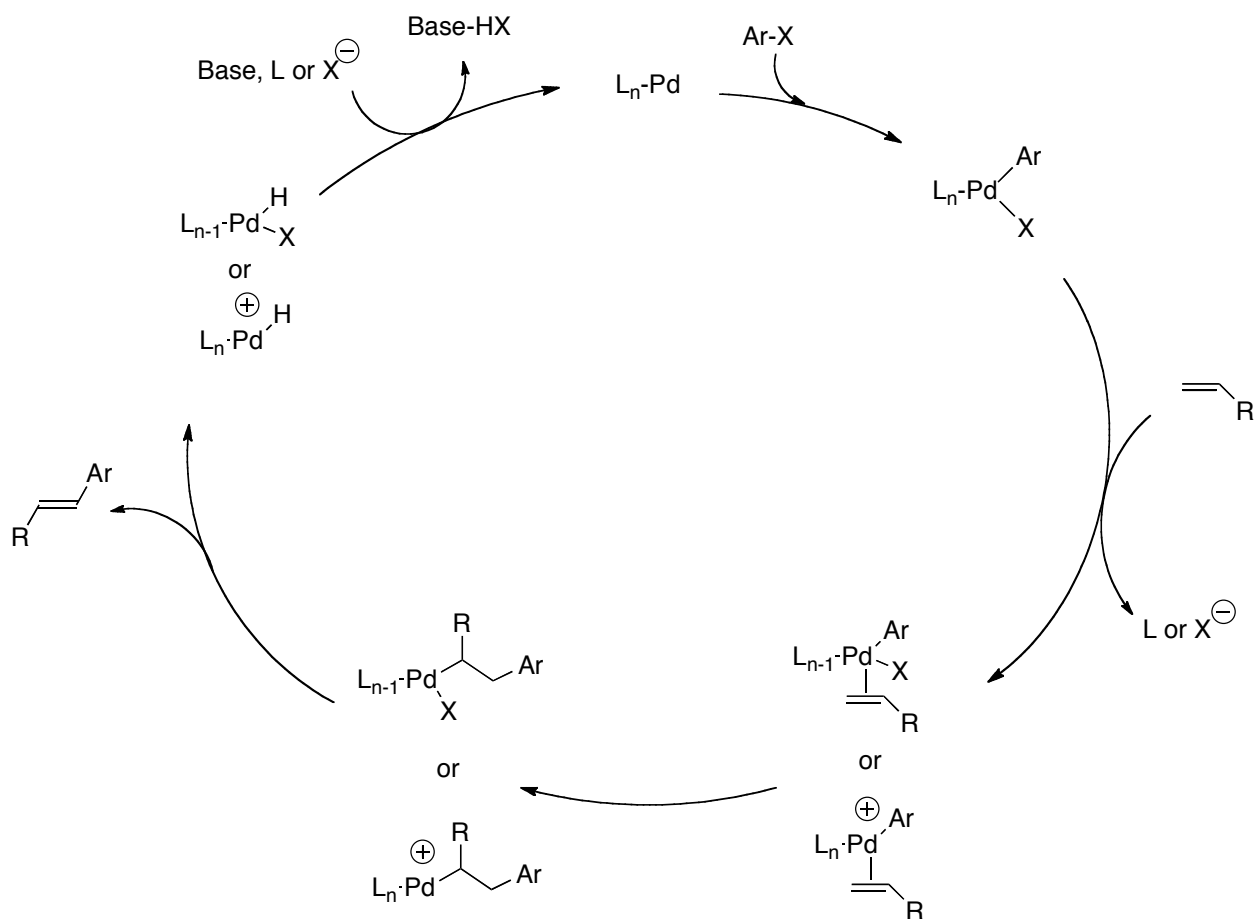
3.1 The Mizoroki-Heck reaction

In the Mizoroki-Heck reaction,^[12] an alkene substrate is coupled to an aryl halide or an equivalent reagent (Scheme 17). During the last decades, continuous research has made the reaction a very convenient and useful way to achieve vinylation or arylation of olefins.^[89]



Scheme 17. The Mizoroki-Heck reaction

The general catalytic cycle is displayed in Scheme 18 (for clarity only the reaction that gives the terminal insertion is displayed). The oxidative addition of the aryl halide (or equivalent reagent) is followed by an alkene coordination and insertion of the aryl into the alkene to form an alkyl intermediate, which through a β -hydride elimination forms the product alkene and a palladium hydride. Through a base-assisted reductive elimination the catalyst is reformed and the catalytic cycle is closed.



Scheme 18. The neutral and cationic catalytic cycle of the Mizoroki-Heck reaction to the terminal product

If the halide in the aryl moiety instead is replaced by a weakly coordinating anion, such as OTf, a cationic catalytic cycle will occur (Scheme 18). In the opposite case, an anionic catalytic cycle can take place if an excess of anions, such as Br^- , is present and replaces the ligand.^[90] The classic Mizoroki-Heck reaction is catalyzed by a Pd^0 species, but in 1975 Pd^{II} was reported as a competent mediator for the reaction.^[91]

Since the oxidative addition and reductive elimination will be scrutinized later in this thesis (see *Section 4.1*), this section will discuss the two steps which separates the Heck reaction from most of the other cross coupling reactions: the alkene insertion and β -hydride elimination steps.

The insertion step of the Heck reaction occurs through a planar or nearly planar complex, where the metal, alkene and aryl/vinyl form a coplanar assembly.^[89b] This feature ensures that the insertion process occurs in a *syn* manner, and is stereospecific, something that was observed experimentally by Heck already in the end of 1960s.^[92] For substituted olefins, the selectivity between the α - and β -insertion is dependent on many different factors. The preferred reaction pathway (neutral or cationic), substitution pattern on the olefin, steric and electronic preferences

of the Pd-ligands, and the solvent are some factors capable of influencing the product distribution.

In general it can be postulated that the electronic properties of the olefin are important for the regioselective outcome. Olefins can be divided into three different groups: electron-rich, neutral, and electron-poor. Electron-poor olefins almost exclusively lead to terminal arylation, which is favored by both electronic and steric effects. The neutral olefins, for example styrenes and aliphatic alkenes, which are governed by steric properties, give rise to predominantly linear products, but can be forced to give branched products by clever selection of reaction conditions.^[89b, 93] For the electron-rich olefins, the important factors, steric and electronic effects, favors different products. The steric hindrance promotes the linear product, but the more electron-rich β -carbon is more prone to bind to the electron-poor Pd(II) moiety resulting in the branched product. This contradiction results in product mixtures. One way to circumvent this problem was the development of the cationic reaction pathway, where the electronic properties are more important and therefore can promote a selective reaction giving the branched product.^[89b, 93]

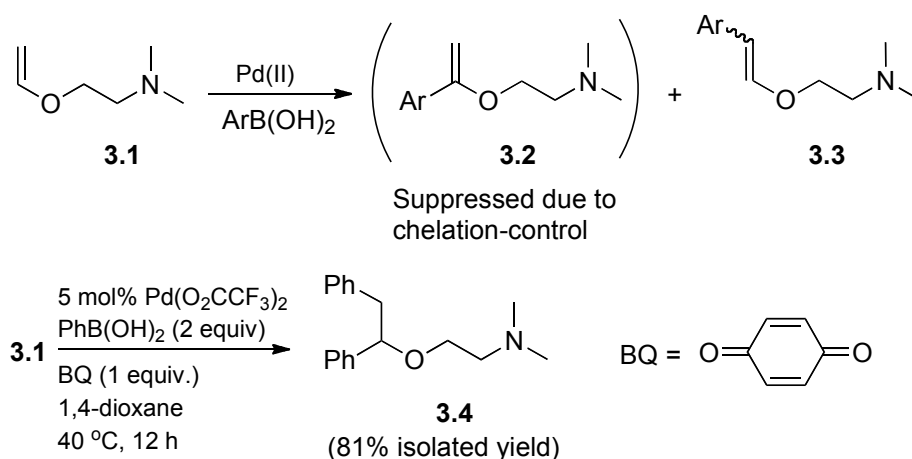
The mechanism of the reverse reaction, the β -hydride elimination, is also stereospecific since it, like the insertion, occurs through a *syn* complex.^[92] It also worth mentioning that since the elimination requires a vacant *cis* coordination site, complexes that are coordinatively saturated give stable metal-alkyl species, and will not easily perform a β -hydride elimination.^[7a]

The palladium(II) catalyzed version of this reaction, often called the *oxidative Heck reaction*, has gathered more attention the last decade, starting with the pioneering work of Uemura and Cho, who presented the first catalytic version of the reaction.^[94] Development of a specific and efficient re-oxidant,^[95] for example the use of molecular oxygen,^[96] has further increased the usefulness of the reaction. The mechanism of the palladium(II) catalyzed oxidative Heck reaction is believed to be analogous to the Pd(0) version. The potential involvement of a Pd(IV) species has been debated but found to be unlikely.^[97] The regioselectivity is also considered to follow the same pattern as the Pd(0) catalyzed reaction, with the insertion step usually being the decisive step.

3.2 Chelation controlled atypical diarylation reaction (Paper III)

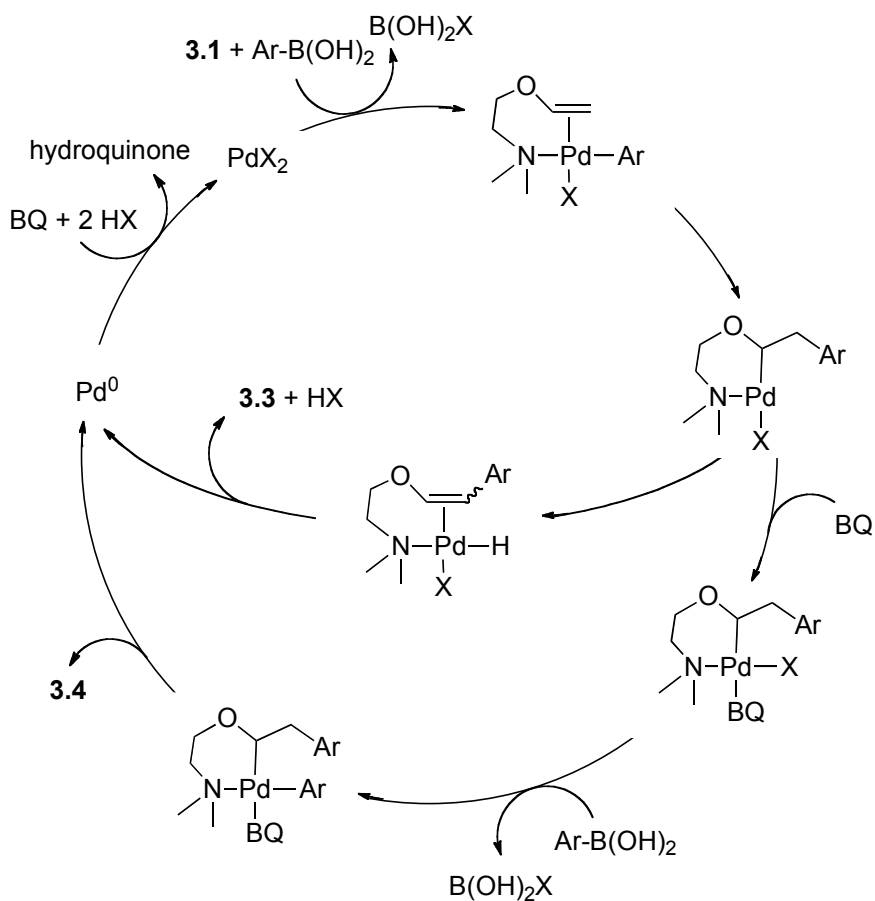
3.2.1 Background

One strategy to control the regio- and stereoselectivity in the Heck reaction is through chelation-control, where the coordination of an auxiliary group creates a pseudointramolecular reaction pathway.^[89b, 98] With the aid of an electron rich nitrogen-containing alkene (**3.1**), Andersson *et al.* could generate a highly regioselective terminal substitution giving **3.3** (Scheme 19).^[98a] Surprisingly, when searching for a Pd(II)-catalyzed protocol for this reaction, the saturated diarylation product **3.4** was isolated (Scheme 19). Optimized conditions for the diarylation reaction, using both electron-rich and electron-deficient aryl boronic acids, have now been established.^[99]



Scheme 19. Conditions for chelation-controlled terminal insertion of the standard Heck reaction (above) and atypical diarylation reaction (below).

The choice of re-oxidant proved to be critical for the formation of the diarylated product as 1,4-benzoquinone (BQ) was the *only* oxidant that resulted in this type of reaction. Mechanistically, the saturated diarylation can be envisioned to proceed via an interception of the σ -alkyl complex by a second transmetalation of the boronic acid, and a subsequent reductive elimination to yield the product. In other words, the second part of the diarylation reaction consists of the final steps in the classic Suzuki-Miyaura reaction (Scheme 20).



Scheme 20. Proposed catalytic cycle of the chelation controlled arylation

A reaction pathway like the one proposed in Scheme 20 would require a preferred pathway for the second transmetalation, outcompeting the β -hydride elimination of the standard oxidative Heck reaction. This phenomenon has been observed earlier when allylic stabilization of the σ -alkyl complex was possible, yielding similar diarylation products of conjugated terminal alkenes and arylstannanes.^[100] However, in the present study, allylic stabilization was not possible, and some other mechanistic motif must be responsible for the repression of the β -hydride elimination. The Heck reaction^[96b, 97d, 101] and the Suzuki-Miyaura reaction^[102] have been the subject of many theoretical investigations that have provided an extensive knowledge about the mechanism of these reactions. In spite of this, no mechanistic insight about the problem at hand was available, and therefore a thorough theoretical examination was needed.

3.2.2 Theoretical investigation of the chelation-controlled diarylation

Due to the complexity of the reaction, the different steps and the free energy state diagram will be presented (Figure 16) and the individual steps will thereafter be thoroughly discussed to provide a complete picture of the reaction. The absence of any additives promoting a cationic pathway and the use of a non-polar solvent (dioxane) ensures that we can focus on the neutral pathway. The

experimentally competent catalyst, Pd(OAc)₂ was chosen as the model catalyst, even if the trifluoroacetate was a more efficient palladium source.^[99] The calculations were performed using the B3LYP functional^[22b, 24a] with the lacvp** basis set, all geometries were optimized in gas phase and the final free energy was found by adding the vibrational contributions and dispersion correction^[26] to the single-point energy with solvation of an optimized gas-phase structure.

The first step of the reaction is the *initial transmetalation*, which generates a Pd(II)-Ph complex **3.6**. Since this complex will be formed regardless of the following reaction steps, the present investigation will focus on the subsequent steps.

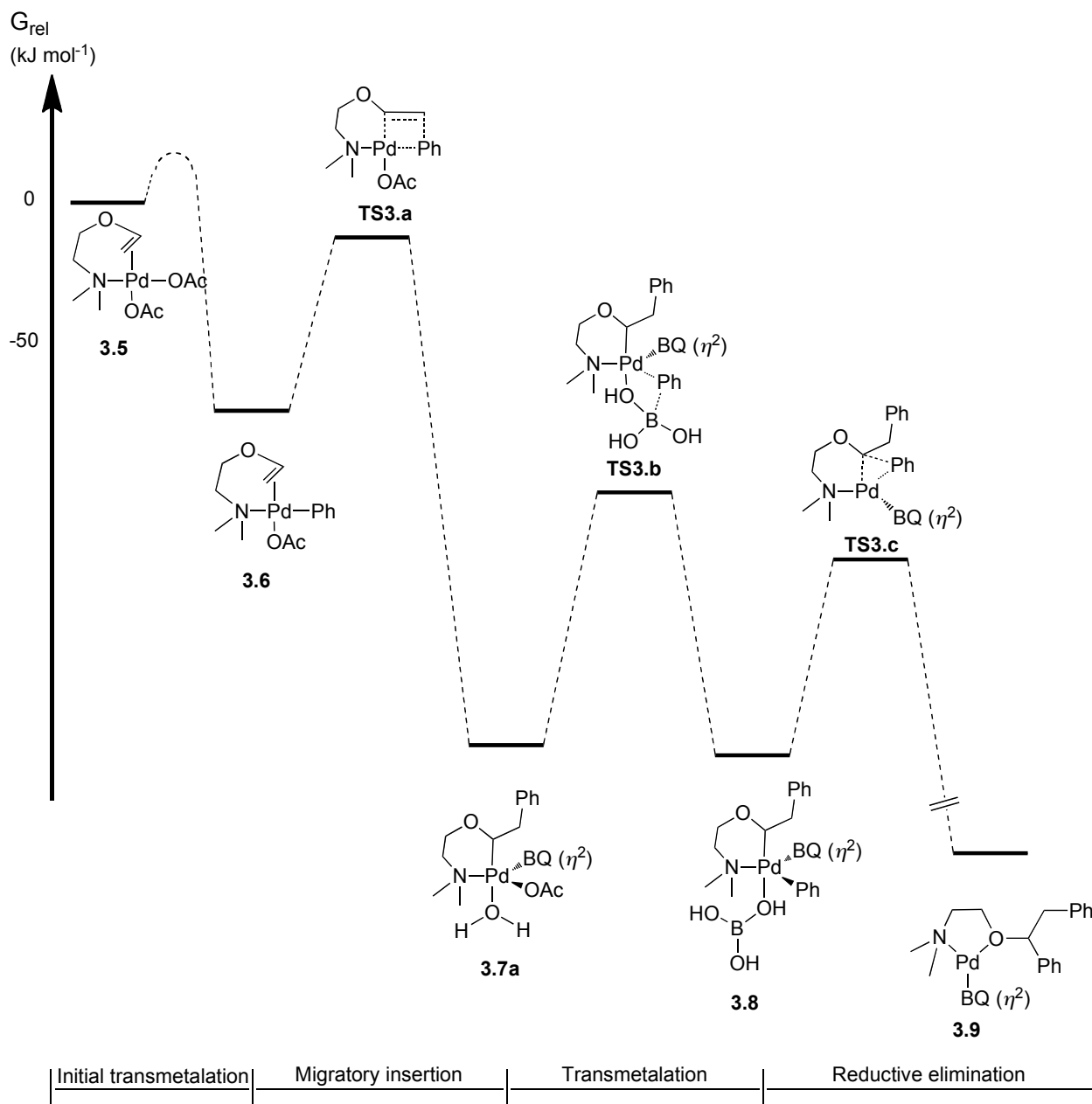


Figure 16. Free energy state diagram of the investigated arylation reaction

The migratory insertion

From complex **3.6** a migratory insertion can lead to either internal or terminal phenylation. Both possibilities were investigated computationally, and the transition state for internal arylation was found to be 25 kJ mol⁻¹ higher in energy compared to the terminal arylation (**TS3.a**) in Figure 16. This result fits the experimental data for the “standard” oxidative Heck reaction, which favors terminal arylation with a selectivity of >50:1,^[99a] and is also in agreement with the outcome of the Pd(II) catalyzed version.^[98a, 103] Consequently, the internal phenylation pathway was not considered for further calculations. Furthermore, a coordination shift of the acetate counterion from monodentate to bidentate after the insertion lowers the energy of the σ -alkyl complex (not shown).

BQ-association

To our surprise, the apparently coordinatively saturated square planar Pd complex formed after the migratory insertion, could gain stability by association with a η^2 -coordination, such as the BQ-ligand (**3.7b**),^[104] giving a new complex with an approximate trigonal bipyramid geometry (Figure 17), which could gain further stabilization by exchange of the acetate moiety with a water molecule (**3.7a**). This discovery was somewhat unexpected, and a natural bond orbital (NBO) analysis^[22a, 105] disclosed a very strong donation-backdonation situation giving a large influence of a metallacyclopropane resonance form with a formal oxidation state of +IV. There are previous examples of the ability of BQ to coordinate to a palladium moiety and influence the rate of a reaction.^[106]

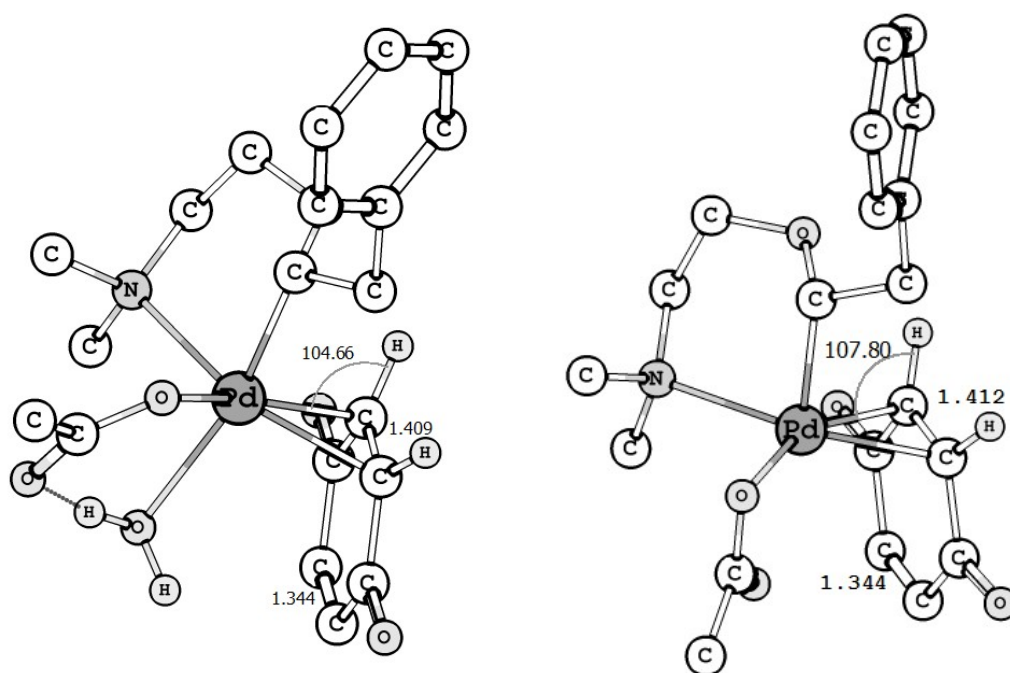
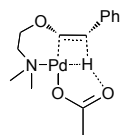
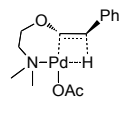
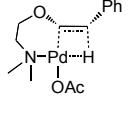
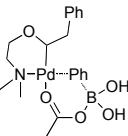
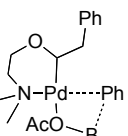
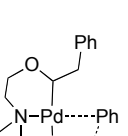
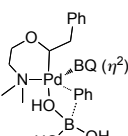


Figure 17. Complex **3.7a** (left) and **3.7b** (right) showing the Pd complexes with the coordinated BQ ligand

Transmetalation vs. β -hydride elimination

The next step in the catalytic cycle is selectivity determining, it is either the β -hydride elimination of the oxidative Heck pathway or the Suzuki-Miyaura transmetalation. Accordingly, two different reaction pathways were investigated (Scheme 20). For the β -hydride elimination, naturally without the BQ-coordination, three different transition states were calculated, forming either (Z)-**3.3** or (E)-**3.3** product. The energies are presented in Table 4. The lowest energy pathway formed (Z)-**3.3** (entry 3), but the difference in energy to the transition state giving (E)-**3.3** (entry 2), was only 1 kJ mol⁻¹. This is in agreement with the poor stereoselectivity observed when the oxidative Heck reaction is carried out.^[99a]

Table 4. Free energy barriers for the investigated β -hydride elimination and transmetalation TSs

Entry	TS	Complex	ΔG (kJ mol ⁻¹)
1	TS3.c β -hydride elim.		121
2	TS3.d β -hydride elim.		116
3	TS3.e β -hydride elim.		115
4	TS3.f Transmetal.		111
5	TS3.g Transmetal.		118
6	TS3.h Transmetal.		105
7	TS3.b Transmetal.		85

For the competing transmetalation several pathways were envisioned, in this investigation both pathways using the associated acetate to activate the boronic acid, as well as pathways including hydroxy complexes have been considered. For some processes, such as the counterion exchange, the association of boronic acid and the following dihedral rotation have not been calculated, since there are numerous pathways possible, and it is improbable that any of the barriers for these processes is higher than the competing β -hydride elimination barrier. Several recent reports have discussed these steps, and none of them have found a high-energy barrier.^[107] Therefore, it is reasonable to assume that the TS for the transmetalation is the highest in this part of the reaction (Figure 18).

The different calculated transition states for the transmetalation can be found in Table 4. The transition states without a coordinated BQ (entries 4-6) were first calculated. The TSs containing an associated acetate, both 4- and 6-atom transmetalations, were found to be 6-12 kJ mol⁻¹ higher in energy than the one utilizing PhB(OH)₃⁻ as the transmetalating agent (entry 6). Interestingly, the barrier for transmetalation is lower than the barrier for the β -hydride elimination by 10 kJ mol⁻¹. On the other hand, these values are calculated for the conditions leading to the diarylated product **3.4**, and not the oxidative Heck product **3.3**. Accordingly, changing the solvent model to DMF, which was employed in the oxidative Heck reaction,^[99a] resulted in a switch to preference for the β -hydride elimination pathway by 17 kJ mol⁻¹. In other words, **TS3.e** was lower in energy than **TS3.h** when BQ was absent and with DMF as solvent. Figure 18 shows the complete free energy surface for the two competing reactions, the transmetalation and the β -hydride elimination.

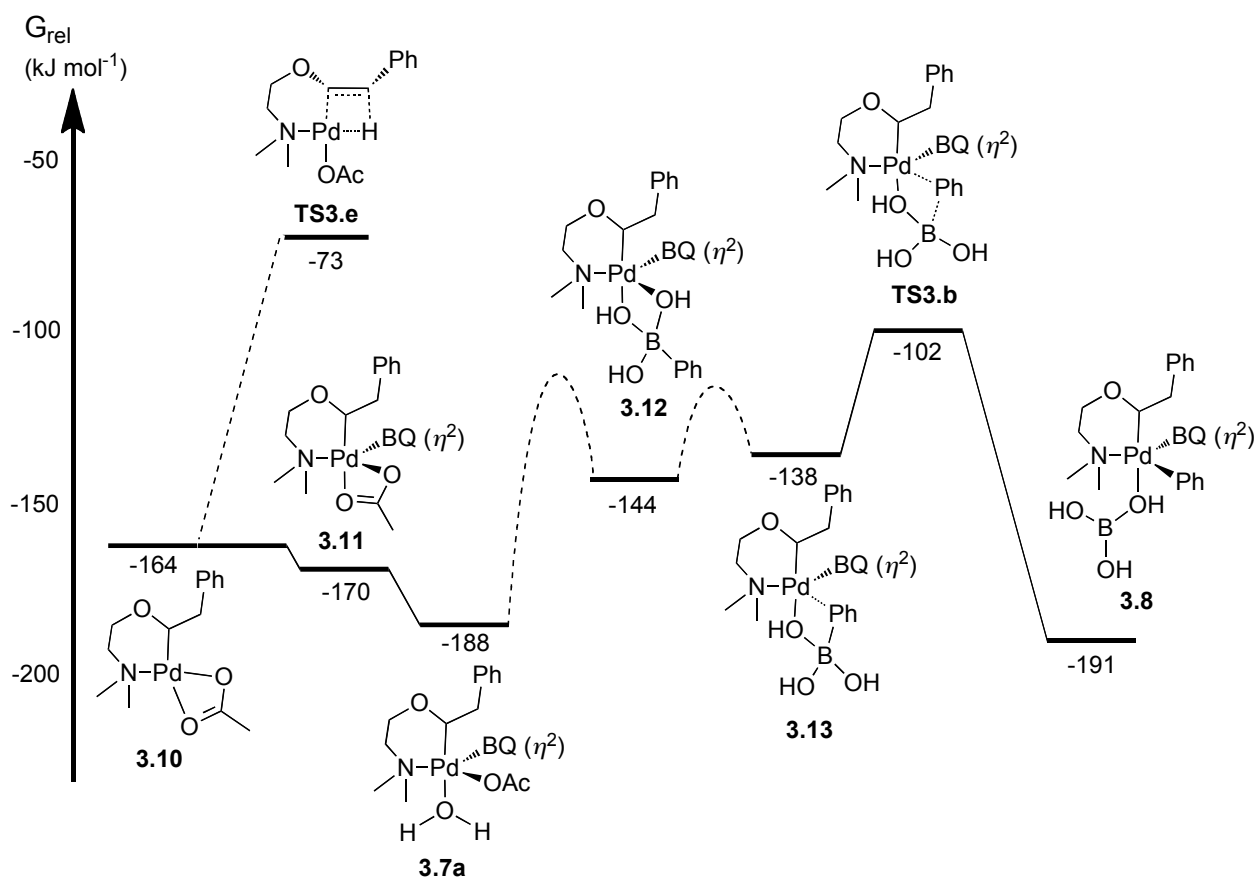


Figure 18. Transmetalation vs. β -hydride elimination

The inclusion of BQ in the transmetalation step resulted in a calculated barrier that was 20 kJ mol⁻¹ lower, suggesting that BQ indeed aids in this step. Due to the above mentioned donation of electrons to the electron-poor BQ in the σ -alkyl complexes, the electrophilicity of the Pd(II) moiety is increased. This should promote the transmetalation and lead to the diarylated product, in agreement with the experimental results.^[99a]

The investigated complexes are sterically encumbered and the inclusion of correction for dispersion had a profound effect on the free energies.^[26] This correction resulted in selective lowering of the activation barriers where BQ was coordinated to the palladium moiety. Without this correction, the β -hydride elimination would in fact have been identified as the favored pathway under all conditions.

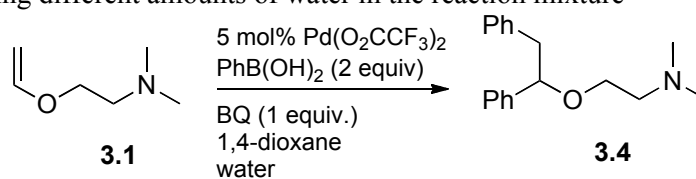
As mentioned before, the conditions for the standard oxidative Heck and the investigated diarylation reaction differ in the solvent of choice. Therefore, parameters suitable for DMF in the solvent model were employed on **TS3.b** and **TS3.e** and resulted in a favored β -hydride elimination (**TS3.e**) by 13 kJ mol⁻¹. This implies that the use of DMF severely diminishes the production of **3.4** compared to **3.3**, regardless of BQ in the mixture, something that is in agreement with the previous experimental results,^[99] even if the effect is slightly overestimated.

Due to the importance of inclusion of dispersion effects, calculations employing the M06 functional were also performed. The energy difference between the two competing transition states, **TS3.b** and **TS3.e**, was found to be reduced from 30 kJ mol⁻¹ to 14 kJ mol⁻¹. Furthermore, the relative energy between complexes **3.10** and **3.7a** (Figure 18) was lowered to only 2 kJ mol⁻¹ with M06. Nonetheless, we can deduce that M06 also identifies the transmetalation as the preferred reaction pathway over the β -hydride elimination.

Water dependence

As shown in Table 4, the complex with the lowest barrier contained a PhB(OH)₃⁻ unit, which only can be formed if water is present in the reaction mixture. The previous protocols did not contain water,^[99] but the solvents and reagents used probably contained small amounts of water. To explore the water effect an experiment was initialized where various controlled amounts of water was added to the reaction mixture. Eight different concentrations of water, starting from anhydrous conditions, were investigated (Table 5).[†]

Table 5. Yield of **3.4** using different amounts of water in the reaction mixture



Entry	Amount water (eq.)	Yield ^a (%)
1	0	3
2	0.01	12
3	0.1	30
4	1	60
5	5	38
6	10	41
7	30	28
8	100	24

^a By ¹H-NMR of the crude product

[†] Water experiments conducted by Alejandro Trejos

The results from the water experiments conclude that water is instrumental for the reaction to work, since the anhydrous conditions gave almost no product. Increasing the amount of water resulted in an increased amount of product up until the addition of one equivalent of water, whereafter the yield dropped steadily with increased amount of water. The unoptimized conditions of this experiment are probably the reason for the discrepancy between the maximum yield of 60% for this experiment and the previously reported 80%.

Reductive elimination

In the final product-forming step, the reductive elimination, the diarylated product is formed. Several different reductive elimination pathways were investigated. As seen before, the transition states without BQ resulted in much higher barriers than the ones containing a coordinated BQ, with the tetra-coordinated BQ-containing complex having the smallest barrier of 72 kJ mol⁻¹ (Figure 19). In this step, the positive effect of BQ as ligand was not a complete surprise, since a similar effect from electron-poor olefins as ligands to promote reductive eliminations has been investigated previously.^[108]

In addition, a possible pathway to the oxidative Heck product **3.3** via β -hydride elimination from **3.8** was investigated. The barrier for this transformation was calculated to be 112 kJ mol⁻¹, well above the competing reductive elimination. In summary, the inclusion of BQ ensures that the reductive elimination pathway to diarylated product is followed through lowering of the barrier for this transformation. Exclusion of BQ would lead to the oxidative Heck product through β -hydride elimination, since the barrier for the reductive elimination would increase above the barrier of the β -hydride elimination.

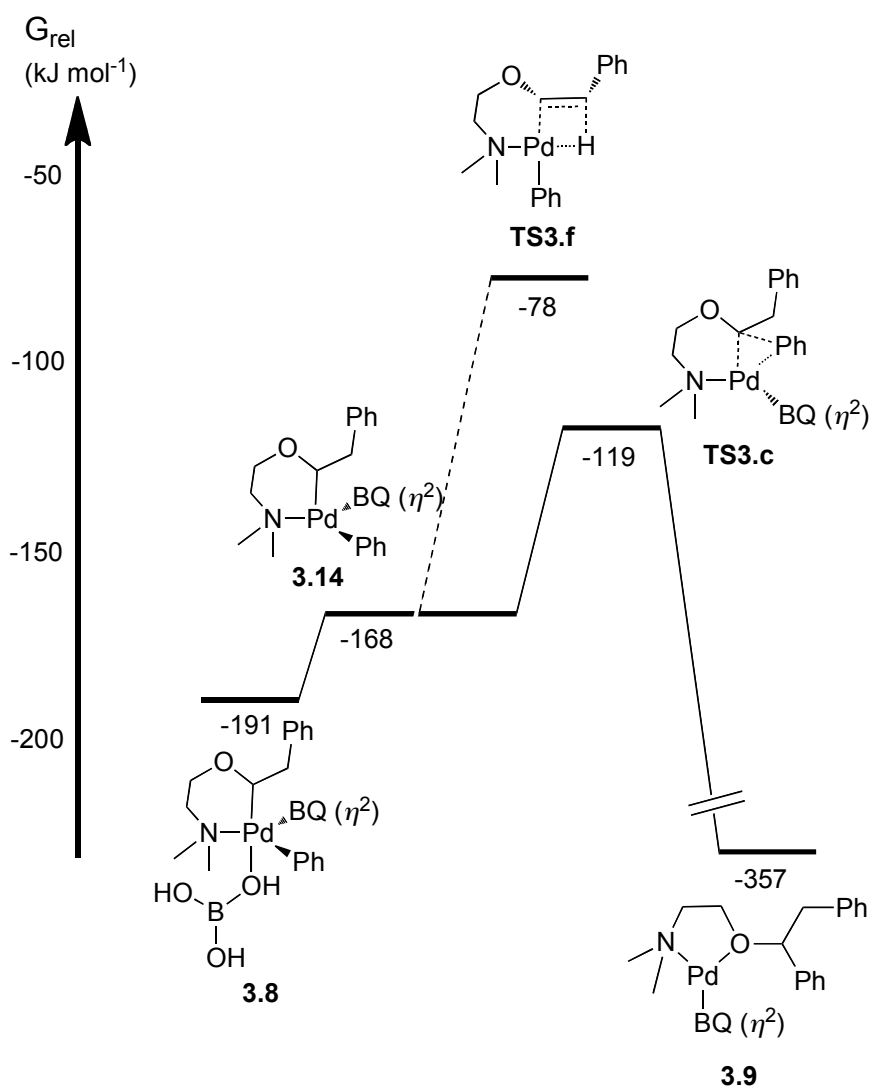


Figure 19. Free energy profile of the lowest found pathway for red. elim. versus β -hydride elimination

The reductive elimination leading to product is highly exergonic, forming the low-energy complex **3.9** (Figure 20). This is a formal Pd(0) complex, coordinated to the product in a bidentate fashion, utilizing both the nitrogen and oxygen to form dative bonds, and to BQ via one of its alkene bonds. The square planar geometry, usually favored by Pd(II) complexes, is due to the π -accepting ability of BQ. A similar complex, reported by Milani *et al.*, with a formal Pd(0) coordinating 2,2'-bipyridine as a bidentate ligand, also adopts a square planar geometry.^[109]

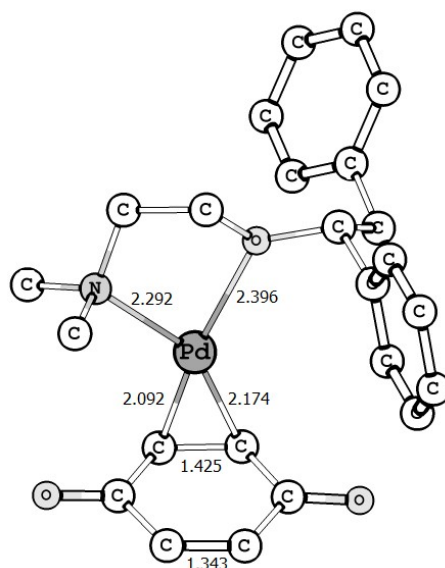
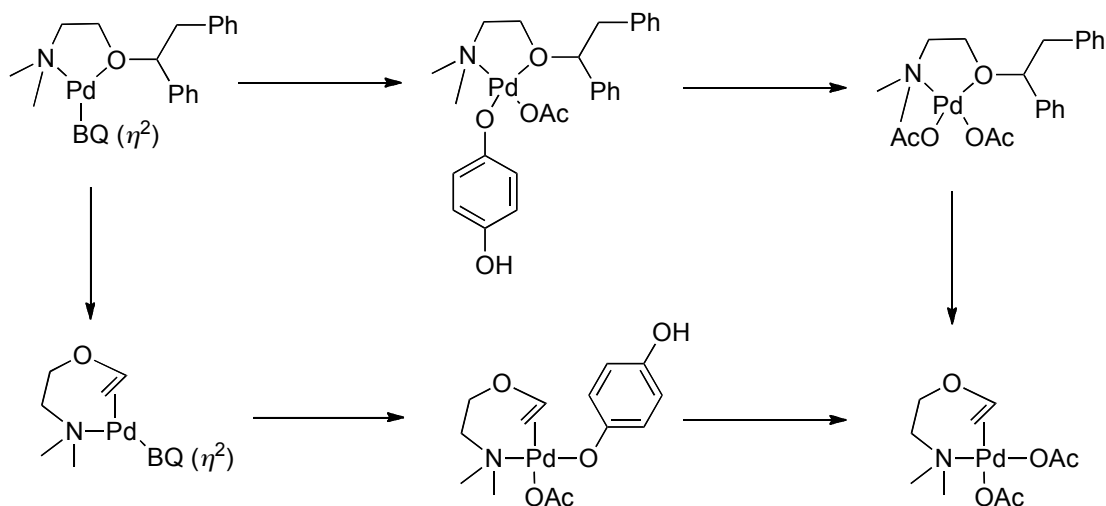


Figure 20. The low-energy complex **3.9** formed after β -hydride elimination, most hydrogens are omitted for clarity

The final steps to close the catalytic cycle is the release of the product, **3.4**, and oxidation of the palladium complex to the starting Pd(II) complex. The transition states for these steps have not been calculated, but two potential pathways are depicted in Scheme 21. The pathway with product-coordinated complexes has lower-energy intermediates, but since the transition states are not calculated, both pathways must be considered viable.



Scheme 21. Two potential pathways of catalyst oxidation to starting point complex **3.5**

3.2.3 Conclusions

In summary, DFT calculations have been used to investigate a reaction that forms a saturated diarylated product in a combination of both a Mizoroki-Heck and a Suzuki reaction. The calculated reaction pathway satisfactorily agrees with the experimental results, and also explains the vital role of BQ in the reaction. Apart from its role as re-oxidant, BQ is also acting as a ligand to the Pd complex and this way opens up a new low-energy pathway to the diarylated product. The BQ-induced lowering of the barriers for both the second transmetalation and the subsequent reductive elimination ensures that the experimental results can be reproduced in this computational study. The crucial second transmetalation is favored over the competing β -hydride elimination by 30 kJ mol⁻¹. The highest free energy barrier is the 86 kJ mol⁻¹ for the second transmetalation, but it is difficult to conclude that this is the rate-determining step since the other steps have similar barriers. Both the migratory insertion and the reductive elimination can be considered to be effectively irreversible, as no subsequent step is close in transition state energy. This is probably also true for the second transmetalation, but the difference with respect to the reductive elimination is small, and the conclusion is therefore less certain. The inclusion of dispersion correlation was imperative for achieving good agreement with experimental data.

3.3 Nickel catalyzed Mizoroki-Heck reaction (Paper IV)

3.3.1 Background

The Mizoroki-Heck reaction, with its amazing functional group tolerance and easy access to enantioselectivity, is sometimes considered to be the most powerful of the cross coupling reactions.^[7a, 89a, 110] During the last decades, the cost and toxicity of the premier catalyst, palladium, has prompted many efforts to replace this noble metal with a less expensive alternative, such as the fellow transition metal nickel.^[111]

Nickel catalysis has several advantages, such as sustainability and the relatively low price of the nickel precursors, which makes it attractive for transition metal catalysis. A wide variety of processes have proven to be nickel catalyzed, including such diverse reactions as cycloadditions^[112] and multicomponent couplings.^[113] However, in this thesis the focus will be on the cross coupling reactions,^[111] which constitute a very important part of the cross coupling family, especially since the nickel catalysts can accommodate a wide range of electrophiles. Not only the classic aryl and vinyl halides, as well as sulfonates, but diverse functional groups, such as ethers, metal alkoxides, carboxylates and carbamates have been efficient coupling partners employed in cross coupling reactions.^[114] This is a resourceful way to achieve orthogonal functionalization of various aromatic systems, where several functional groups can offer multiple reactive sites.

The versatility of nickel in cross coupling reactions has further been shown by the ability to create both C(sp³) - C(sp³) and C(sp³) - C(sp²) bonds through coupling reactions.^[115] Also enantioselective versions of this reaction have been presented.^[116]

In spite of all this, there has been a considerable lack of nickel catalyzed version of the Heck reaction in the literature, something that could be accounted either to the inherent reluctance of nickel towards performing a β -hydride elimination, a transformation vital to the Mizoroki-Heck reaction, or to the strong Ni-H bond, which has a larger bond energy than the similar Pd-H bond.^[117] To overcome this problematic reaction step, the reported nickel catalyzed Mizoroki-Heck reactions have been hampered by harsh conditions, such as high temperatures, highly polar solvents, long reaction times and metal additives, in order to progress.^[118] In order to achieve a milder version of the nickel catalyzed Mizoroki-Heck reaction, a way to facilitate both the β -hydride elimination and the proton abstraction must be uncovered.

Previous studies on the nickel catalyzed vinylation of allylic ethers and carbonates have suggested that a cationic nickel(II) complex, formed via the addition of triethylsilyl

trifluoromethanesulfonate (TESOTf), could accomplish a β -hydride elimination.^[119] Triflates have been used earlier in the palladium catalyzed Mizoroki-Heck reactions,^[120] as well as in nickel catalyzed benzylation of olefins,^[121] even if the cationic palladium(II) intermediate has been difficult to form, something that has been solved through the addition of ionic liquids or halide scavengers.^[122] Since the cationic pathway seems to work for other types of nickel catalyzed transformations, it might be possible to extend this to the cross coupling reaction as well.

3.3.2 Experimental results[†]

In the light of the above-mentioned reports, the nickel catalyzed Mizoroki-Heck reaction was envisioned to proceed with the aid of Ni(COD)₂, a bidentate phosphine ligand and a tertiary amine base, catalyzing the reaction between aryl triflates and butyl vinyl ether. The initial catalyst and base screenings revealed that the reaction was possible and Scheme 22 shows the optimized conditions for the test reaction between 4-biphenyl triflate (**3.15**) and butyl vinyl ether (**3.16**) yielding the acetophenone (**3.17**) after hydrolysis with HCl/H₂O.



Scheme 22. Optimized conditions for the nickel catalyzed Heck reaction between aryl triflates and butyl vinyl ether

The successful results prompted further investigation and a study of the triflate scope was initialized. A range of different aryl triflates proved to be competent coupling partners with good to excellent yields, giving the aryl methyl ketone. Both electron withdrawing and donating groups were viable in the reaction, as well as different functional groups, such as esters, amides, cyano, diazo, and trifluoromethyl groups. Electron donating groups in *para* position or *ortho* substituents lowered the yield to some degree, but the high yields could be restored by a slight increase in catalytic loading.

The role of the leaving group was investigated by switching to arylsulfonates instead of triflates. Unfortunately, the reaction did not demonstrate the same good results with sulfonates. In most cases mixtures of regioisomers were observed when isolating the products, and for the nitro

[†] Study performed by Thomas Gøgsig

containing leaving groups the catalytic ability was greatly reduced, probably because of the chelating effects of the nitro moiety. The only exception from the negative results was the pentafluoro-containing sulfonate, which showed yields in the same region as the triflates, and only produced one regioisomer.

Halide additives, such as LiCl and TBAB, completely inhibited the reaction, most likely because of strong coordination to the Ni(II) complex, and thereby encumbering the cationic pathway.

A range of different olefins was tested in the reaction with 4-biphenyl triflate. Steric hindrance significantly lowered the yield and essentially no reaction was achieved when employing *N*-vinyl acetamide, *N*-vinyl 2-pyrrolidine or vinyl acetate. The lack of reactivity for the latter can potentially be explained with a coordination of the carbonyl group to the nickel complex, most probably after the insertion step, where the cationic Ni(II) complex would be stabilized by such an interaction, leading to an unwillingness to perform the following β -hydride elimination.

Finally, a competition experiment was initialized. A 1:1 mixture of butyl vinyl ether and *N*-vinyl acetamide was added to a solution of 4-biphenyl triflate, DPPF, Cy₂NMe and nickel catalyst. Only traces of the two possible alkene products were detected, further strengthening the hypothesis that the carbonyl containing substrates can coordinate to the nickel complex and inhibit the catalyst.

In summary, the experimental results indicated that a cationic nickel intermediate was responsible for the catalytic activity. To further explore this pathway, theoretical studies were needed.

3.3.3 DFT study of the nickel catalyzed Heck reaction

The aim of the DFT study was to examine the catalytic cycle, and especially to investigate the role of cationic nickel intermediates. The model system for the computational study was the catalytically active Ni(dppp) complex with the substrates phenyl triflate and ethyl vinyl ether. The experimentally viable THF was chosen as the solvent for the study. The initial state of the reaction was opted to be the pre-complex of the oxidative addition where the phenyl triflate is coordinated to the nickel complex via the phenyl ring (complex **3.18**).

The first step of the catalytic cycle is the oxidative addition of phenyl triflate to yield the Ni(II) complex **3.19** (Figure 21). This reaction proved to be highly exergonic, -131 kJ mol^{-1} , with a low barrier of only 15 kJ mol^{-1} (**TS3.g**). The following exchange of the labile OTf anion with the substrate vinyl can be expected to be a facile process; particularly since the OTf anion is known to be a weakly coordinating species.^[123] The resulting cationic complex **3.20** is somewhat more stable than the neutral precursor.

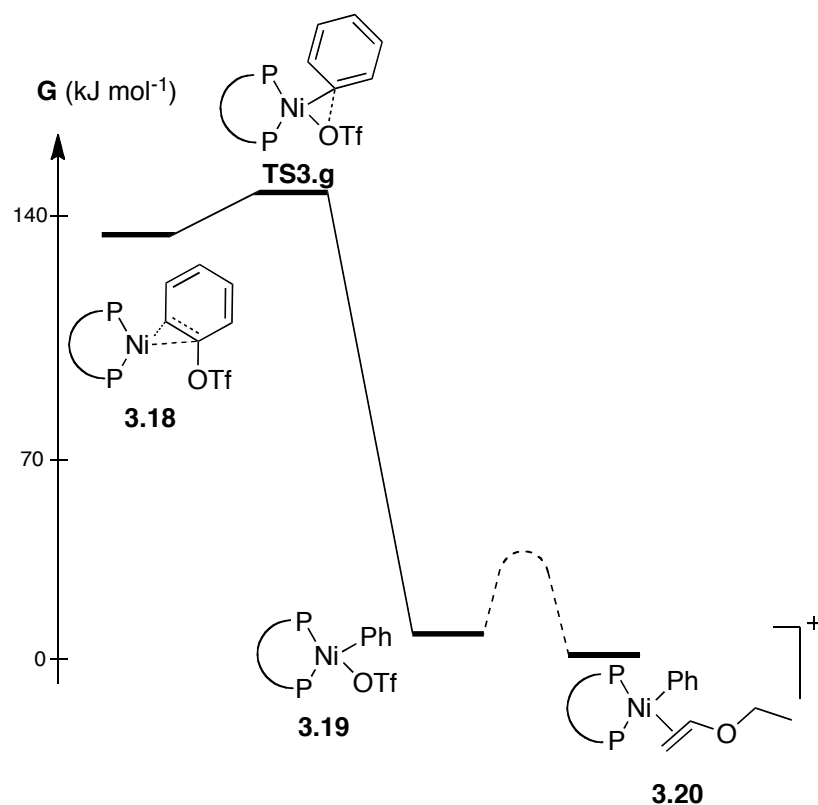


Figure 21. The oxidative addition and the subsequent ligand exchange

In the subsequent step, the vinyl ether is inserted into the phenyl-Pd bond. Two pathways are possible, internal and terminal insertion, giving two different products. Experimentally, the only observed product was from the internal insertion (Scheme 22). To encompass as large part of the conformational space as possible, 20 and 15 transition state structures for internal and terminal insertion were inspected, respectively. The final free energy difference between the best transition state for internal (**TS3.h**) and terminal insertion (**TS3.i**) was found to be 20 kJ mol⁻¹ in favor of the internal attack (Figure 22). This corresponds to less than 1% of the internal product, which mirrors the experimental results.

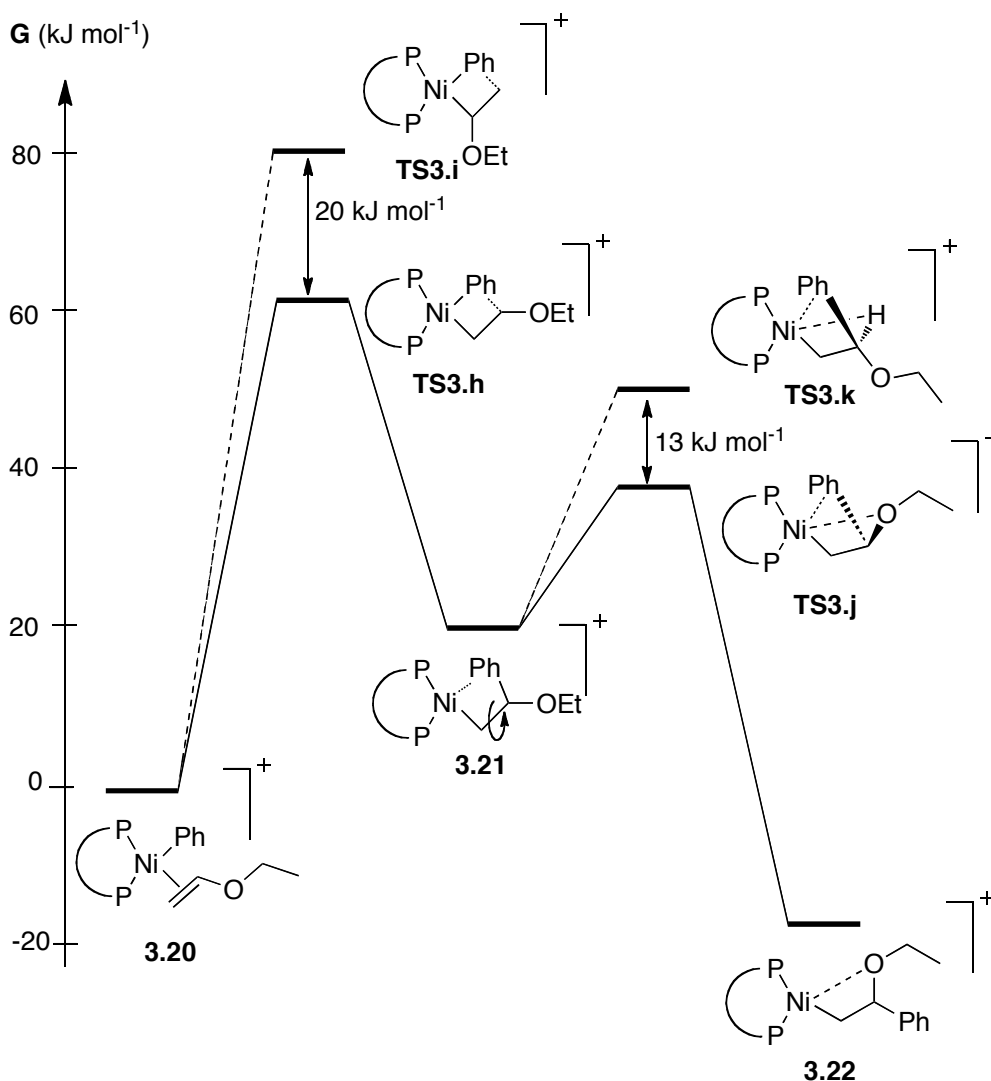


Figure 22. The selectivity for the insertion step, and the subsequent torsional rotation to the more stable O-coordinated complex

The post insertion complex **3.21** has a Ni-phenyl π -interaction, and can, through a torsional rotation about the former alkene C-C bond, form either an agostic complex (through **TS3.k**) or the oxygen coordinated complex **3.22** (via **TS3.j**). The barrier for the latter is 13 kJ mol^{-1} lower in energy, giving complex **3.22** that is 37 kJ mol^{-1} lower in energy than the preceding complex **3.21**. In order to be able to perform a β -hydride elimination, another torsional rotation must take place, to form the agostic complex **3.23**, via **3T3.I** (Figure 23). The barrier for this rotation is fairly large, 68 kJ mol^{-1} , and is followed by the β -hydride elimination (**TS3.m**) with a smaller barrier of only 22 kJ mol^{-1} . The importance of torsional rotations in similar reactions has been observed before, and even been found to be the selectivity-determining step.^[101s]

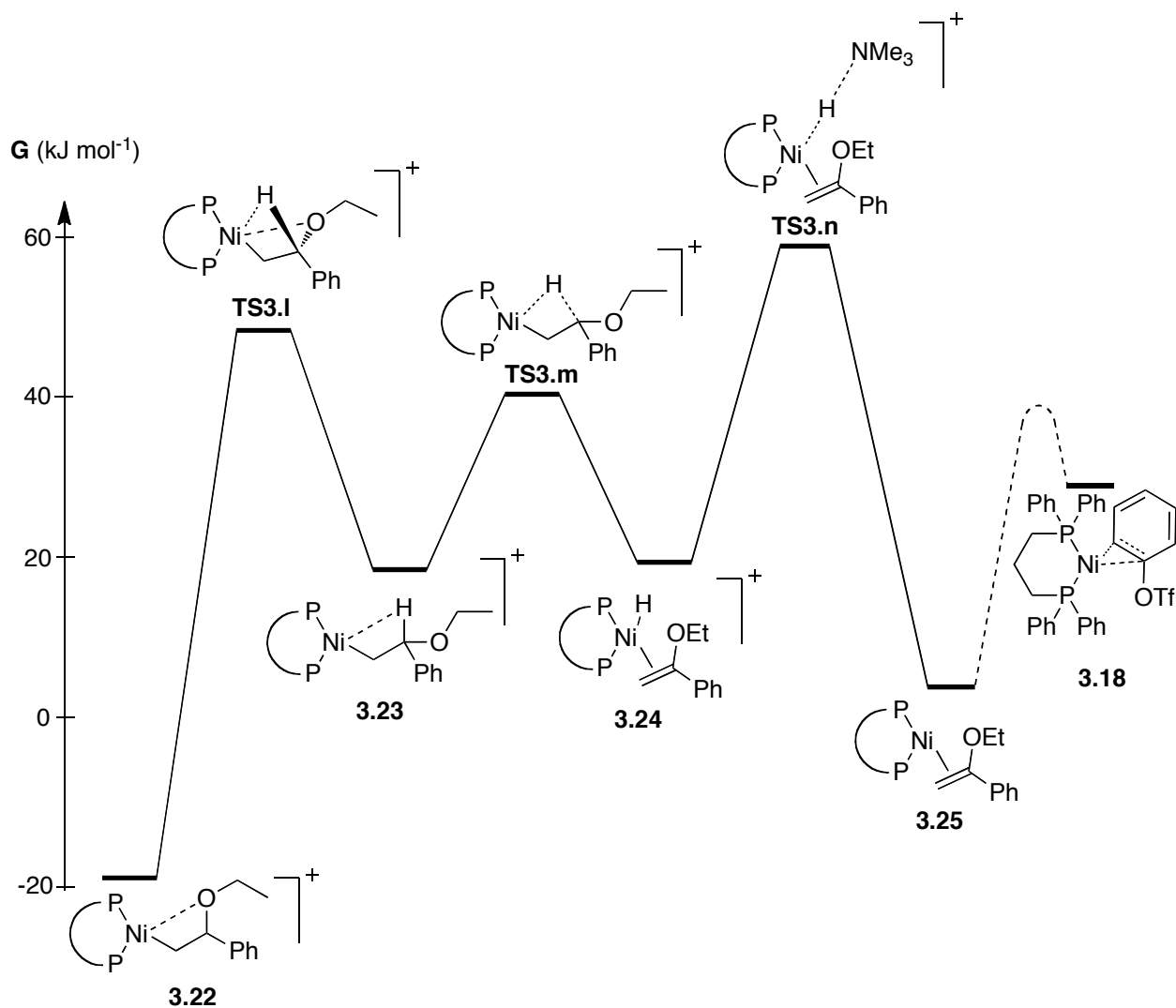


Figure 23. The elimination and proton abstraction steps to give product and complex **3.18**

The resulting Ni-hydride, **3.24**, coordinated to the product alkene, is subjected to a proton abstraction by an amine base, modeled by the computationally simpler NMe₃ instead of the experimentally favored Cy₂NMe. The barrier for this reaction was found to be 47 kJ mol⁻¹ (Figure 23). Several other possible base-assisted proton abstractions were examined, for example without the coordinated alkene or a reductive elimination from a Ni-complex with a coordinated base, but none was found to be more effective than via **TS3.n**, depicted in Figure 23. The last transformation in the catalytic cycle is a ligand exchange to give complex **3.18**, from complex **3.25**. This reaction is slightly endergonic, 30 kJ mol⁻¹, and regenerates the starting structure for the catalytic cycle.

The free energy state diagram of two catalytic cycles of the reaction is shown in Figure 24. As can be seen in the figure, the final two steps of each catalytic cycle, the β -hydride elimination and the proton abstraction, going from complex **3.22** to complex **3.18**, are slightly endergonic.

Nevertheless, the subsequent catalytic cycle will ensure a total lowering in energy due to the strongly exergonic first step, the oxidative addition.

There are two transition states in this reaction that can be considered *effectively irreversible*, that is, transition states that are higher than any subsequent points on the free energy surface, in this catalytic cycle. These are **TS3.g** and **TS3.n**, and this would imply that the insertion step would be a reversible step, but it is important to note that even if this is true, the competing pathway to terminal insertion is still energetically inaccessible, since **TS3.n** is lower than **TS3.i**.

In total, the resting state can be identified as complex **3.22** and the total barrier is 87 kJ mol^{-1} , which is satisfactorily compatible with the experimental conditions. These results are also in good agreement with a previous study that also identified the catalyst regeneration as the rate-determining step.^[117]

G (kJ mol^{-1})

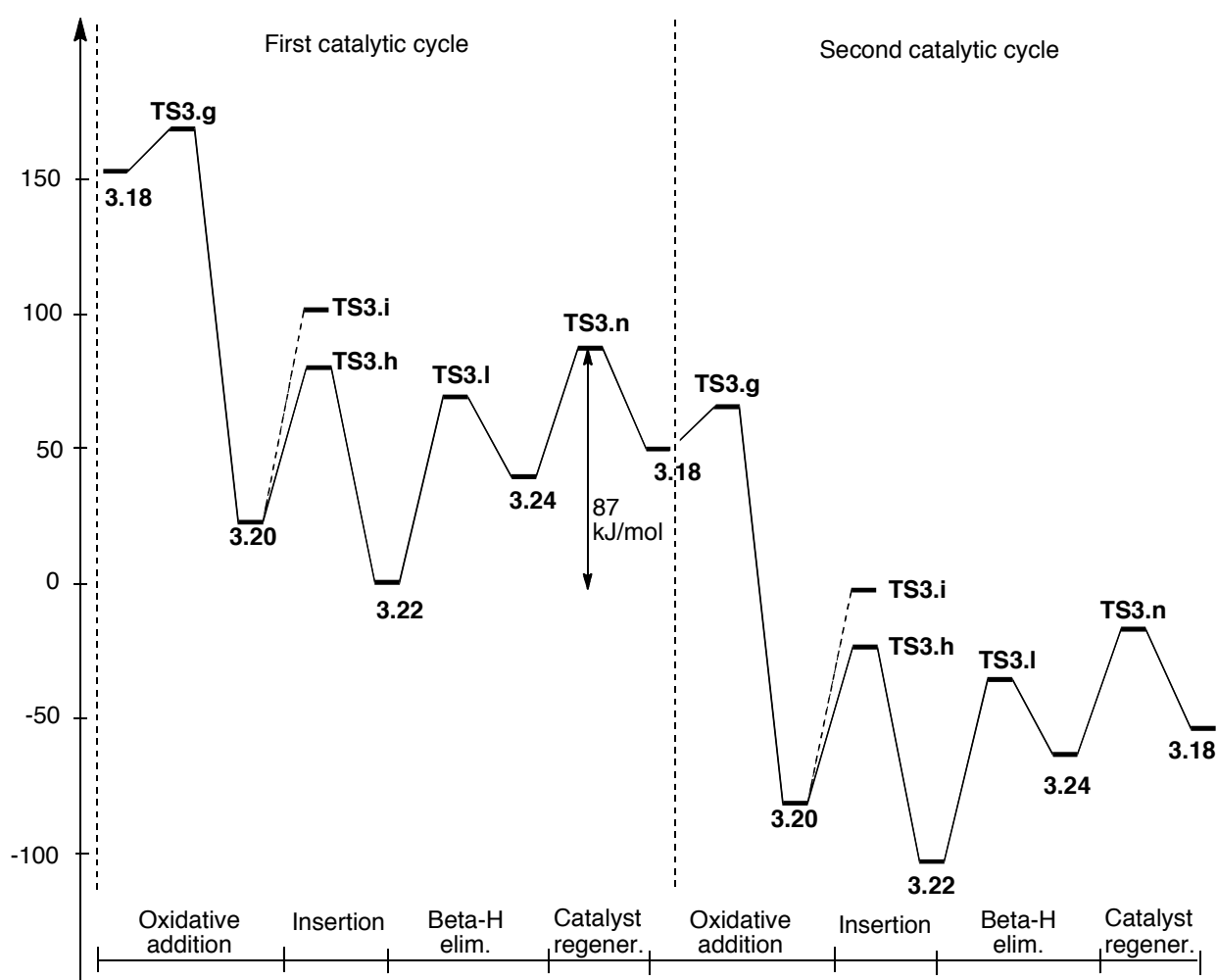
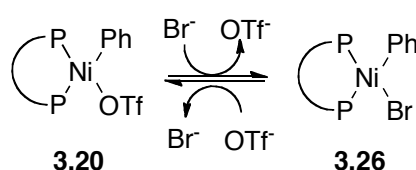


Figure 24. Free energy state diagram showing two catalytic cycles in sequence

The two lowest points on the free energy surface, complex **3.20** and **3.22**, are likely points for inhibition of the reaction. Since several conditions have proven to induce non-reactivity for the

present reaction conditions, such as certain olefins or halide additives, we decided to examine this further.

Complex **3.20**, the Ni(II) species after oxidative addition, is sensitive to stabilization by, for example other more coordinating anions. Since halides had proven to inhibit the reaction it is easy to envision the halide anion coordinating to this complex and stabilizing it enough to prevent further reaction. To investigate this, an analogous version of complex **3.20**, with a Br anion instead of an OTf anion was constructed and the energy for this (complex **3.26**) was calculated (Scheme 23). Indeed, it was found that complex **3.26** was 69 kJ mol^{-1} lower in energy, strengthening the hypothesis that halide anions can lead to the formation of stable Ni(II) species that cannot react further.



Scheme 23. Potential bromide stabilization of complex **3.20**.

For the post-insertion complex **3.22**, the inhibition of the reaction when adding N-vinyl acetamide to the reaction mixture was examined (Figure 25). The additional chelating ability by the carbonyl oxygen of the acetamide was considered the reason for the lack of reactivity, especially since the similar substrate vinyl acetate did not react either. The post-insertion complex of vinyl acetamide was envisioned as analogous to complex **3.22** and is depicted in Figure 25, with a stable six-membered ring formed via the covalent bond and the coordination of the carbonyl oxygen (complex **3.27**) to nickel.

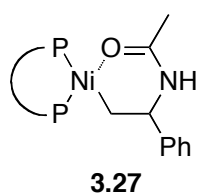


Figure 25. Stable Ni-complex **3.27** after insertion to the vinyl acetamide substrate.

From complex **3.27** the transition state of the subsequent β -hydride elimination was located and the free energy barrier of this transformation was found to be 94 kJ mol^{-1} , a barrier sufficiently large to inhibit this reaction pathway, and therefore making the reaction ineffective for this class of substrates. This reasoning is further strengthened by the results from the base optimization, where the strongly coordinating bases, DBU and pyridine, give almost no reactivity. On the other hand, the sterically encumbered bases, which do not coordinate as well, such as DIPEA, Et_3N and Cy_2NMe , give good conversions.

3.3.4 Conclusions

In summary, a new efficient protocol for the nickel catalyzed Heck reaction of aryl triflates with vinyl ethers has been presented. New and mild reaction conditions, corresponding to the palladium catalyzed Heck reaction, are applied, giving a practical and sustainable alternative to the classic regioselective arylation of vinyl ethers. The catalytic system consisting of Ni(COD)₂, DPPF, and the amine base Cy₂NMe, proved to work effectively, coupling both electron deficient and electron rich arenes, yielding the corresponding aryl methyl ketone after hydrolysis in very good yields with good functional group tolerance.

Mechanistic studies, primarily DFT calculations, revealed the cationic nickel pathway as a viable path for the catalytic cycle. The extremely exergonic oxidative addition of phenyl triflate was followed by an insertion where the internal product was found to be favored, in agreement with the experimental results. The subsequent β -hydride elimination and catalyst regeneration are slightly endergonic but the overall energy of the catalytic cycle is ensured by the oxidative addition in the following catalytic cycle.

The inhibiting effect of halide additives could be explained by the trapping of inactive Ni(II) species, and the reason for the lack of reactivity for certain carbonylic vinyls was explained with the inability of these complexes to perform the β -hydride elimination due to the stabilizing effect from the coordinating carbonyl oxygen.

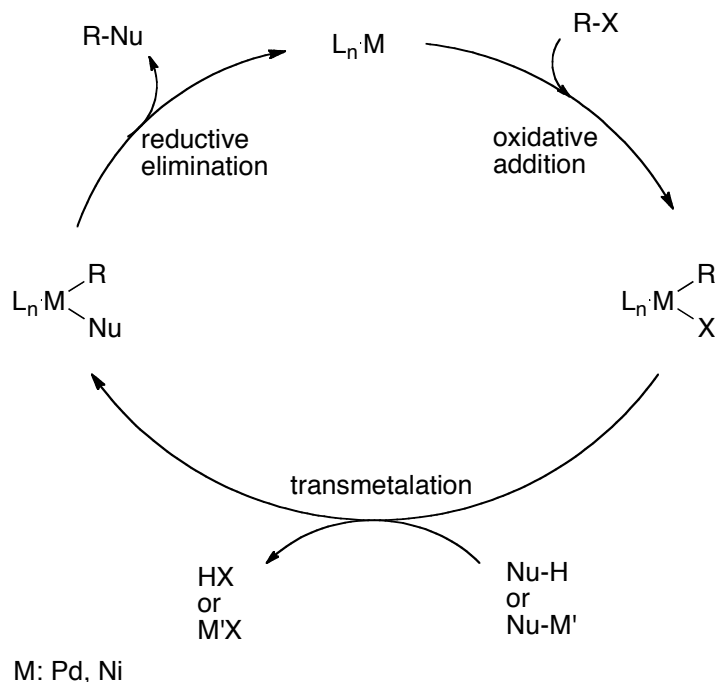
4. Iron catalyzed cross coupling reactions (Papers V-VI)

Cross coupling reactions are today widely used in organic chemistry. They have since their emergence in the 1970s been a seminal tool for many synthetic chemists. However, even though much is known about this reaction class, there is still much to understand and many potential developments are possible to envision. For example, the last decade has seen a rise in the interest to perform more environmentally friendly versions of these reactions.

4.1 Background

4.1.1 Catalytic cycle and mechanism of the C-C bond-forming reaction

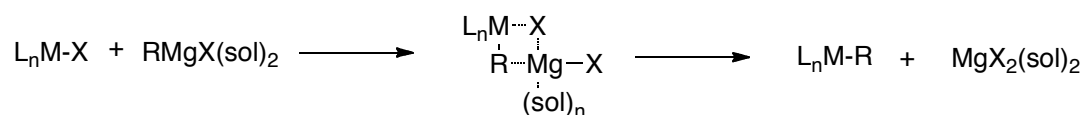
The catalytic cycle of the cross coupling reaction involves three different steps: *oxidative addition*, *transmetalation*, and a *reductive elimination* to close the cycle. The mechanism for a cross coupling reaction, exemplified with a coupling between an aryl halide and a carbon nucleophile, is shown in Scheme 24. The most common metals involved in this reaction is palladium and nickel.



Scheme 24. Catalytic cycle of a cross coupling reaction

The oxidative addition occurs at a low-valent metal species and the relative rate of the reaction usually follows the trend Ar-I > Ar-Br > Ar-Cl. The bromide and chloride electrophiles require ligands, such as a phosphine ligand, coordinated to palladium to be able to perform the oxidative addition.

The subsequent transmetalation is a more complex reaction than the preceding oxidative addition. Scheme 25 shows a simple mechanistic suggestion for the reaction between a Grignard reagent and the metal center.



Scheme 25. Mechanistic suggestion for the transmetalation

One can envision the other organometallic reagents transferring the carbon group in the same manner, but in reality the reaction is more complex. Different studies have been performed and revealed a more complicated mechanism than expected. A number of studies on the organoboron transmetalation have been presented,^[124] and several other examinations concerning this crucial step have been performed, dealing with organotin, organosilicon and organostannanes, among others.^[7a]

The closing step of the catalytic cycle is the reductive elimination, which must occur from a *cis* orientation of the coupling partners. The rate of the reaction is faster for aryl and vinyl complexes than from the alkyl species, this is one reason to why sp²-sp² and sp²-sp³ couplings are favored over the sp³-sp³ couplings.^[7a]

A thorough review of the mechanistic aspects for the palladium catalyzed cross coupling reactions has been published by Amatore and Jutand.^[125]

4.1.2 Carbon-heteroatom bond-forming cross coupling reactions

In recent years the scope of the cross coupling reaction has been extended to include also carbon-heteroatom bond-forming reactions. The most common of these is the carbon-nitrogen bond-forming reaction, with the palladium catalyzed variant known as “the Buchwald-Hartwig reaction”.^[126] The mechanism of this reaction is similar to the above-mentioned mechanism for the carbon-carbon counterpart, but differs in the second step, where the transmetalation is replaced with an amination of the metal-complex. Several informative texts have been published regarding this subject.^[127] Other cross coupling reactions forming carbon-heteroatom bonds are carbon-phosphorous,^[128] carbon-sulfur,^[129] carbon-oxygen,^[130] and carbon-boron^[131] bond-forming reactions.

4.1.3 Drawbacks of today's catalysts for cross coupling reactions

The classic catalysts for cross coupling reactions are palladium and nickel. These metals are unfortunately toxic and in the case of Pd also expensive and fairly non-abundant. There is also the environmental and medicinal problem with leaching of the catalyst. The potential risk of having small amounts of toxic metals in our medicines is something that the companies must invest large sums of money in trying to avoid.

Another way of circumventing this problem is to use other metals, which are not as dangerous to the environment, and humans, and if possible, also cheap and abundant. One such metal, which in fact can overcome all the mentioned obstacles, is *iron*. It is cheap, abundant, environmentally friendly and non-toxic for humans. It has also been shown to be able to perform cross coupling reactions.

4.2 Possibilities for iron catalyzed cross coupling

4.2.1 Scope and limitations

Already in the 1940s Kharasch could show the ability of stoichiometric amounts of iron salts to mediate a cross coupling reaction between a Grignard reagent and a alkyl or aryl halide.^[132] Almost 30 years later Kochi and co-workers, along with some other groups, picked up the trail again, making the reaction catalytic in iron and broadening the scope to include both alkyl/aryl Grignard reagents coupled to aryl/alkyl halides to give the cross coupling product, even if the yield and selectivity were somewhat unpredictable.^[133]

The introduction of NMP as co-solvent by Cahiez and Avedissian in the 1990s was a major breakthrough, which increased the yield and stereospecificity.^[134] Further broadening of the scope was achieved in the years that followed, with the use of heteroaryl halides^[135] and application in synthesis of complex molecules.^[136]

The seminal work of Fürstner and co-workers in the last decade has been the source of the standard experimental setup for conducting an iron catalyzed cross coupling reaction. Furthermore, Fürstner and co-workers have greatly extended the scope, introducing important features such as secondary alkyl halides^[137] and investigated the tolerance for different functional groups as coupling partners,^[138] as well as screened the possible iron catalysts,^[137-138] found new halide-equivalent groups, for example triflates^[139] and made extensive mechanistic studies (*vide infra*). In addition to this, several other groups have made large contributions to the advancement of the field of iron catalyzed cross coupling reactions. Some of the development has concerned alkyl halides bearing β -hydrogens,^[140] and further development of sp^3 - sp^3 couplings.^[141]

The development of ligands for the iron catalyst has resulted in the discovery of the salen-type ligands as very well suited for the coupling of secondary alkyl halides,^[138, 140a] and the use of TMEDA as additive for the coupling between aryl Grignard and alkyl halides,^[140b, 142] where the preformed Fe-TMEDA complexes proved to be competent catalysts.^[143] Additional research in this area has provided a range of different ligands suited for this cross coupling reaction.^[144] Also iron nanoparticles have shown catalytic ability.^[145]

For mechanistic reasons, Fürstner and co-workers explored low-valent iron complexes and their abilities in the cross coupling reaction. An important study concerned the use of the tetrakis(ethylene)ferrate complex $[\text{Li}(\text{tmeda})]_2[\text{Fe}(\text{C}_2\text{H}_4)_4]$ isolated by Jonas *et al.*^[146] It proved to be a capable catalyst in the reaction, able to catalyze both the aryl Grignard/alkyl halide and the alkyl Grignard/aryl halide coupling with good results.^[147] Several other low-valent complexes have also shown catalytic activity, and Fürstner and co-workers have been able to demonstrate the potential of iron at different oxidation states, -II to +III (except -I), to promote the cross coupling reaction.^[148] For further information about these low-valent iron complexes, see *section 4.2.2* in this thesis.

The homocoupling of the Grignard reagent, both aryl-aryl and alkyl-alkyl, has been examined by Xu *et al.*, and found to give moderate to good yields in short times.^[149] In addition to this, unsymmetrical biaryls, an important structural unit, can be synthesized through iron catalyzed cross coupling, at first using aryl copper reagents as a coupling partner,^[150] and later with aryl Grignard reagents where iron fluoride showed an ability to suppress the amount of homocoupling.^[111c, 151]

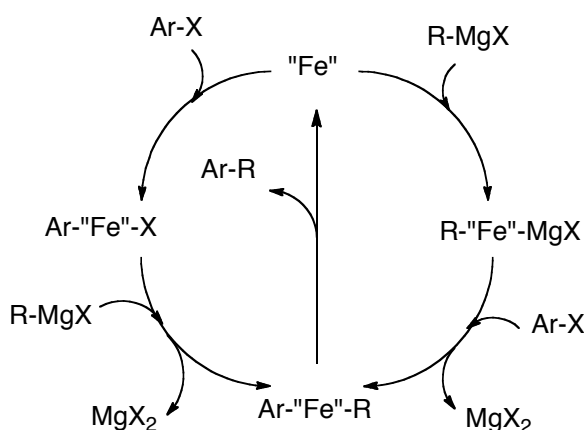
Grignard reagent generated *in situ* can also complete a cross coupling reaction, which has been demonstrated by von Wangelin and co-workers.^[152] This technique has showed an ability to work nicely in iron catalyzed domino reactions.^[152a, 153]

In order to extend the nucleophilic scope, several groups have been able to use zinc reagents instead of the more reactive Grignard reagent. Nakamura *et al.* coupled both primary and secondary halides with arylzinc reagents under iron catalysis,^[154] Bedford and co-workers managed to develop a coupling utilizing benzyl halides and phosphates as electrophiles,^[155] and recently Nakamura *et al.* have been able to use complex sulfonates as electrophiles in this coupling.^[156] Even though these findings are an important step towards a more versatile iron catalyzed cross coupling, it is important to point out that all the “zinc reagents” so far require a fair amount of Mg in order to carry out the coupling. The need for MgX_2 is vital for the reaction, and one can therefore speculate what the actual reagent is.

Several examples of iron catalyzed cross coupling used in synthesis of complex molecules is present in the literature, and represents a diverse array of different structures.^[157]

4.2.2 Mechanistic suggestions

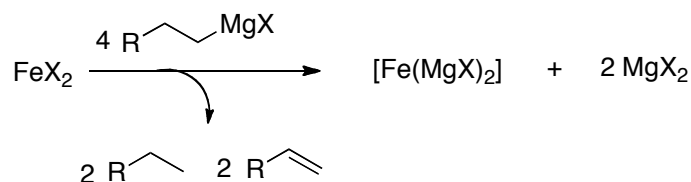
The mechanistic investigations by Kochi and co-workers reached the conclusion, based on by-product formations, that the active catalyst must be an Fe^{I} -species, even if this never could be isolated.^[133b-d] This elusive species was formed from reduction of the iron salt by the Grignard reagent.^[133d] Furthermore, Kochi and co-workers proposed that the mechanism was analogous to the Kumada-Tamao-Corriu reaction mechanism with an oxidative addition, transmetalation and reductive elimination, but they could not determine which of the oxidative addition and transmetalation was the first step in the cycle.^[133b, c] Scheme 26 shows the two different pathways of the cross coupling reaction. Both the suggested mechanistic paths are valid and fit the kinetic data from Kochi and co-workers.



Scheme 26. Catalytic cycle for iron catalyzed cross coupling

Regarding the catalytically active iron species, the Fe^{I} -catalyst put forward by Kochi and co-workers was not entirely proven and other, low-valent iron species such as Fe^0 , could not be excluded.^[133b, c]

In the last decade several new suggestions regarding the mechanism have been presented. Fürstner and co-workers have reported that “inorganic Grignard reagents” of the type $\text{Fe}(\text{MgX})_2$,^[158] with iron in the formal oxidation state $-II$, can be formed in the presence of excess Mg or organomagnesium.^[137-138] These highly unorthodox reagents were proposed to be the catalytically active species in iron catalyzed cross coupling and were formed in the same way as Kochi and co-workers suggested, through reduction of the iron by the Grignard reagent according to Scheme 27.



Scheme 27. Generation of the potentially catalytically active “inorganic Grignard reagent”

In fact, it could be shown that isolated complexes of this type could enter the catalytic cycle and work as catalysts for the cross coupling reaction.^[147] Some examples of these complexes are shown in Figure 26. In an extensive study, Fürstner and co-workers showed that almost the entire range of oxidation states, -II to +III (except for -I, which could not be isolated) can perform the cross coupling reaction.^[148] Recently, Wolf and co-workers prepared several Fe(-I) complex (Figure 26) and employed them in the cross coupling reaction, achieving moderate yields.^[159]

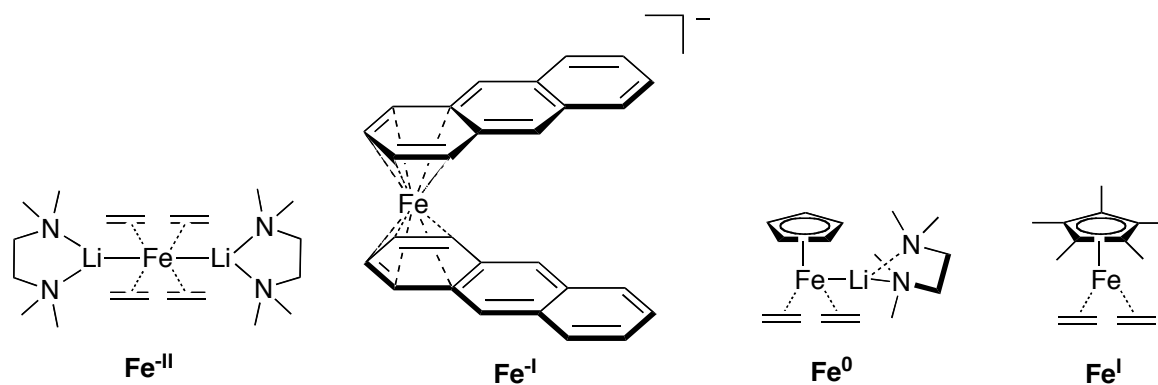


Figure 26. Some low-valent iron complexes that are competent catalysts for iron catalyzed cross coupling

Several other research groups have performed mechanistic studies on the iron catalyzed cross coupling. Cahiez *et al.* have proposed a Fe^0 - Fe^{II} cycle with a two-step electron transfer with poly-aryl iron species as important intermediates.^[160] A radical mechanism has been proposed by various groups, and some evidence has been presented, for example by reactions with radical clocks such as cyclopropylmethyl bromide.^[140b, 141, 143, 145, 161]

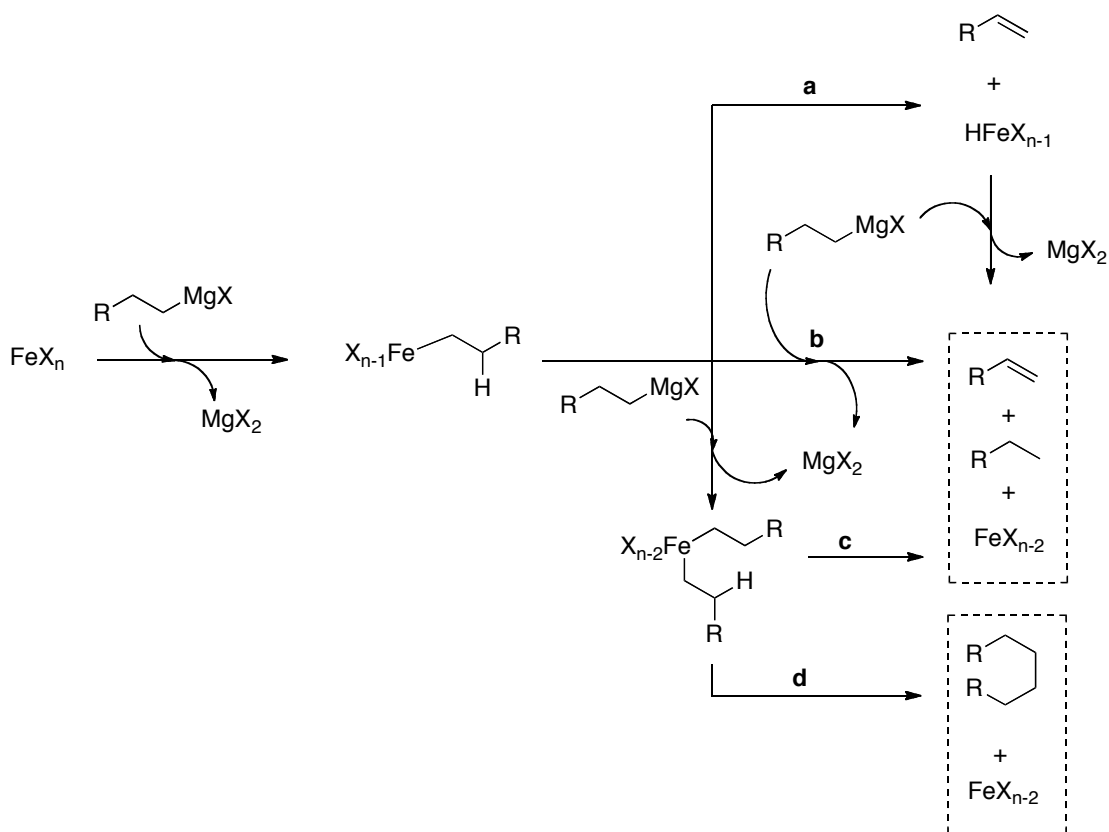
4.3 Mechanistic investigation of iron catalyzed cross coupling (Papers V and VI)

In order to improve and develop a catalytic reaction, a thorough knowledge of the mechanism is imperative. It is the best way to understand which conditions or features to change to further advance the reaction. Therefore, the following section will reveal our efforts to provide additional insights to the knowledge of the mechanism and catalytic activity of the iron catalyzed cross coupling reaction.

4.3.1 Active catalyst

With inspiration from Kochi and co-workers, a titration experiment was designed in order to elucidate the nature of the active catalyst. Analysis of the potential pathways for formation of the reduced active iron specie revealed that it could be achieved through four different paths leading to three different organic products, alkene, alkane and the homocoupling of two alkyls (Scheme 28).

Alkene and alkane are formed through either a β -hydride elimination followed by a reductive elimination (path **a**) or via a direct elimination (path **b**) from the pre-formed alkyl iron complex, or by a second transmetalation, which yields a dialkyl iron, followed by internal elimination (path **c**). The homocoupling product is generated through reductive elimination from the above-mentioned dialkyl iron complex (path **d**).

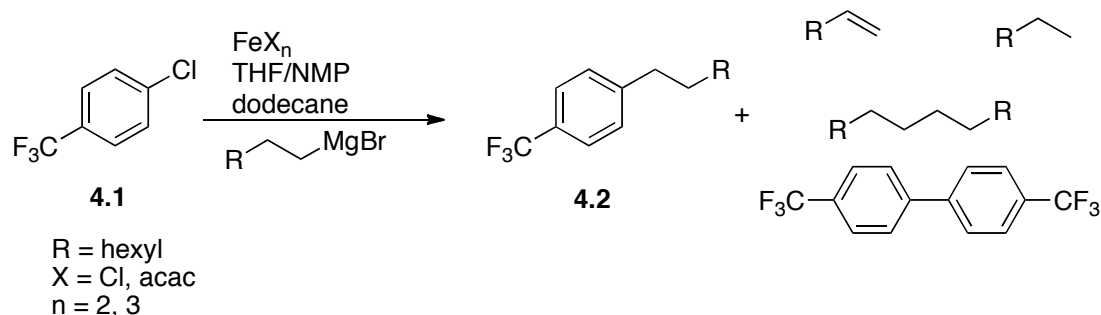


Scheme 28. The four different pathways of catalyst activation and their byproducts

In these processes, two electrons are transferred to the iron moiety and a reduced iron species and an oxidized organic byproduct (alkene or homocoupling) are formed. By measuring the amount of oxidized byproduct, one can calculate the number of electrons relocated to iron, and from that deduce the nature of the oxidation state of the catalytically active iron.

4.3.2 Titration experiments: a way to deduce the oxidation state of the active catalyst

The experimental study was conducted as a titration on a “standard” iron catalyzed cross coupling reaction between octyl Grignard and an aryl chloride (**4.1**) in a THF/NMP mixture (35 - 105 mL THF), with dodecane as the internal standard, to yield a *p*-substituted octyl benzene (**4.2**). Four different iron catalysts, $\text{Fe}(\text{acac})_n$ and FeCl_n ($n = 2, 3$) were employed in different amounts (5 – 15 mol%) (Scheme 29).



Scheme 29. The cross coupling employed in the titration study

The Grignard reagent was added in small portions (10% of the total amount in each addition), allowed to react for the time required for the reaction to use up all the Grignard, whereupon a small sample was collected, and the next portion of Grignard was added. The amounts of product and byproducts were analyzed by GC. The mass balance of the aryl was monitored, and found to be constant indicating that all the added aryl fragments were accounted for, and the total sum of alkyl fragments was verified to match the amount of Grignard added. All components were then plotted against the amount of added Grignard reagent (Figure 27).

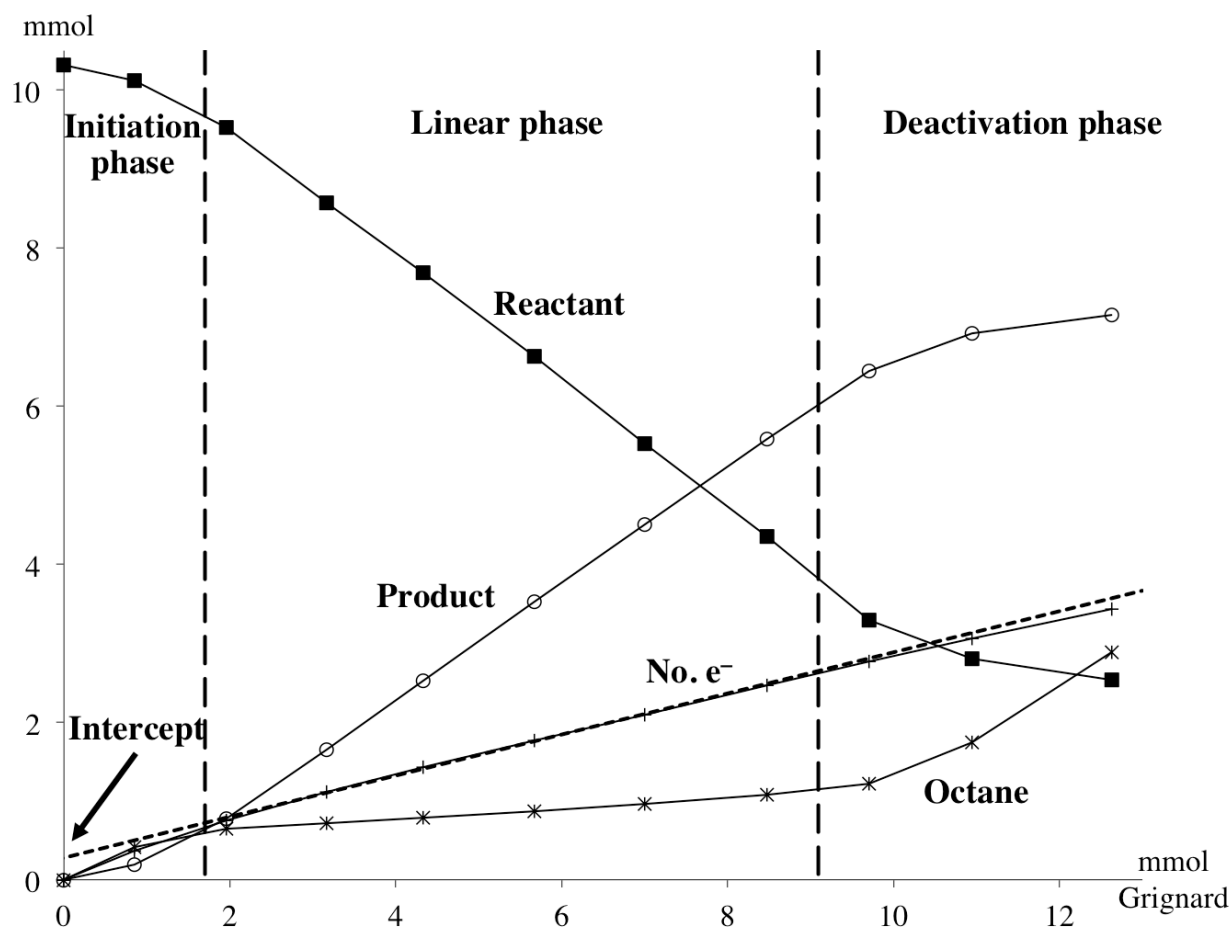


Figure 27. An example of a titration reaction plot

The resulting plot can be divided into three different sections:

1. The initiation phase, where the iron is reduced to the catalytically active form
 2. The linear phase, where the cross coupling reaction is running, determined through a F-test selection of the points for each experiment.
 3. The deactivation phase, where the catalytic activity is diminished and the Grignard reagent remains unreacted until the work-up, as indicated by the increasing amount of octane formed.
- The line showing the number of electrons is represented with a dotted line, in an ideal situation it should be constant in the linear region, but contaminants of both alkene and alkane in the Grignard reagent results in a positive slope. However, when extrapolating this line to $x = 0$ the y-intercept will give the amount of electrons added to the iron precatalyst in the initiation phase. Dividing this number with the amount of iron complex added in each experiment yields the number of electrons transferred to each Fe atom. The results from the different reaction conditions can be seen in Table 6.

Table 6. Number of electrons added to each Fe atom including regression standard error

Entry	Catalyst	Fe (mol%)	THF (ml)	Ratio e ⁻ /Fe
1	FeCl₂	5	50	0.256 ± 0.004
2		10	50	0.146 ± 0.004
3		15	50	0.237 ± 0.006
4		5	70	0.566 ± 0.007
5		5	105	0.699 ± 0.067
6	Fe(acac)₂	5	50	0.684 ± 0.001
7		10	50	0.705 ± 0.010
8		15	50	0.695 ± 0.013
9		5	70	0.809 ± 0.010
10		5	105	0.736 ± 0.063
11	FeCl₃	5	50	0.605 ± 0.006
12		10	50	0.614 ± 0.005
13		15	50	0.642 ± 0.014
14		5	70	1.094 ± 0.039
15		5	105	1.026 ± 0.029
16	Fe(acac)₃	5	50	0.991 ± 0.011
17		10	50	0.903 ± 0.040
18		15	50	1.127 ± 0.021
19		5	70	1.123 ± 0.023
20		5	105	1.169 ± 0.031

As can be seen from Table 6, the results from the titration experiment are hard to interpret. There is no doubt that we can measure the reduction of the iron precatalyst, but it seems like only part of the added iron participates in the reaction, especially at higher concentrations. In more diluted solutions, a greater amount of iron appear to be reduced, at least this is the case for the FeCl_n complexes. This is probably due to oligomerization, which is easier at high concentrations. The acetylacetonate complexes behave somewhat more consistent, something that could be explained by the fact that they are more coordinatively saturated and therefore less prone to oligomerize.

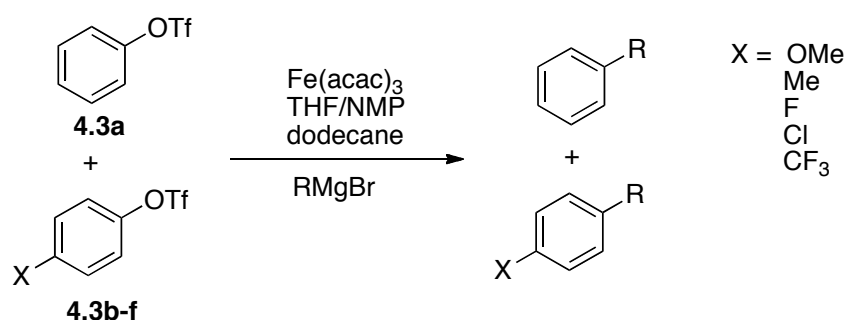
One could easily think that the results from these studies indicate that one mol of electrons is added to each mol of Fe^{III} precatalyst, but that is in fact not the situation. This can simply be deduced from the fact that the Fe^{III} complexes do not show ratios that are one higher than the Fe^{II} counterpart. Instead, we conclude that only a part of the added iron is actually reduced to the active form and can then participate in the catalytic cycle. This would imply that a large part of the iron resides in the +II or +III oxidation state, something that is a strong indication that iron in low-valent states, such as -II, is highly unlikely since these iron complexes would

comproportionate with the iron remaining in higher oxidation states. However, the oxidation state of the active catalyst cannot be determined with certainty from this experiment.

Several pieces of valuable information about the reaction conditions could be extracted from the titration experiments. The importance of the co-solvent NMP was verified and several ways of stabilizing the active catalyst were identified. These ways include dilution or the addition of coordinating ligands such as TMEDA. Slow addition of the Grignard reagent prolonged the catalyst lifetime, as well as excess amounts of the aryl substrate. As mentioned before, the catalyst deactivation seems to be via oligomerization of iron complexes and if these processes could be shifted towards the monomeric forms, the deactivation can be avoided.

4.3.3 Hammett study

To extract more kinetic information, a Hammett study was performed by reacting a mixture of two different substrates, and measuring the disappearance of both. Due to low reactivity of the aryl chlorides, the more reactive aryl triflates (**4.3a-f**) were chosen as substrates (Scheme 30).



Scheme 30. Competitive Hammett study performed with aryl triflates

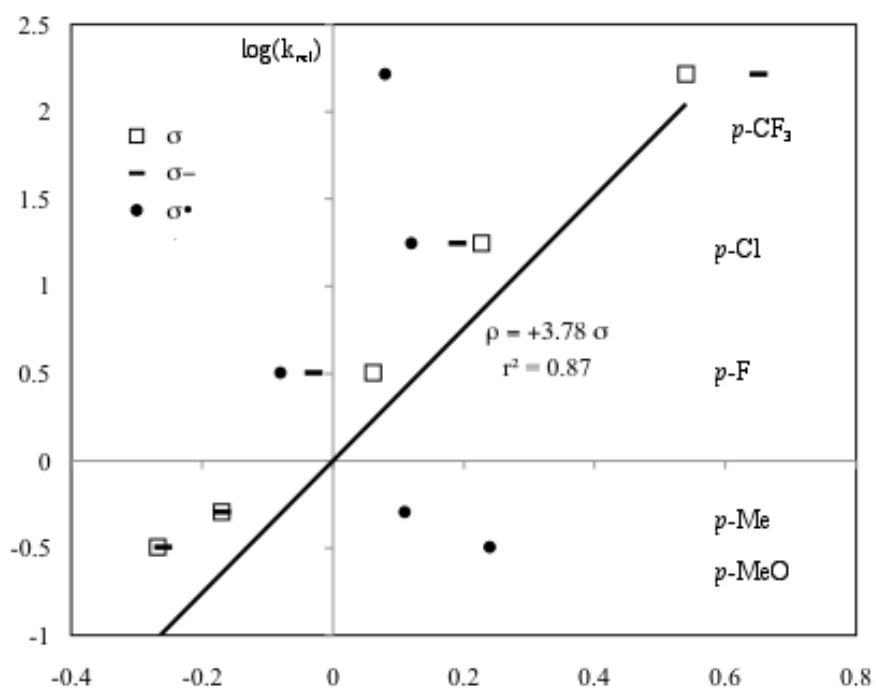
The kinetic dependence was assumed to be the same for both substrates A and B, and the relative rate of reaction, $k_{\text{rel}}=k_A/k_B$ was obtained from fitting to the expression $\ln([A]_0/[A]) = k_{\text{rel}}\ln([B]_0/[B])$. Furthermore, the analysis was made in the linear region (Figure 27) and the relative rates were then fitted to literature σ values^[162] using the Hammett expression $\log(k_x/k_H) = \rho\sigma_x$ (Table 7).

Table 7. Relative rates and literature values of the substrates

<i>p</i> -Substituent	k_{rel}	σ	σ^-	σ^\bullet
OMe	0.32	-0.268	-0.26	0.24
Me	0.51	-0.17	-0.17	0.11
F	3.2	0.062	-0.03	-0.08
Cl	17.7	0.227	0.19	0.12
CF ₃	165 ^a	0.54	0.65	0.08

[a]Determined in competition with the *p*-Cl substrate, $k(\text{CF}_3)/k(\text{Cl}) = 9.34$

The linear correlation to the different σ values was calculated and the best correlation was achieved with the standard σ scale, giving $\rho = +3.8$ (Figure 28).

Figure 28. Hammett correlation against the different σ values

Several important facts were obtained from the Hammett study, first of all the low reactivity of aryl chlorides was noted; only *p*-substituted aryl chlorides with electron-withdrawing substituents could perform the coupling. For the aryl triflates, a full range of *p*-substituted aryl triflate could be used in the competition experiments.

Secondly, the reaction showed a large preference for electron withdrawing *p*-substituted aryl triflates yielding a ρ -value of +3.8. The large positive value indicates that the oxidative addition is an effectively irreversible step in the catalytic cycle. In comparison, the oxidative addition using Pd^0 is close to 1, sometimes up to 1.5.^[97c, 101p, 163] Even though this also means that a considerable amount of negative charge is donated to the aromatic ring in the oxidative addition,

the correlation is still better with σ than σ^- . The correlation is not good to σ^\bullet either, and we can therefore rule out a possible SET mechanism with an aryl radical anion since this would correlate to a combination of σ^- and σ^\bullet . The relative rate of the *p*-fluoride substituted aryl is higher than the unsubstituted substrate, which indicates a positive σ_F value, something that we only can find in the standard σ scale.

However, few reactions show strong correlation to σ^\bullet only, therefore we constructed a combination between σ^\bullet and σ . A considerable improvement was achieved when using this combination, with a correlation coefficient of $r^2 = 0.956$ compared to 0.87 in the previous correlation to only σ values (Figure 29).

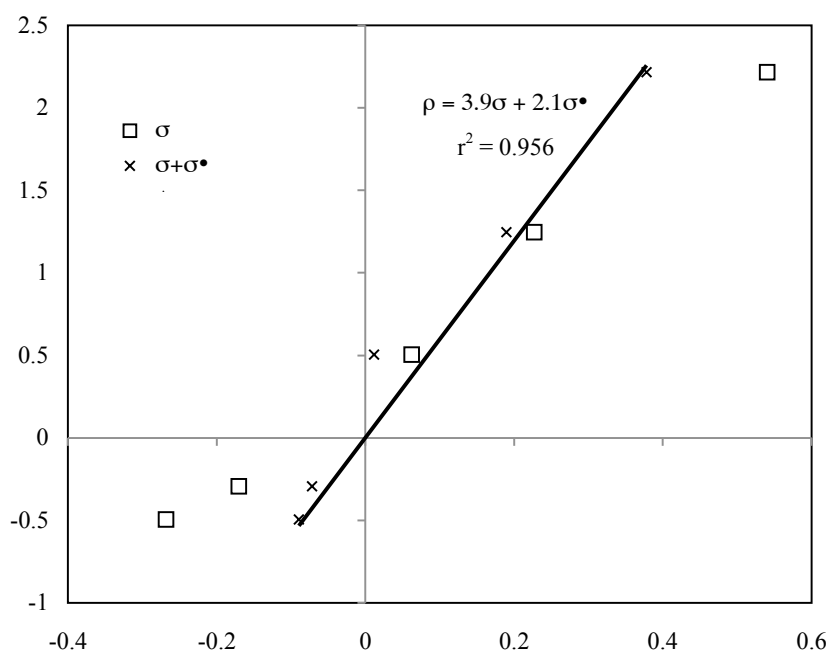


Figure 29. Hammett correlation with σ and a combination of σ and σ^\bullet

This points toward a transfer of spin from iron to the aryl moiety in the oxidative addition transition state. This was also confirmed by the calculated transition states of this step, showing a large spin density on the aromatic carbons (*vide infra*).

4.3.4 Computational investigation of the catalyst activation and the catalytic cycle

In a catalytic cycle all steps must be exergonic (in the worst case they can be slightly endergonic) in order to result in a complete cycle. In our investigation of the active catalyst in the iron catalyzed cross coupling reaction we therefore began our efforts with calculating the reaction free energy for each step in the two postulated catalytic cycles (Scheme 26), for each plausible oxidation state of iron. All cycles where one single step was above 80 kJ mol^{-1} were excluded due

to the improbability for this to have a lower barrier than 100 kJ mol⁻¹, something that would be required in order for the reaction to run at room temperature. For the most promising cycles, transition states were located to achieve an energy profile.

Four different oxidation states, Fe^{-II} to Fe^I, were employed in the study, and were modeled with the simplest, but active, catalytic system, ferrous chloride. The charge was compensated with Cl⁻, ClMg⁺ or Mg²⁺, and all possible spin states were explored. The reaction system was represented with phenyl chloride and ethyl magnesium chloride. The solvent, THF, was modeled by a variable number of coordinated dimethyl ether molecules, where the number of explicit solvent molecules for each complex were determined from the final free energy of the system. All geometries were determined *in vacuo*.

The only step that is common for the two catalytic cycles in Scheme 26 is the final reductive elimination; therefore we decided to investigate this step first. The favored spin states for the complexes were high spin, except for the aryl substituted Fe^{III}-complexes where an intermediate spin (S = 3/2) was found to be preferred. The results from this initial study are shown in Table 8.

Table 8. Free energies (kJ mol⁻¹) for postulated reductive elimination steps.

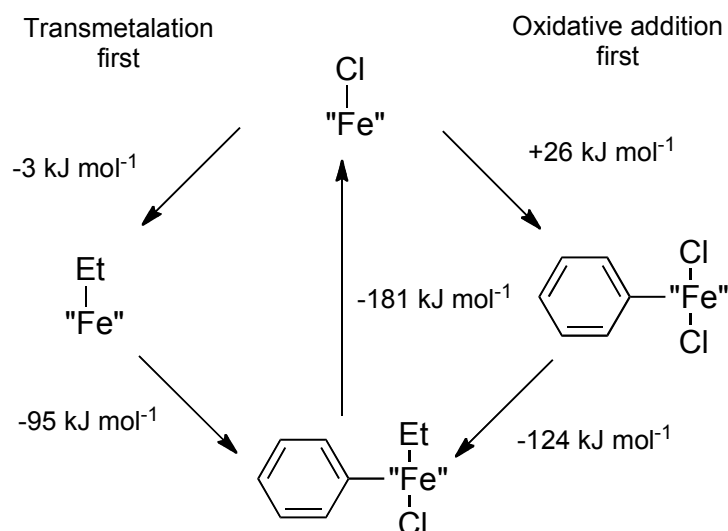
"Fe"	No Sol. ^a	Ox. State ^b	ΔG	ΔG [‡]
FeMg	3	-II	195	–
FeMgCl	3	-I	94	–
Fe	2	0	30	191
FeCl	2	+I	-181	10

^aNumber of explicit solvent molecules (Me₂O) used in the calculation. ^bOxidation state of Fe after reductive elimination.

The most important conclusion from these results is that iron in the two lowest oxidation states cannot perform a reductive elimination, due to the endergonicity of this step. For the other two oxidation states, transition states were located and reaction barriers were determined. The Fe^I - Fe^{III} cycle shows a small barrier, giving a facile elimination, whereas the Fe⁰ - Fe^{II} cycle has a barrier of 191 kJ mol⁻¹, which indicates that this step is not realistic for this cycle.

In conclusion, only the Fe^I - Fe^{III} cycle is likely for the reaction, something that also is in agreement with the proposal by Kochi and co-workers.^[133b, c]

The next step in our examination of this reaction was to study the first steps in the catalytic cycle, the oxidative addition and the transmetalation. As shown in Scheme 26, the order of these steps has not been previously determined. The reaction energies for the different steps are shown in Scheme 31.



Scheme 31. The two $\text{Fe}^{\text{I}} - \text{Fe}^{\text{III}}$ cycles with reaction free energies (kJ mol^{-1}), “Fe” is a solvated iron species.

The left side of Scheme 31, depicting the cycle with transmetalation as the first step consists of steps that all are exergonic. Nevertheless, the opposite reaction path, with the oxidative addition as the initial step cannot be excluded since the highest endergonicity is only 26 kJ mol^{-1} . To get a deeper understanding of which one of these cycles that is the most favored, we calculated the transition states for both cycles and constructed the complete free energy surface (Figure 30).

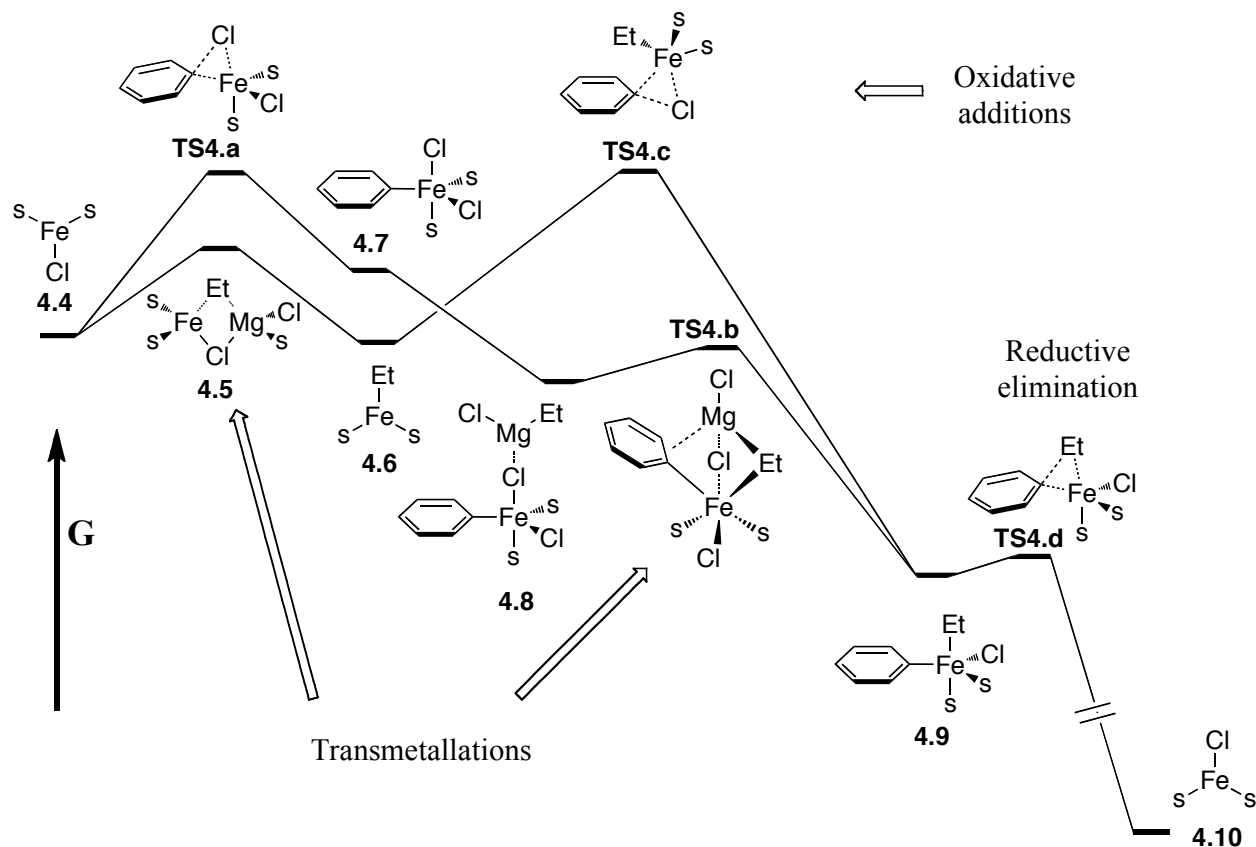


Figure 30. Free energy surface of the two $\text{Fe}^{\text{I}} - \text{Fe}^{\text{III}}$ cycles, explicit solvent molecules are denoted by “s”

The more “classic” cycle (right side of Scheme 31) has the oxidative addition (**TS4.a**) as the first step, with a barrier of 65 kJ mol⁻¹ (Figure 31). The reaction is endergonic, but the resulting complex **4.7** can be stabilized by coordinating EtMgCl through one of the chlorides (**4.8**). The subsequent transmetalation step was assumed to go through a four-center transition state, in accordance with previous computational studies on similar reactions,^[102e, 164] and such a transition state could be localized (**TS4.b**, Figure 31), with a 18 kJ mol⁻¹ barrier to form the resulting aryl-alkyl-Fe^{III} complex (**4.9**), which is a common point for both cycles. Due to the strong *trans* effect of both the alkyl and aryl groups, they end up *cis* to each other, well set up for the reductive elimination.

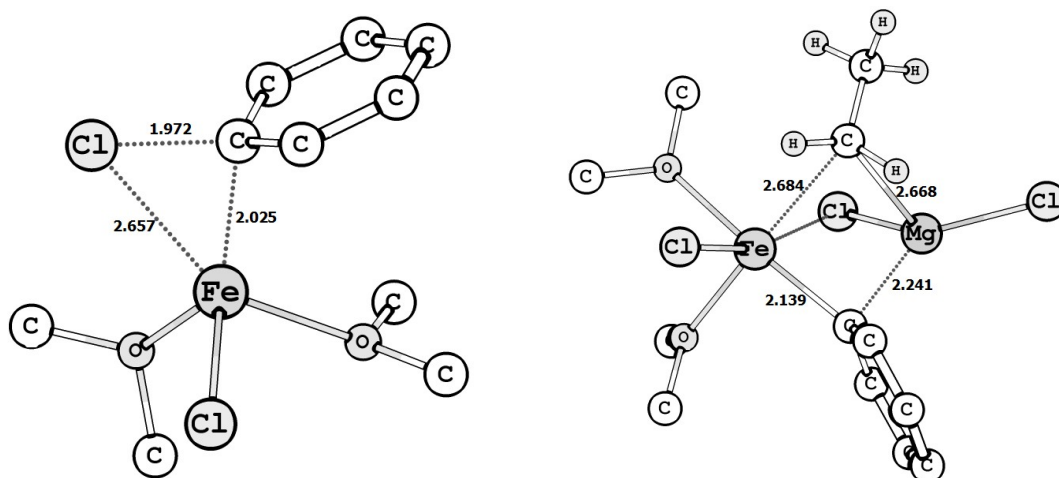


Figure 31. Transition states for OA (**TS4.a**, left) and TM (**TS4.b**, right) for the "OA first" cycle, most H are omitted for clarity

The other possible cycle (left side of Scheme 31) starts with the transmetalation. However, in this case it was not possible to form the pre-complex with the Grignard reagent coordinated to the iron moiety through one of the chlorides. This structure collapses, forming a bis- μ complex (**4.5**, Figure 32), where the ethyl group has been partially transferred to the iron. This complex is a minimum on the potential energy surface but, due to entropic and desolvation costs, most likely close to a saddle point on the free energy surface. Dissociation of this complex forms the alkyl-Fe^I complex **4.6** that can perform an oxidative addition with a barrier of 69 kJ mol⁻¹ (**TS4.c**, Figure 32).

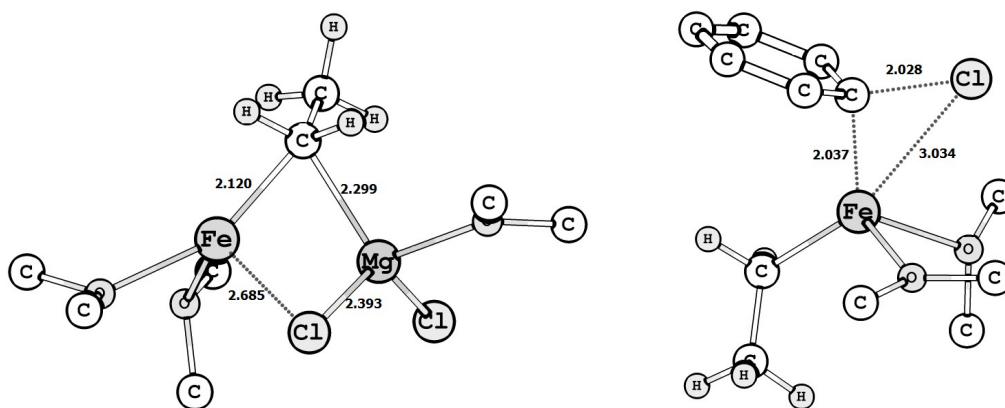


Figure 32. TM intermediate (**4.5**) and TS for OA (**TS4.c**) in the "TM first" cycle, most hydrogens are omitted for clarity

The final step, common for both cycles, is the reductive elimination, which has a barrier of only 10 kJ mol^{-1} , closing the catalytic cycle (**TS4.d**, Figure 33).

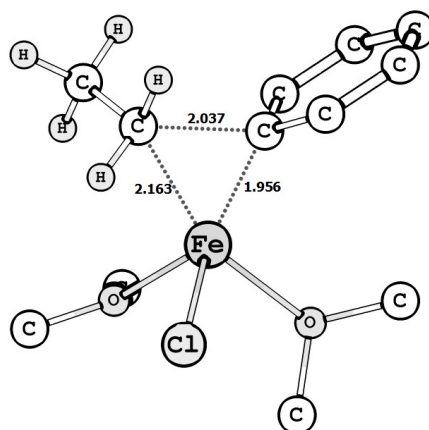


Figure 33. Transition state for the reductive elimination (**TS4.d**), most hydrogens are omitted for clarity

As can be seen from Figure 30 the oxidative addition is the rate-limiting step for both catalytic cycles. Unfortunately it is not possible to differentiate between the two cycles, the highest point differ only by 1 kJ mol^{-1} . In fact, it is likely that both pathways are active simultaneously. As already mentioned, both oxidative addition transition states show significant spin polarization of the aromatic moiety, with Mulliken spin densities between 0.07 and 0.16 on the aromatic carbons.

In the calculations a $\text{Fe}^0\text{-Fe}^{\text{II}}$ cycle was found to be non-feasible for the reaction, since it could not close the catalytic cycle in a reductive elimination from R_2Fe (Table 8). This is in contrast to the experimental results (Table 6) where the added Fe^{II} pre-catalyst can perform the reaction. However, as mentioned before, we have indications of that iron easily can oligomerize in solution, we therefore postulate that a reductive elimination of R_2Fe can be assisted by another Fe^{II} species, such as FeCl_2 . To inspect this hypothesis we performed a computational analysis on a

small model system with the alkyl groups modeled with methyl groups (Figure 34). This reaction forms two Fe^I-Cl species, and is by that a viable path into the Fe^I - Fe^{III} cycle. In solution the barrier for this transformation is only 85 kJ mol⁻¹ (TS4.e).

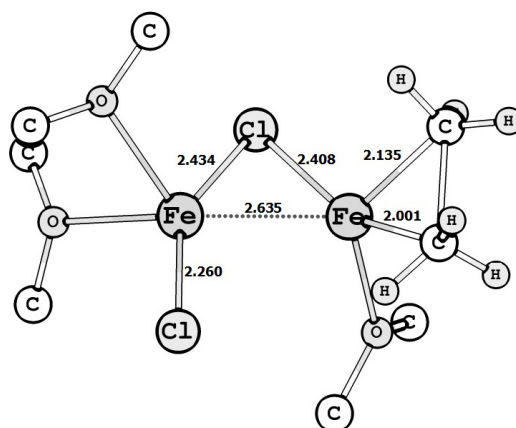
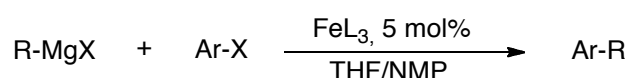


Figure 34. Reductive elimination from a bis-Fe^{II} complex through TS4.e, most hydrogens are omitted for clarity.

4.3.5 Low temperature cross coupling – scope and possibilities[†]

The scope of the low-temperature iron cross coupling was investigated by reacting a selection of aryl electrophiles with an alkyl Grignard reagent at three different temperatures, -78 °C, -20 °C, and ambient temperature (Scheme 32). The Grignard reagent was added in small portions at intervals to avoid precipitation of the catalyst, which had been previously detected. The results were analyzed by GC, and the threshold for a “successful” reaction was 50% yield or more.



Scheme 32. Iron catalyzed cross coupling between an alkyl Grignard and an aryl electrophile

The result from the screening of the low-temperature coupling are shown in Figure 35. The need for a strongly electron withdrawing group for the aryl chlorides to perform the coupling at very low temperatures (-78 °C) are apparent. At somewhat elevated temperature, -20 °C, the unsubstituted aryl chlorides still do not participate in the cross coupling, but both aryl triflates and chloropyridine reacted well. When ambient temperature was reached, the unsubstituted aryl chloride finally conceded and were able to partake in the reaction. The results are in total agreement with the previously reported Hammett study (Paper V) and support the hypothesis of a rate-limiting oxidative addition.

[†] Experimental study performed by Parisa Emamy

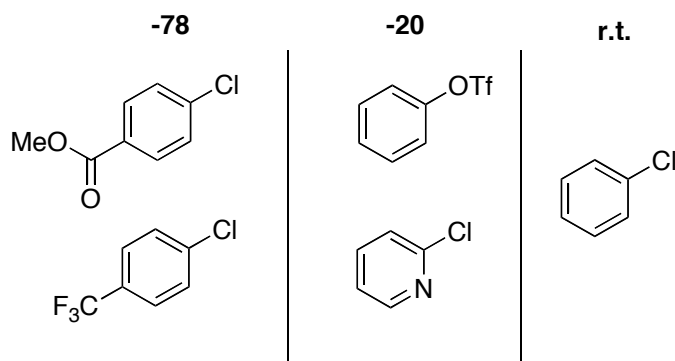


Figure 35. Substrates used in the cross coupling and the temperatures at which they reacted

4.3.6 Computational investigation of the low temperature cross coupling

A computational investigation was undertaken in order to give an explanation to the results from the substrate screen. The rate-limiting step for this reaction is the oxidative addition, and therefore we calculated barriers for this step for some selected substrates (Table 9). The calculated barriers agree fairly well with the experimental results in Figure 35. The highest barrier is found for the only substrate requiring a room temperature reaction, chlorobenzene. Phenyl triflate has a lower barrier, and *p*-CF₃-substituted chlorobenzene even lower, as anticipated. Somewhat surprisingly, the lowest barrier overall was found for 2-chloropyridine, a substrate that was only active at -20 °C. The moderate reactivity observed for this substrate could be due to coordination of the nitrogen lone pair, to magnesium or iron, in a geometry that inhibits the oxidative addition. It is also important to note that this is the only substrate that would give a coupling product without any iron catalyst at room temperature, presumably through an S_NAr reaction.

Table 9. Calculated barriers to oxidative addition for selected substrates

Substrate	ΔE^\ddagger (kJ/mol)
Phenyl-Cl	65
Phenyl-OTf	52
<i>p</i> CF ₃ -Phenyl-Cl	49
2-Cl-pyridine	40

4.3.7 Kinetic investigation of low temperature cross coupling

The further kinetic investigations involved an initial-rate study at -25 °C of the cross coupling between octyl Grignard and phenyl triflate, using Fe(acac)₃ as the catalyst (Scheme 32). The standard reaction utilized 0.5 mmol of substrate and Grignard, and 0.025 mmol (5 mol%) of iron

catalyst. The total THF-volume was adjusted to 20 mL in all cases. During the investigation, the initial concentration of each of the principal components, Grignard reagent, substrate and catalyst, was varied systematically. The reaction was followed by GC monitoring until ca. 10% product formation was reached, which made sure that all plots should be linear unless a change in mechanism occurs.

The suggested mechanism (Paper V) which proposed a rate-limiting oxidative addition, would give a first order dependence of both substrate and catalyst, and between 0 and 1 for the Grignard reagent, depending on the order of the transmetalation and oxidative addition. As the active Fe^{I} catalyst is formed from the Fe^{III} pre-catalyst via a reductive elimination of two alkyl groups on the Fe, we could identify hexadecane in all reaction mixtures, in an amount approximately proportional to the amount of added Fe pre-catalyst.

The concentration of Grignard reagent was the first to be varied, using between 0.025 M and 0.5 M. At low concentrations the reaction rate is doubled when increasing the concentration of Grignard from 0.025 M to 0.05 M, indicating a positive reaction order and an involvement of the reagent in the rate-limiting step. However, the curvature of the plots shows a slow decline of the catalyst activity over time (Figure 36).

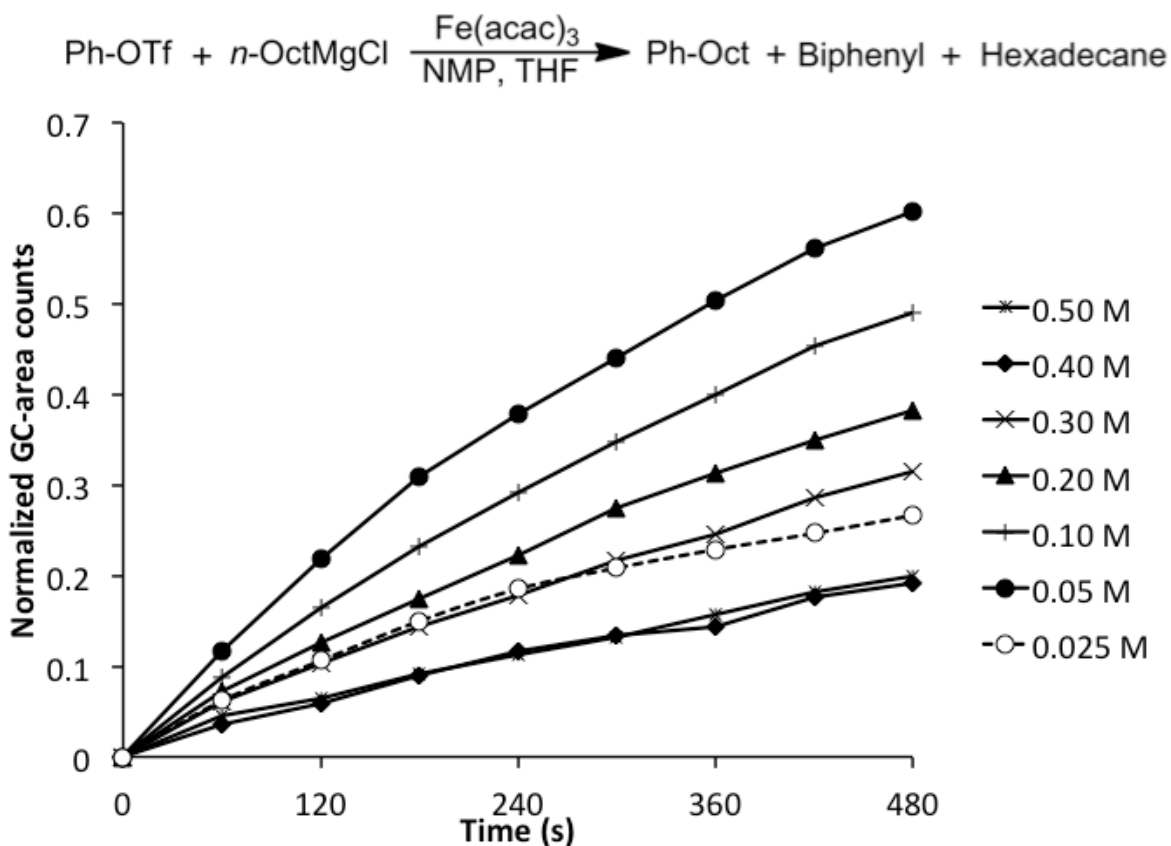


Figure 36. Product formation at different Grignard concentrations

At higher concentrations, the catalyst activity is decreasing, reaching a minimum at 0.4 M which stays constant at 0.5 M as well. For these two highest concentrations the rate seems to be constant after the first minute of reaction. Consequently, comparative F-tests revealed that exclusion of the first point resulted in a straight line, indicating no further deactivation of the catalyst. At the lower concentrations, the behaviour is different, the plots show curvature throughout the entire reaction time. In summary, the results are consistent with a dual catalyst activity, where the initially formed, highly active, iron catalyst is converted by excess Grignard to a less active form. With higher Grignard concentrations, the rate of this catalyst deterioration increases. When considering one of the strongest features of the Grignard reagent, its strong reducing ability, one can speculate if the lowering of the catalytic activity is due to formation of more reduced iron species, which are inferior catalysts or inactive. We can also observe minor formation of biphenyl at the lowest Grignard concentrations, but this is suppressed at higher concentrations.

The second factor to be studied was the substrate concentration, phenyl triflate, which was varied in the range 0.025-0.2 M. The reaction order was positive with a clear increase in the initial rate with increased concentration (Figure 37).

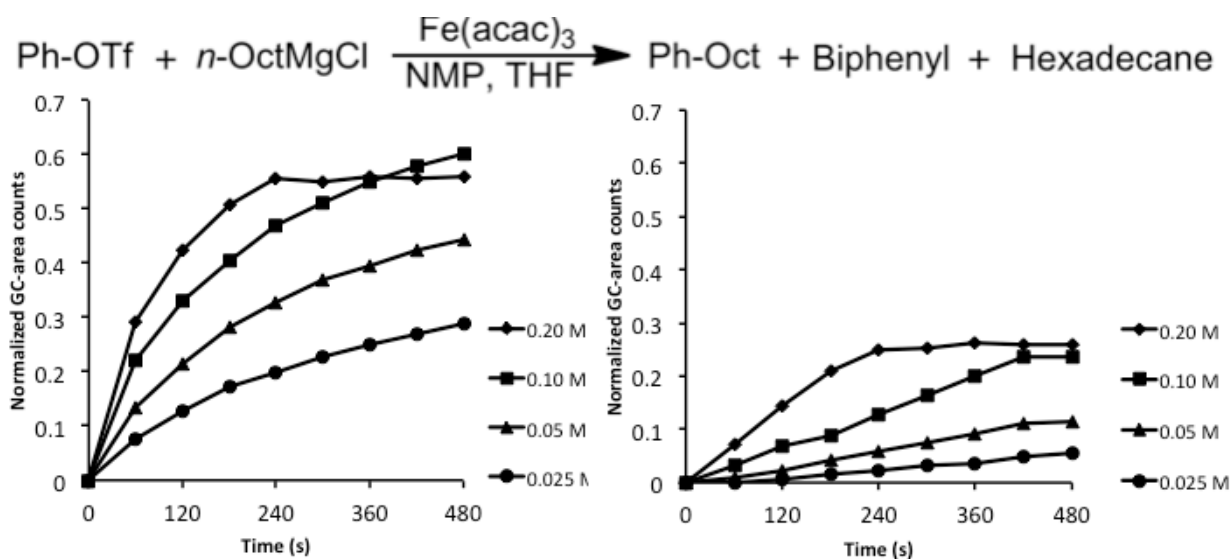
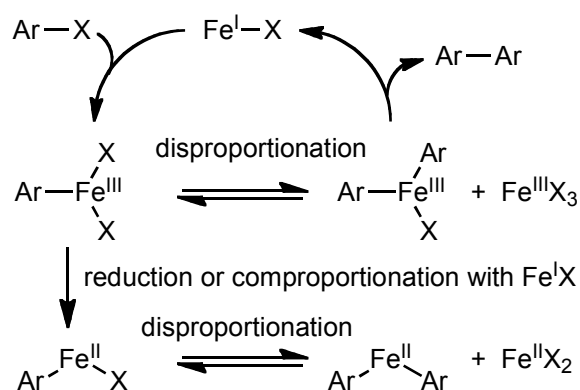


Figure 37. Formation of the coupling product octyl benzene (left) and biphenyl (right) at varying concentrations

Unfortunately, catalyst deactivation was observed at all concentrations, most notably at higher concentrations of substrate, where the catalyst activity diminished almost completely after an initial eruption. This behavior was somewhat surprising, since our previous report stated that increased amount of substrate protected the active catalyst (Paper V). However, when comparing

these two studies, it is important to remember that the experimental systems were very different. In the previously conducted examination, the concentration of the Grignard reagent was constantly low, whereas in the later study there was a higher concentration of Grignard reagent at all times, yielding a more reducing environment. Nevertheless, we did not expect the iron catalyst to deactivate faster in an environment consisting of more of the “oxidant”, phenyl triflate. We can only explain this behavior with the existence of several catalyst deactivation pathways.

Alonso *et al.* have shown that poly-aryl iron species can be isolated.^[160a] These complexes are formed from exchange reactions between iron centers, or by several oxidative additions and electron transfer reductions in succession. Reactions like this would inevitably give rise to biphenyl formation through reductive elimination from diphenyl Fe^{III} complexes. Indeed, the formation of biphenyl increases more rapidly than the desired product when increasing the concentration of phenyl triflate (Figure 37). The catalytically inactive species that is formed could be a Ph₄Fe^{III} anion,^[160a] which would not undertake a reductive elimination, or, due to the reducing environment, a Ph₂Fe^{II} species, which also is known to be reluctant to perform a reductive elimination as shown in Scheme 33 (Paper V).



Scheme 33. Disproportionation pathways to arylated iron species

The final component that was varied was the iron catalyst, Fe(acac)₃, which was varied from 0.25-5 mM, corresponding to 1-20 mol%. Following the pattern from the previous reagents, the reaction order was positive at low concentrations, and the reaction rate increased up to ca 2 mM (Figure 38).

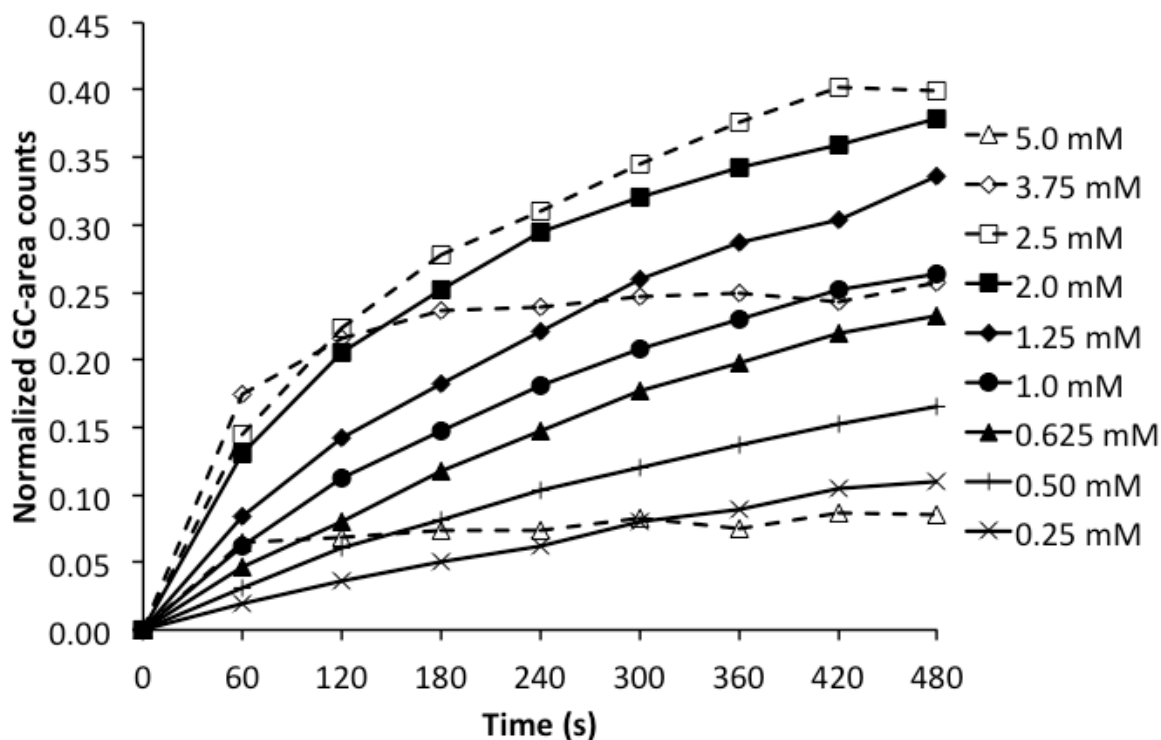
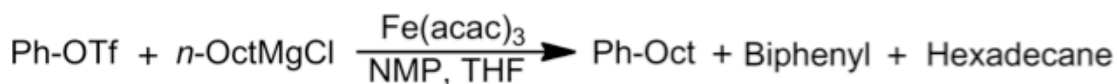


Figure 38. Formation of octylbenzene with varying amount of the iron catalyst

With increasing concentrations of the catalyst, the level of catalyst deactivation seemed to increase as well. As can be seen in Figure 38, the most dilute catalyst has almost no curvature, indicating an absence of catalyst deactivation, and the highest catalyst concentration exhibits a short burst of catalytic activity followed by catalyst death, similar to what could be observed for the aryl triflate experiment series. We can only interpret this as a bimolecular catalyst deactivation. Previous work has shown that reductive elimination from mononuclear Fe^{II} is disfavored, but that a binuclear Fe^{II} can occur (Paper V). To explain the observed plots, one can envision a comproportionation between Fe^{I} and Fe^{III} to Fe^{II} . The formed Fe^{II} species can react to form product in a bimolecular process, albeit it would be slower than the $\text{Fe}^{\text{I}} - \text{Fe}^{\text{III}}$ cycle, giving Fe^{I} . The same processes, instead forming unreactive Ph_nFe complexes, could rationalize the catalyst deactivation. The increased amounts of biphenyl at higher concentration of iron catalyst support this suggestion (Figure 39).

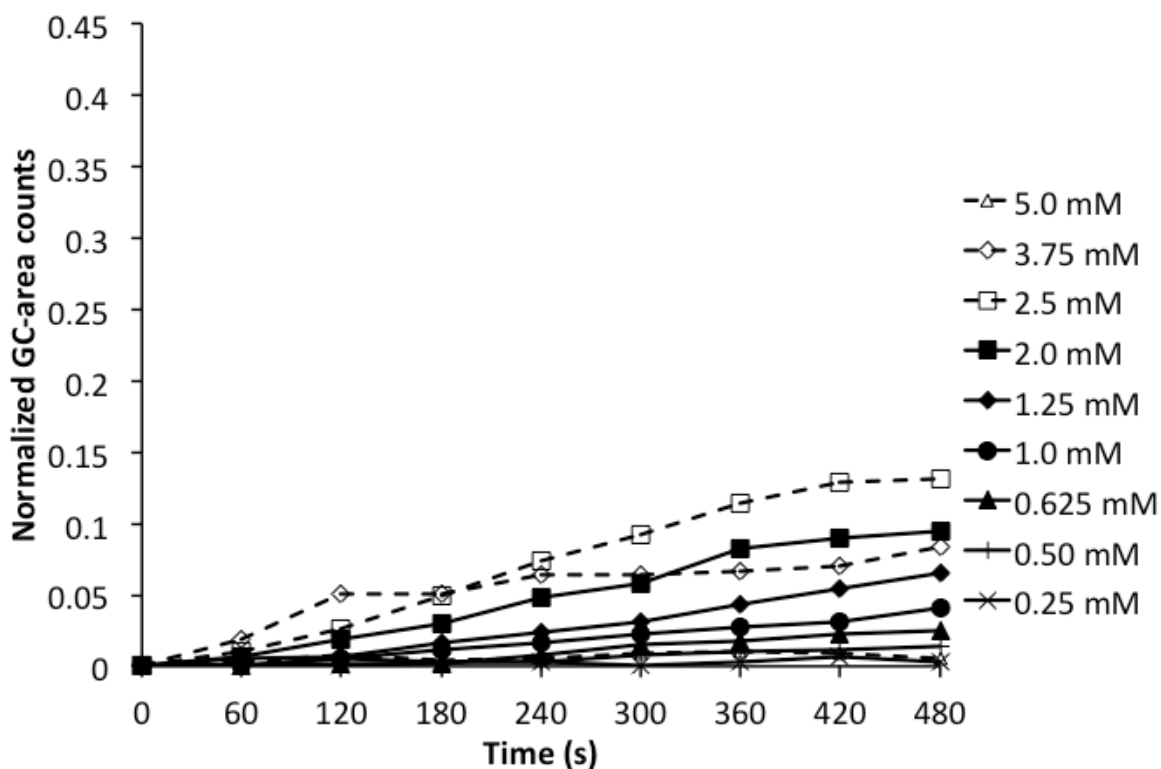
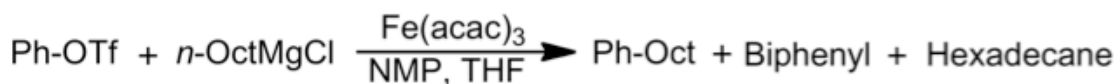


Figure 39. Formation of biphenyl at varying concentrations of iron catalyst

4.3.8 Theoretical examination of low temperature cross coupling in a reducing environment

The strongly reducing environment in the kinetic investigation might suppress the catalytically active $\text{Fe}^{\text{I}} - \text{Fe}^{\text{III}}$ cycle, and replace this with the more reduced $\text{Fe}^0 - \text{Fe}^{\text{II}}$ cycle. As a comparison, the free energy surface of the $\text{Fe}^0 - \text{Fe}^{\text{II}}$ cycle was calculated (Figure 40), in order to investigate whether this cycle could perform the catalytic cycle. According to the free energy surface, all steps of this more reduced cycle, are less efficient than in the $\text{Fe}^{\text{I}} - \text{Fe}^{\text{III}}$ cycle. Common knowledge suggests that a Fe^0 species should more easily perform a oxidative addition than a similar Fe^{I} species. That is not true here however, probably because the oxidative addition involves additional steps, such as the coordination of a π -system.

The barrier for the oxidative addition (**TS4.f**) in the $\text{Fe}^0 - \text{Fe}^{\text{II}}$ cycle is 87 kJ mol^{-1} , which is rather modest, but hard to fit with the low-temperature setting of this reaction. The subsequent transmetalation has an insignificant barrier from a bimetallic complex. The structure (**4.13**) in Figure 40 is in fact an energy minimum, which on the potential energy surface is lower in energy than the flanking structures. On the PES, this reaction is almost barrierless, and takes place without saddle points, indicating very low free energy barriers.^[107b] The final reductive

elimination is definitely the prohibiting step with a barrier of 204 kJ mol⁻¹ (TS4.g), making it impossible to reform the Fe⁰ species required to close the catalytic cycle.

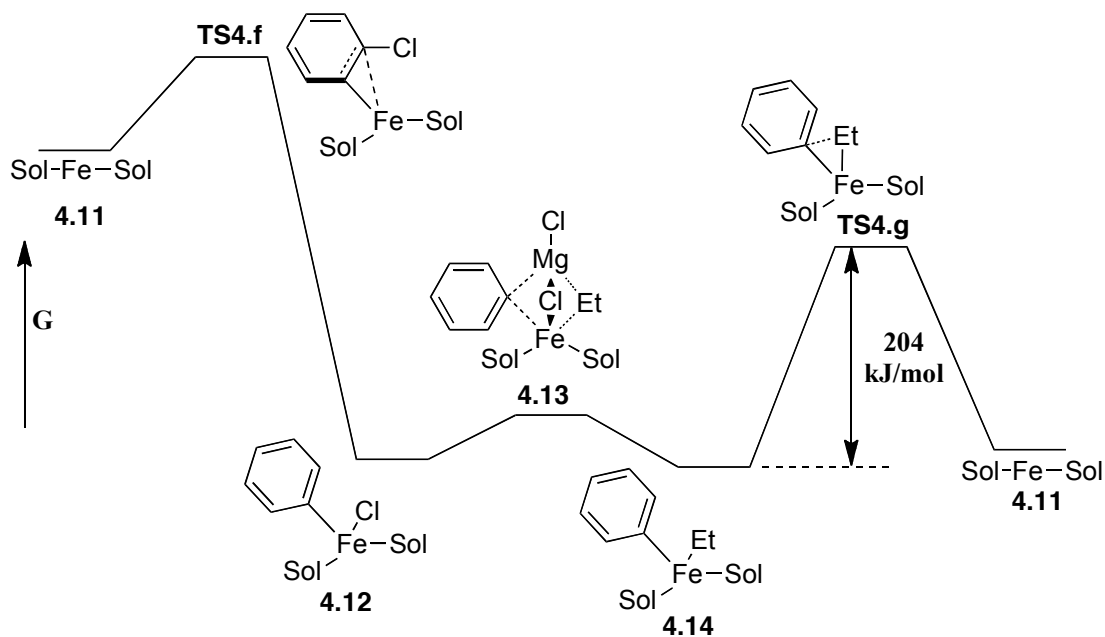
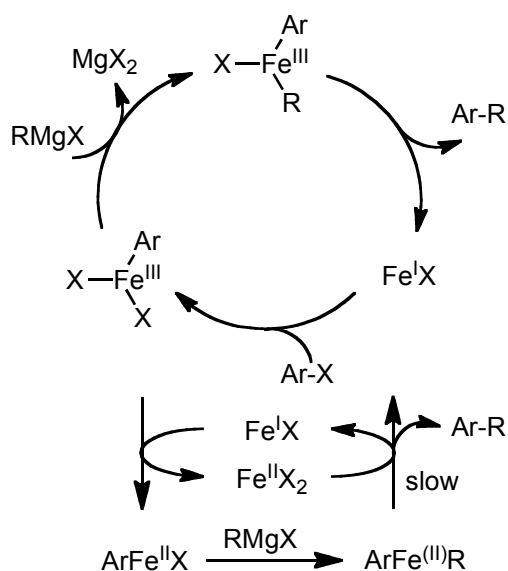


Figure 40. Free energy surface of the Fe⁰-Fe^{II} cycle

The above-mentioned results indicate that the iron catalyst is reduced but not as far as to Fe⁰. This would imply that Fe^{III} complexes that are reduced to less active Fe^{II} species is the main path towards catalyst deactivation. This process can occur through single electron transfer (SET) from the Grignard reagent or through comproportionation (Scheme 34). Fe^{II} species cannot perform a mononuclear reductive elimination, but can partake in a transmetalation or inefficient binuclear couplings. Coupling, leading to the reformation of Fe^I catalyst is still viable, even if this is a slow reaction (Paper V).



Scheme 34. Plausible catalytic cycles in a highly reducing environment

4.3.9 Conclusions

A titration experiment of the iron catalyzed cross coupling reaction has disclosed that the active catalyst, most probably is a Fe^{I} species. Furthermore, a computational study supported this suggestion, and revealed that the catalytic cycle is a $\text{Fe}^{\text{I}} - \text{Fe}^{\text{III}}$ cycle closed by a reductive elimination and preceded by a rate-limiting oxidative addition and a transmetalation, even if the order of these two steps could not be deduced. Iron in lower oxidation states can enter the catalytic cycle, but is unable to complete the catalytic cycle with a reductive elimination.

In the oxidative addition, a significant spin transfer to the aryl moiety could be shown, and this can explain why electron-rich substrates still perform the coupling rather unhindered. In spite of this, the radical character on the aromatic ring is not sufficiently strong to cause the electron-rich substrates to be faster than the unsubstituted versions as would be expected from a purely radical reaction.

The cross coupling has been shown to tolerate low temperatures, even if the scope is somewhat narrow, with electron-withdrawing substrates being able to complete the reaction at much lower temperatures than the unsubstituted or electron-rich counterparts.

Initial rate studies could further strengthen the hypothesis that a $\text{Fe}^{\text{I}} - \text{Fe}^{\text{III}}$ cycle is responsible for the catalytic activity of the iron catalyst, and several potentially problematic catalyst deactivation pathways were identified. The main process of these non-productive paths seems to be a bimolecular process, forming Fe^{II} complexes with low or no reactivity. In particular, stable poly-aryl iron complexes appear to be inert in further catalytic reactions.

Computational studies have supported this hypothesis and shown good agreement between experimental reactivity and calculated barriers. In addition, the inability of Fe^0 to close a catalytic cycle has been presented, and an alternative way for Fe^{II} species to re-enter the catalytic cycle through a slow bi-nuclear step has been suggested.

In conclusion, the $\text{Fe}^{\text{I}} - \text{Fe}^{\text{III}} - \text{Fe}^{\text{I}}$ cycle is the most plausible catalytic cycle for the iron catalyzed cross coupling, with lower oxidation states unable to perform the necessary reductive elimination step. The existence of several rapid deactivation pathways has been identified, and measures to avoid these have been presented.

5. Summary and concluding remarks

The importance of transition metal catalyzed reactions has been proven many times during the last 50 years, most notably by the many Nobel laureates in the field. One of the most important ways to advance the research has been through careful mechanistic investigations, which have revealed many significant properties for the different reactions. The areas covered in this thesis have not been an exception, and several studies of the palladium catalyzed allylic alkylation or Mizoroki-Heck reactions, as well as cross coupling reactions, have been performed. Nevertheless, there is still a great need for more knowledge about the mechanisms for these reactions.

In the field of the palladium catalyzed allylic alkylation, many different factors can influence the regioisomeric outcome of the reaction. In an attempt to isolate and study some of these effects, a tethered ligand was employed. An initial experimental study was followed by a computational investigation that could reproduce the experimental results. The factors controlling the regioselectivity of the reaction were investigated and revealed that the preference for the nucleophilic attack depended heavily on the steric hindrance as well as on the enforced rotation of the allylic moiety.

The mechanism for the synthesis of sulfoxides through a palladium catalyzed sulfinylation reaction was studied computationally. A new viable method to study this system was presented and could accurately reproduce the experimental results. The importance of a palladium catalyzed Mislow-Braverman-Evans rearrangement to reach the correct product was also shown.

The Mizoroki-Heck reaction has been investigated in two different studies. The reason for the importance of the re-oxidant benzoquinone in a domino Mizoroki-Heck-Suzuki reaction has been revealed. It was shown to allow access to a low-energy pathway to the new diarylation reaction. In addition to this, a new nickel catalyzed Mizoroki-Heck reaction has been presented. The novel mild conditions provide new possibilities for this cross coupling reaction. The computational study supported the mechanistic proposal of a cationic catalytic cycle and the free energy surface was compatible with the reaction conditions. The investigation could also explain the reason why some additives reduced the reactivity of the nickel catalysts.

The mechanism for iron, as an environmentally friendly alternative to the classic cross coupling metals, has also been studied. Several kinetic and computational studies have been performed. The plausible oxidation state for the active catalyst, as well as pathways leading to catalyst deactivation have been revealed. The catalytic cycle for the proposed Fe(I) – Fe(III) cycle was presented, revealing two possible pathways with either the oxidative addition or the transmetalation as the initial step. Since the difference between the reaction barriers is small, the

preferred reaction pathway could not be determined. In addition, the scope of the reaction at low temperatures and the reaction orders of the participating reactants and the catalyst have been investigated. The results from the study of the reaction order showed positive orders for both reactants and the catalyst. However, irregularities, such as the curvature of the plots indicated a dual catalyst activity. Most probably, the initially formed, highly active iron catalyst, was converted by excess Grignard to a less active form. Also, excess of the substrate and large catalyst loadings displayed catalyst deactivation. Oligomerization or over-reduction of the catalyst have been presented as reasons for these effects.

6. Outlook

The need for more thorough knowledge about the mechanisms and optimal conditions for new and existing reactions is still large. The kinetic investigation methods employed in this thesis have been used for many years, but can still give much mechanistic information about a reaction. In conjunction with computational efforts, which has seen great progress the last decades, a versatile tool to uncover mechanistic details is available.

The continuous development of processing speed for computers has enabled computational chemists to explore new areas, such as biochemical reactions with large enzymes, but also made it possible to do more exact calculations on moderately large systems, such as transition metal catalyzed reactions. One example of this is the different dispersion correction methods that have emerged lately. The importance of these interactions has been exemplified in this thesis for the palladium catalyzed domino Mizoroki-Heck-Suzuki reaction. Here the inclusion of a correction term was imperative in order to achieve accurate results. Even if these methods to date are not perfect, the impact they have had must be stressed. In the future, inclusion of a dispersion correction will probably be mandatory in all computational work.

In this thesis the calculations on the iron catalyzed cross coupling reactions have been without adding any dispersion correction. This was done because of the small size of the system, and assumed lack of important dispersion interaction. However, several issues such as the number of explicit solvent molecules to include can probably be influenced by inclusion of a correction method. These reactions are still not thoroughly understood, and much research is required to fully comprehend this area. One interesting topic to study further would be the possibility to synthesize a stable iron(I) complex that can be used in a coupling reaction. So far, only pre-catalysts are employed, or synthetically challenging or unstable iron complexes. Therefore, there is a need for a stable and reliable source for an iron(I) catalyst able to carry out the cross coupling.

Further studies of the palladium catalyzed allylic alkylation can include other nucleophiles, such as substituted malonates, or heteroatom nucleophiles. The influence on the selectivity by changing the nucleophiles would be an interesting continuation of the project. The computational part of this research extension will of course include the above-mentioned dispersion correction, since possible van der Waals interactions will be an important part of the nature of the nucleophile.

Another possible area for further research, as well as the employment of the dispersion effects, is the arylation version of the sulfinylation reaction. This reaction has not been mechanistically

studied and would be interesting to explore. The computational part would certainly benefit from dispersion corrections, most notably due to the presence of aryl groups.

The newly developed nickel catalyzed Mizoroki-Heck reaction can be further improved. The scope of the vinyls can be extended beyond the vinyl ethers, and also the need for aryl triflates as substrate might be possible to alleviate. Since a computational study already has been performed, a combination of calculations and experimental work is probably the best way to advance this reaction.

7. Acknowledgements

Det är många som ska ha ett stort tack för stöd, idéer, uppmuntran, sällskap, kärlek, tålamod, kunskap och allt annat som kan tänkas ha hjälpt mig under de här nästan fem åren.

Först och allra främst, **Per-Ola Norrby**, fantastisk handledare, och världens största idéspruta. I mitt projekt har många idéer blivit testade, vissa har funkade, andra nästan, somliga definitivt inte, men det är oerhört skönt att alltid kunna få mer att göra! Sedan är det inte fel att PO lyckas kombinera idéerna med en fantastisk kunskap, som han gärna delar med sig av, samt med en entusiasm som är få förunnad.

Min examinerare, **Kristina Luthman**, frågar, lyssnar, förstår som få andra.

Mina två biträdande handledare. **Sten Nilsson Lill**, med din fantastiska förmåga att alltid hjälpa till och dela med sig av tips och tricks, om det fanns ett Nobelpris i hjälpsamhet skulle du prenumerera på det! **Göran Hilmersson**, med framförallt de träningsrelaterade diskussionerna, det är skönt att det finns någon mer på våning 8 som uppskattar att röra på sig.

Medlemmar i grupp Norrby är värda ett stort tack, in order of appearance.

Anna, för din pålitlighet, hjälpsamhet och trevligt sällskap på konferenser, men tänk på att Dagmar inte är ett killnamn!

PF, framförallt för din humor, konferenssällskap, för tillfällena att få diskutera annat än kemi på jobbet, och för 10 år i kemihuset.

Charlotte, för trevligt rumssällskap, bra samarbete samt dålig humor!

Carina, Petra och **Elaine** för trevligt sällskap.

Jobbar man i POs grupp duggar samarbetena tätt, så en runda tacksamhet till de som jag har samarbetat med under åren:

Prof. **Giovanni Poli**, for letting me stay for 5 weeks in his group in Paris, also **Steven Giboulot** was a great support during my STSM.

Prof. **Troels Skrydstrup** and his group, especially **Thomas Gøgsig**, in Aarhus, Denmark, for providing an excellent scientific challenge and great collaboration.

Christian Sköld, Uppsala, för ett mycket bra samarbete, samt intressant projekt.

Många andra har passerat genom grupp Norrby, som exjobbare, STSM-gäster eller annat. **Kenan, Parisa, Albin, Emelie, Peter, Erik, Volker, Julie, Helene, Steffi, Aaron** och **Javier**. Ni förtjänar ett tack för att ni alla bidragit med kunskap, stämning samt i vissa fall ett tillfälle till att öva på engelskan.

Mina medförfattare, vissa har redan nämnts ovan, **Guillaume Prestat, Sverker Hansson, Björn Åkermark, Susanne Olsson** (grym röntgeninsats!), **Mikael Håkansson, Mats Larhed, Alejandro Trejos** samt **Luke Odell** ska ha ett stort tack för bra samarbete.

Alla andra på våning 8 och 9 för att ni lyckas göra det till en plats som är roligt att gå till, fortsatt som ni gör! Ett speciellt tack riktas till **Bisse** för trevligt sällskap i SF, samt för alla rövarhistorier, utan dem skulle åren varit mycket tråkigare.

Alla andra som jag umgås med utanför kemihuset förtjänar en stor eloge för att ha bidragit med möjligheten att slappna av, ha roligt och tänka på annat. Framförallt **Kalle** ska en medalj för alla träningstimmar som han har ställt upp på.

Min **familj**, tack för stödet, även om det finns lite att jobba på när det gäller förståelsen.

Charlie, inga ord kan förklara hur mycket du betyder.

Hard pressed on my right; my left is in retreat.
My centre is yielding. Impossible to maneuver.
Situation excellent. I am attacking.

General Ferdinand Foch

7. References

- [1] a) G. Natta, P. Pino, P. Corradini, F. Danusso, E. Mantica, G. Mazzanti, G. Moraglio, *J. Am. Chem. Soc.* **1955**, *77*, 1708-1710; b) K. Ziegler, E. Holzkamp, H. Breil, H. Martin, *Angew. Chem. Int. Ed.* **1955**, *67*, 541-547; c) G. Natta, *Angew. Chem. Int. Ed.* **1956**, *68*, 393-403.
- [2] R. Jira, *Angew. Chem. Int. Ed.* **2009**, *48*, 9034-9037.
- [3] a) http://www.nobelprize.org/nobel_prizes/chemistry/laureates/2001/;
b) http://www.nobelprize.org/nobel_prizes/chemistry/laureates/2005/;
c) http://www.nobelprize.org/nobel_prizes/chemistry/laureates/2010/;
- [4] a) S. M. Ma, Z. Lu, *Angew. Chem. Int. Ed.* **2008**, *47*, 258-297; b) B. M. Trost, M. L. Crawley, *Chem. Rev.* **2003**, *103*, 2921-2943; c) B. M. Trost, D. L. VanVranken, *Chem. Rev.* **1996**, *96*, 395-422.
- [5] J. Tsuji, H. Takahashi, M. Morikawa, *Tetrahedron Lett.* **1965**, 4387-4388.
- [6] a) B. M. Trost, T. J. Dietsche, *J. Am. Chem. Soc.* **1973**, *95*, 8200-8201; b) B. M. Trost, T. J. Fullerton, *J. Am. Chem. Soc.* **1973**, *95*, 292-294; c) B. M. Trost, P. E. Strege, *J. Am. Chem. Soc.* **1977**, *99*, 1649-1651; d) B. M. Trost, T. R. Verhoeven, *J. Org. Chem.* **1976**, *41*, 3215-3216.
- [7] a) J. Hartwig, *Organotransition Metal Chemistry*, University Science Books, **2010**; b) L. S. Hegedus, *Organometallics in synthesis, A manual*, (Ed. M. Schlosser) John Wiley & Sons Ltd., West Sussex, **2001**.
- [8] a) J. C. Fiaud, J. L. Malleron, *J. Chem. Soc. Chem. Comm.* **1981**, 1159-1160; b) M. Braun, T. Meier, *Synlett* **2006**, 661-676; c) M. Braun, T. Meier, *Angew. Chem. Int. Ed.* **2006**, *45*, 6952-6955; d) X. L. Hou, W. H. Zheng, B. H. Zheng, Y. Zhang, *J. Am. Chem. Soc.* **2007**, *129*, 7718-7719.
- [9] M. Peuckert, W. Keim, *Organometallics* **1983**, *2*, 594-597.
- [10] J. Chatt, B. L. Shaw, *J. Chem. Soc.* **1962**, 5075-5084.
- [11] P. L. Watson, D. C. Roe, *J. Am. Chem. Soc.* **1982**, *104*, 6471-6473.
- [12] a) T. Mizoroki, K. Mori, A. Ozaki, *Bull. Chem. Soc. Jpn.* **1971**, *44*, 581; b) R. F. Heck, J. P. Nolley, *J. Org. Chem.* **1972**, *37*, 2320-2322.
- [13] K. Tamao, K. Sumitani, M. Kumada, *J. Am. Chem. Soc.* **1972**, *94*, 4374-4376.
- [14] J. P. Corriu, J. P. Masse, *J. Chem. Soc. Chem. Comm.* **1972**, 144.
- [15] a) L. Cassar, *J. Organomet. Chem.* **1975**, *93*, 253-257; b) H. A. Dieck, F. R. Heck, *J. Organomet. Chem.* **1975**, *93*, 259-263; c) K. Sonogashira, Y. Tohda, N. Hagihara, *Tetrahedron Lett.* **1975**, 4467-4470; d) M. Yamamura, I. Moritani, S. I. Murahashi, *J. Organomet. Chem.* **1975**, *91*, C39-C42; e) S. I. Murahashi, M. Yamamura, N. Mita, *J. Org. Chem.* **1977**, *42*, 2870-2874; f) S. I. Murahashi, M. Yamamura, K. Yanagisawa, N. Mita, K. Kondo, *J. Org. Chem.* **1979**, *44*, 2408-2417.
- [16] a) N. Miyaura, K. Yamada, A. Suzuki, *Tetrahedron Lett.* **1979**, *20*, 3437-3440; b) N. Miyaura, H. Suginome, A. Suzuki, *Tetrahedron Lett.* **1981**, *22*, 127-130; c) N. Miyaura, K. Yamada, H. Suginome, A. Suzuki, *J. Am. Chem. Soc.* **1985**, *107*, 972-980.
- [17] E. Negishi, A. O. King, N. Okukado, *J. Org. Chem.* **1977**, *42*, 1821-1823.
- [18] Y. Hatanaka, T. Hiyama, *J. Org. Chem.* **1988**, *53*, 918-920.
- [19] J. K. Stille, *Pure Appl. Chem.* **1985**, *57*, 1771-1780.
- [20] C. J. Cramer, *Essentials of Computational Chemistry: Theories and Models*, Wiley-VCH, Weinheim, **2004**.
- [21] F. Jensen, *Introduction to Computational Chemistry*, Wiley-VCH, Weinheim, **2006**.
- [22] a) A. D. Becke, *J. Chem. Phys.* **1993**, *98*, 5648-5652; b) A. D. Becke, *J. Chem. Phys.* **1993**, *98*, 1372-1377.
- [23] M. J. Ramos, S. F. Sousa, P. A. Fernandes, *J. Phys. Chem. A* **2007**, *111*, 10439-10452.
- [24] a) C. T. Lee, W. T. Yang, R. G. Parr, *Phys. Rev. B* **1988**, *37*, 785-789; b) P. J. Stephens, F. J. Devlin, C. F. Chabalowski, M. J. Frisch, *J. Phys. Chem.* **1994**, *98*, 11623-11627.

- [25] Y. Zhao, D. G. Truhlar, *Acc. Chem. Res.* **2008**, *41*, 157-167.
- [26] S. Grimme, J. Antony, S. Ehrlich, H. Krieg, *J. Chem. Phys.* **2010**, *132*, 154104.
- [27] P. J. Hay, W. R. Wadt, *J. Chem. Phys.* **1985**, *82*, 299-310.
- [28] J. Tomasi, B. Mennucci, R. Cammi, *Chem. Rev.* **2005**, *105*, 2999-3093.
- [29] a) D. J. Tannor, B. Marten, R. Murphy, R. A. Friesner, D. Sitkoff, A. Nicholls, M. Ringnalda, W. A. Goddard, B. Honig, *J. Am. Chem. Soc.* **1994**, *116*, 11875-11882; b) B. Marten, K. Kim, C. Cortis, R. A. Friesner, R. B. Murphy, M. N. Ringnalda, D. Sitkoff, B. Honig, *J. Phys. Chem.* **1996**, *100*, 11775-11788.
- [30] S. Kozuch, S. Shaik, *Acc. Chem. Res.* **2011**, *44*, 101-110.
- [31] H. Maskill, *The Physical Basis of Organic Chemistry*, Oxford University Press, Oxford, **1985**.
- [32] R. Crabtree, *The Organometallic Chemistry of the Transition Metals*, John Wiley & Sons, Inc., Hoboken, New Jersey, **2005**.
- [33] A. Miyashita, A. Yasuda, H. Takaya, K. Toriumi, T. Ito, T. Souchi, R. Noyori, *J. Am. Chem. Soc.* **1980**, *102*, 7932-7934.
- [34] B. M. Trost, D. L. Vanvraken, C. Bingel, *J. Am. Chem. Soc.* **1992**, *114*, 9327-9343.
- [35] a) G. J. Dawson, C. G. Frost, J. M. J. Williams, *Tetrahedron Lett.* **1993**, *34*, 3149-3150; b) J. Sprinz, G. Helmchen, *Tetrahedron Lett.* **1993**, *34*, 1769-1772; c) P. von Matt, A. Pfaltz, *Angew. Chem., Int. Ed.* **1993**, *32*, 566-569.
- [36] a) T. Hayashi, T. Hagihara, M. Konishi, M. Kumada, *J. Am. Chem. Soc.* **1984**, *105*, 7767-7768; b) T. Hayashi, M. Konishi, M. Kumada, *J. Chem. Soc., Chem. Commun.* **1984**, 107-108.
- [37] a) J. E. Backvall, P. G. Andersson, *J. Am. Chem. Soc.* **1992**, *114*, 6374-6381; b) C. G. Frost, J. Howarth, J. M. J. Williams, *Tetrahedron Asymm.* **1992**, *3*, 1089-1122.
- [38] a) B. Åkermark, S. Hansson, B. Krakenberger, A. Vitagliano, K. Zetterberg, *Organometallics* **1984**, *3*, 679-682; b) B. Åkermark, K. Zetterberg, S. Hansson, B. Krakenberger, A. Vitagliano, *J. Organomet. Chem.* **1987**, *335*, 133-142; c) B. Åkermark, S. Hansson, B. Krakenberger, K. Zetterberg, A. Vitagliano, *Chem. Scr.* **1987**, *27*, 525.
- [39] a) T. Hayashi, K. Kishi, A. Yamamoto, Y. Ito, *Tetrahedron Lett.* **1990**, *31*, 1743-1746; b) R. Pretot, A. Pfaltz, *Angew. Chem. Int. Ed.* **1998**, *37*, 323-325; c) S. L. You, X. Z. Zhu, Y. M. Luo, X. L. Hou, L. X. Dai, *J. Am. Chem. Soc.* **2001**, *123*, 7471-7472.
- [40] a) M. Prat, J. Ribas, M. Morenomanas, *Tetrahedron* **1992**, *48*, 1695-1706; b) N. Vicart, B. Cazes, J. Gore, *Tetrahedron Lett.* **1995**, *36*, 535-538; c) N. Vicart, J. Gore, B. Cazes, *Synlett* **1996**, 850-852.
- [41] For some recent examples, see: a) D. Liu, F. Xie, W. B. Zhang, *Tetrahedron Lett.* **2007**, *48*, 7591-7594; b) D. J. Weix, J. F. Hartwig, *J. Am. Chem. Soc.* **2007**, *129*, 7720-7721.
- [42] E.-I. Negishi, S.-Y. Liou, *Handbook of Organopalladium Chemistry for Organic Synthesis*, (Ed. E.-I. Negishi) Wiley-Interscience, New York, **2002**.
- [43] a) E. Negishi, H. Matsushita, S. Chatterjee, R. A. John, *J. Org. Chem.* **1982**, *47*, 3188-3190; b) E. Negishi, F. T. Luo, A. J. Pecora, A. Silveira, *J. Org. Chem.* **1983**, *48*, 2427-2430; c) E. I. Negishi, S. Chatterjee, *Tetrahedron Lett.* **1983**, *24*, 1341-1344; d) F. T. Luo, E. Negishi, *Tetrahedron Lett.* **1985**, *26*, 2177-2180.
- [44] a) J. Tsuji, I. Minami, I. Shimizu, *Chem. Lett.* **1983**, 1325-1326; b) T. Baba, K. Nakano, S. Nishiyama, S. Tsuruya, M. Masai, *J. Chem. Soc. Chem. Comm.* **1990**, 348-349.
- [45] T. Tsuda, Y. Chujo, S. Nishi, K. Tawara, T. Saegusa, *J. Am. Chem. Soc.* **1980**, *102*, 6381-6384.
- [46] B. M. Trost, F. D. Toste, *J. Am. Chem. Soc.* **1999**, *121*, 4545-4554.
- [47] a) I. D. G. Watson, S. A. Styler, A. K. Yudin, *J. Am. Chem. Soc.* **2004**, *126*, 5086-5087; b) I. D. G. Watson, A. K. Yudin, *J. Am. Chem. Soc.* **2005**, *127*, 17516-17529; c) A. M. Johns, Z. J. Liu, J. F. Hartwig, *Angew. Chem. Int. Ed.* **2007**, *46*, 7259-7261.

- [48] a) A. Pfaltz, M. Lautens in *Comprehensive Asymmetric Catalysis*, (Eds.: E. N. Jacobsen, A. Pfaltz and H. Yamamoto), Springer, Berlin, **1999**, pp. 833 - 886; b) B. M. Trost, C. Lee in *Catalytic Asymmetric Synthesis*, (Ed. I. Ojima), Wiley-VCH, New York, **2000**, pp. 593-694.
- [49] a) B. M. Trost, D. L. Vanvrancen, *Angew. Chem. Int. Ed. Engl.* **1992**, *31*, 228-230; b) G. Knuhl, P. Sennhenn, G. Helmchen, *J. Chem. Soc. Chem. Comm.* **1995**, 1845-1846; c) B. M. Trost, B. Breit, S. Peukert, J. Zambrano, J. W. Ziller, *Angew. Chem. Int. Ed. Engl.* **1995**, *34*, 2386-2388; d) B. M. Trost, A. C. Krueger, R. C. Bunt, J. Zambrano, *J. Am. Chem. Soc.* **1996**, *118*, 6520-6521; e) B. Wiese, G. Helmchen, *Tetrahedron Lett.* **1998**, *39*, 5727-5730; f) O. Pamies, M. Dieguez, C. Claver, *J. Am. Chem. Soc.* **2005**, *127*, 3646-3647.
- [50] a) V. Branchadell, M. Moreno-Manas, F. Pajuelo, R. Pleixats, *Organometallics* **1999**, *18*, 4934-4941; b) K. J. Szabo, *Chem. Soc. Rev.* **2001**, *30*, 136-143.
- [51] G. C. Lloyd-Jones, S. C. Stephen, *Chem.-Eur. J.* **1998**, *4*, 2539-2549.
- [52] a) M. Sjogren, S. Hansson, P. O. Norrby, B. Åkermark, M. E. Cucciolito, A. Vitagliano, *Organometallics* **1992**, *11*, 3954-3964; b) P. Fristrup, T. Jensen, J. Hoppe, P.-O. Norrby, *Chem.-Eur. J.* **2006**, *12*, 5352-5360.
- [53] S. Hansson, P. O. Norrby, M. P. T. Sjogren, B. Åkermark, M. E. Cucciolito, F. Giordano, A. Vitagliano, *Organometallics* **1993**, *12*, 4940-4948.
- [54] U. Kazmaier, D. Stolz, K. Kramer, F. L. Zumpe, *Chem.-Eur. J.* **2008**, *14*, 1322-1329.
- [55] a) T. Hayashi, A. Yamamoto, Y. Ito, E. Nishioka, H. Miura, K. Yanagi, *J. Am. Chem. Soc.* **1989**, *111*, 6301-6311; b) M. Kranenburg, P. C. J. Kamer, P. W. N. M. van Leeuwen, *Eur. J. Inorg. Chem.* **1998**, 25-27; c) A. Frolander, S. Lutsenko, T. Privalov, C. Moberg, *J. Org. Chem.* **2005**, *70*, 9882-9891; d) S. M. Ma, Z. Lu, *Angew. Chem. Int. Ed.* **2008**, *47*, 258-297.
- [56] J. D. Oslob, B. Åkermark, P. Helquist, P. O. Norrby, *Organometallics* **1997**, *16*, 3015-3021.
- [57] a) A. Dedieu, *Chem. Rev.* **2000**, *100*, 543-600; b) J. Kleimark, P.-O. Norrby in *Transition Metal Catalyzed Enantioselective Allylic Substitution in Organic Synthesis*, (Ed. U. Kazmaier), Springer, **2011**.
- [58] H. Hagelin, B. Åkermark, P. O. Norrby, *Organometallics* **1999**, *18*, 2884-2895.
- [59] N. Svensen, P. Fristrup, D. Tanner, P. O. Norrby, *Adv. Synth. Catal.* **2007**, *349*, 2631-2640.
- [60] C. Johansson, G. C. Lloyd-Jones, P. O. Norrby, *Tetrahedron Asymm.* **2010**, *21*, 1585-1592.
- [61] a) P. O. Norrby, *Ph. D. Thesis*, **1992**; b) P. O. Norrby, B. Åkermark, F. Haeffner, S. Hansson, M. Blomberg, *J. Am. Chem. Soc.* **1993**, *115*, 4859-4867.
- [62] M. E. Krafft, M. Sugiura, K. A. Abboud, *J. Am. Chem. Soc.* **2001**, *123*, 9174-9175.
- [63] a) M. E. Krafft, Z. Fu, M. J. Procter, A. M. Wilson, O. A. Dasse, C. Hirose, *Pure Appl. Chem.* **1998**, *70*, 1083-1090; b) M. E. Krafft, A. M. Wilson, Z. Fu, M. J. Procter, O. A. Dasse, *J. Org. Chem.* **1998**, *63*, 1748-1749.
- [64] K. Itami, T. Koike, J. Yoshida, *J. Am. Chem. Soc.* **2001**, *123*, 6957-6958.
- [65] M. P. T. Sjogren, S. Hansson, B. Åkermark, A. Vitagliano, *Organometallics* **1994**, *13*, 1963-1971.
- [66] B. Åkermark, B. Krakenberger, S. Hansson, A. Vitagliano, *Organometallics* **1987**, *6*, 620-628.
- [67] R. Mccrindle, E. C. Alyea, G. Ferguson, S. A. Dias, A. J. Mcalees, M. Parvez, *J. Chem. Soc. Dalton* **1980**, 137-144.
- [68] a) O. Reiser, *Angew. Chem. Int. Ed. Engl.* **1993**, *32*, 547-549; b) E. PenaCabrera, P. O. Norrby, M. Sjogren, A. Vitagliano, V. DeFelice, J. Oslob, S. Ishii, D. O'Neill, B. Åkermark, P. Helquist, *J. Am. Chem. Soc.* **1996**, *118*, 4299-4313; c) P. Dierkes, S. Ramdeehul, L. Barloy, A. De Cian, J. Fischer, P. C. J. Kamer, P. W. N. M. van Leeuwen, J. A. Osborn, *Angew. Chem. Int. Ed.* **1998**, *37*, 3116-3118.
- [69] a) R. P. Bell, *Proc. R. Soc. Lond. A* **1936**, *154*, 414-429; b) M. G. Evans, M. Polanyi, *Trans. Faraday Soc.* **1936**, *32*, 1333-1360; c) F. Jensen, *Introduction to Computational Chemistry*, Wiley, Chichester, **1999**.
- [70] G. S. Hammond, *J. Am. Chem. Soc.* **1955**, *77*, 334-338.

- [71] P. O. Norrby, *J. Mol. Struct. - Theochem* **2000**, *506*, 9-16.
- [72] M. Mellah, A. Voituriez, E. Schulz, *Chem. Rev.* **2007**, *107*, 5133-5209.
- [73] M. C. Carreno, *Chem. Rev.* **1995**, *95*, 1717-1760.
- [74] a) R. Bentley, *Chem. Soc. Rev.* **2005**, *34*, 609-624; b) J. Legros, J. R. Dehli, C. Bolm, *Adv. Synth. Catal.* **2005**, *347*, 19-31.
- [75] a) S. Patai, Rappoport, Z., Stirling, C. J. M. in *The Chemistry of Sulphones and Sulphoxides*, John Wiley, New York, **1988**, p. 56; b) P. C. B. Page, *Organosulfur Chemistry II.*, Springer, Berlin, Germany, **1999**; c) *Organosulfur Chemistry in Asymmetric Synthesis*, (Ed. T. B. Toru, C.) Wiley-VCH, Weinheim, **2008**.
- [76] G. Maitro, G. Prestat, D. Madec, G. Poli, *J. Org. Chem.* **2006**, *71*, 7449-7454.
- [77] C. B. Caupéne, C.; Perrio, S.; Metzner, P., *J. Org. Chem.* **2005**, *70*, 2812-2815.
- [78] G. Maitro, S. Vogel, G. Prestat, D. Madec, G. Poli, *Org. Lett.* **2006**, *8*, 5951-5954.
- [79] G. Maitro, S. Vogel, M. Sadaoul, G. Prestat, D. Madec, G. Poli, *Org. Lett.* **2007**, *9*, 5493-5496.
- [80] a) E. Bernoud, G. Le Duc, X. Bantreil, G. Prestat, D. Madec, G. Poli, *Org. Lett.* **2010**, *12*, 320-323; b) G. Maitro, G. Prestat, D. Madec, G. Poli, *Tetrahedron Asymm.* **2010**, *21*, 1075-1084.
- [81] a) D. R. Rayner, E. G. Miller, P. Bickart, A. J. Gordon, K. Mislow, *J. Am. Chem. Soc.* **1966**, *88*, 3138-3139; b) S. Braverman, Y. Stabinsky, *Chem. Commun.* **1967**, 270-271; c) P. Bickart, F. W. Carson, J. Jacobus, E. G. Miller, K. Mislow, *J. Am. Chem. Soc.* **1968**, *90*, 4869; d) D. A. Evans, G. C. Andrews, C. L. Sims, *J. Am. Chem. Soc.* **1971**, *93*, 4956-4957; e) D. A. Evans, G. C. Andrews, *Acc. Chem. Res.* **1974**, *7*, 147-155.
- [82] D. K. Jones-Hertzog, W. L. Jorgensen, *J. Am. Chem. Soc.* **1995**, *117*, 9077-9078.
- [83] D. K. Jones-Hertzog, W. L. Jorgensen, *J. Org. Chem.* **1995**, *60*, 6682-6683.
- [84] a) T. H. Dunning, *J. Chem. Phys.* **1989**, *90*, 1007-1023; b) R. A. Kendall, T. H. Dunning, R. J. Harrison, *J. Chem. Phys.* **1992**, *96*, 6796-6806; c) D. E. Woon, T. H. Dunning, *J. Chem. Phys.* **1993**, *98*, 1358-1371; d) D. E. Woon, T. H. Dunning, *J. Chem. Phys.* **1994**, *100*, 2975-2988.
- [85] a) J. Amaudrut, D. J. Pasto, O. Wiest, *J. Org. Chem.* **1998**, *63*, 6061-6064; b) J. Amaudrut, O. Wiest, *J. Am. Chem. Soc.* **2000**, *122*, 3367-3374.
- [86] L. E. Overman, F. M. Knoll, *Tetrahedron Lett.* **1979**, 321-324.
- [87] E. D. Glendening; J. K. Badenhop; A. E. Reed; J. E. Carpenter, J. A. Bohmann, C. M. Morales, F. Weinhold in *NBO 5.0*, Theoretical Chemistry Institute, University of Wisconsin, Madison, WI, **2001**, <http://www.chem.wisc.edu/~nbo5>
- [88] a) P. Fristrup, M. Ahlquist, D. Tanner, P. O. Norrby, *J. Phys. Chem. A* **2008**, *112*, 12862-12867; b) C. P. Butts, E. Filali, G. C. Lloyd-Jones, P. O. Norrby, D. A. Sale, Y. Schramm, *J. Am. Chem. Soc.* **2009**, *131*, 9945-9957.
- [89] a) I. P. Beletskaya, A. V. Cheprakov, *Chem. Rev.* **2000**, *100*, 3009-3066; b) W. Cabri, I. Candiani, *Acc. Chem. Res.* **1995**, *28*, 2-7; c) A. De Meijere, F. E. Meyer, *Angew. Chem. Int. Edit.* **1994**, *33*, 2379-2411.
- [90] B. P. Carrow, J. F. Hartwig, *J. Am. Chem. Soc.* **2010**, *132*, 79-81.
- [91] H. A. Dieck, R. F. Heck, *J. Org. Chem.* **1975**, *40*, 1083-1090.
- [92] R. F. Heck, *J. Am. Chem. Soc.* **1969**, *91*, 6707-6714.
- [93] P. Fristrup, S. Le Qument, D. Tanner, P. O. Norrby, *Organometallics* **2004**, *23*, 6160-6165.
- [94] C. S. Cho, S. Uemura, *J. Organomet. Chem.* **1994**, *465*, 85-92.
- [95] X. L. Du, M. Suguro, K. Hirabayashi, A. Mori, T. Nishikata, N. Hagiwara, K. Kawata, T. Okeda, H. F. Wang, K. Fugami, M. Kosugi, *Org. Lett.* **2001**, *3*, 3313-3316.
- [96] a) Y. C. Jung, R. K. Mishra, C. H. Yoon, K. W. Jung, *Org. Lett.* **2003**, *5*, 2231-2234; b) M. M. S. Andappan, P. Nilsson, H. von Schenck, M. Larhed, *J. Org. Chem.* **2004**, *69*, 5212-5218.
- [97] a) B. L. Shaw, *New. J. Chem.* **1998**, *22*, 77-79; b) B. L. Shaw, S. D. Perera, *Chem. Commun.* **1998**, 1863-1864; c) V. P. W. Bohm, W. A. Herrmann, *Chem.-Eur. J.* **2001**, *7*, 4191-4197; d) D. J. Cardenas, B. Martin-Matute, A. M. Echavarren, *J. Am. Chem. Soc.* **2006**, *128*, 5033-5040.

- [98] a) C. M. Andersson, J. Larsson, A. Hallberg, *J. Org. Chem.* **1990**, *55*, 5757-5761; b) N. D. Duezo, J. C. de la Rosa, J. Priego, I. Alonso, J. C. Carretero, *Chem.-Eur. J.* **2001**, *7*, 3890-3900; c) M. Oestreich, *Eur. J. Org. Chem.* **2005**, 783-792.
- [99] a) M. Larhed, A. Trejos, A. Fardost, S. Yahiaoui, *Chem. Commun.* **2009**, 7587-7589; b) M. Larhed, S. Yahiaoui, A. Fardost, A. Trejos, *J. Org. Chem.* **2011**, *76*, 2433-2438.
- [100] M. S. Sigman, K. B. Urkalan, *Angew. Chem. Int. Ed.* **2009**, *48*, 3146-3149.
- [101] a) R. J. Deeth, A. Smith, K. K. Hii, J. M. Brown, *Tetrahedron Lett.* **1998**, *39*, 3229-3232; b) K. K. Hii, T. D. W. Claridge, J. M. Brown, A. Smith, R. J. Deeth, *Helv. Chim. Acta.* **2001**, *84*, 3043-3056; c) H. von Schenck, B. Åkermark, M. Svensson, *Organometallics* **2002**, *21*, 2248-2253; d) C. Amatore, A. Jutand, F. Lemaitre, J. L. Ricard, S. Kozuch, S. Shaik, *J. Organomet. Chem.* **2004**, *689*, 3728-3734; e) D. Balcells, F. Maseras, B. A. Keay, T. Ziegler, *Organometallics* **2004**, *23*, 2784-2796; f) R. J. Deeth, A. Smith, J. M. Brown, *J. Am. Chem. Soc.* **2004**, *126*, 7144-7151; g) L. J. Goossen, D. Koley, H. Hermann, W. Thiel, *Chem. Commun.* **2004**, 2141-2143; h) S. Kozuch, S. Shaik, A. Jutand, C. Amatore, *Chem.-Eur. J.* **2004**, *10*, 3072-3080; i) A. Stadler, H. von Schenck, K. S. A. Vallin, M. Larhed, A. Hallberg, *Adv. Synth. Catal.* **2004**, *346*, 1773-1781; j) Q. Chen, B. L. Lin, Y. Fu, L. Liu, Q. X. Guo, *Res. Chem. Intermediat.* **2005**, *31*, 759-767; k) G. T. de Jong, F. M. Bickelhaupt, *J. Phys. Chem. A* **2005**, *109*, 9685-9699; l) L. J. Goossen, D. Koley, H. L. Hermann, W. Thiel, *Organometallics* **2005**, *24*, 2398-2410; m) G. K. Datta, H. von Schenck, A. Hallberg, M. Larhed, *J. Org. Chem.* **2006**, *71*, 3896-3903; n) G. T. de Jong, F. M. Bickelhaupt, *J. Chem. Theory. Comput.* **2006**, *2*, 322-335; o) S. Kozuch, S. Shaik, *J. Am. Chem. Soc.* **2006**, *128*, 3355-3365; p) M. Ahlquist, P. O. Norrby, *Organometallics* **2007**, *26*, 550-553; q) C. H. Hu, M. T. Lee, H. M. Lee, *Organometallics* **2007**, *26*, 1317-1324; r) T. B. Marder, K. C. Lam, Z. Y. Lin, *Organometallics* **2007**, *26*, 758-760; s) I. Ambrogio, G. Fabrizi, S. Cacchi, S. T. Henriksen, P. Fristrup, D. Tanner, P. O. Norrby, *Organometallics* **2008**, *27*, 3187-3195; t) M. B. Hall, P. Surawatanawong, Y. Fan, *J. Organomet. Chem.* **2008**, *693*, 1552-1563; u) S. T. Henriksen, P. O. Norrby, P. Kaukoranta, P. G. Andersson, *J. Am. Chem. Soc.* **2008**, *130*, 10414-10421; v) P. O. Norrby, S. T. Henriksen, D. Tanner, S. Cacchi, *Organometallics* **2009**, *28*, 6201-6205; w) P. O. Norrby, C. Backtorp, *J. Mol. Catal. A-Chem.* **2010**, *328*, 108-113; x) L. Xue, Z. Lin, *Chem. Soc. Rev.* **2010**, *39*, 1692-1705.
- [102] a) I. W. Davies, J. Wu, J. F. Marcoux, M. Taylor, D. Hughes, P. J. Reider, R. J. Deeth, *Tetrahedron* **2001**, *57*, 5061-5066; b) A. A. C. Braga, N. H. Morgon, G. Ujaque, F. Maseras, *J. Am. Chem. Soc.* **2005**, *127*, 9298-9307; c) Y. C. Chang, J. C. Lee, F. E. Hong, *Organometallics* **2005**, *24*, 5686-5695; d) L. J. Goossen, D. Koley, H. L. Hermann, W. Thiel, *J. Am. Chem. Soc.* **2005**, *127*, 11102-11114; e) A. A. C. Braga, G. Ujaque, F. Maseras, *Organometallics* **2006**, *25*, 3647-3658; f) F. Maseras, A. A. C. Braga, G. Ujaque, *Organometallics* **2006**, *25*, 3647-3658; g) F. E. Hong, Y. L. Huang, C. M. Weng, *Chem.-Eur. J.* **2008**, *14*, 4426-4434.
- [103] M. Larhed, C. M. Andersson, A. Hallberg, *Tetrahedron* **1994**, *50*, 285-304.
- [104] J. E. Backvall, A. Gogoll, *Tetrahedron Lett.* **1988**, *29*, 2243-2246.
- [105] F. Weinhold, C. Landis, *Valancy and Bonding. A Natural Bond Orbital Donor-Acceptor Perspective*, Cambridge University Press, Cambridge, **2005**.
- [106] A. Ishikawa, Y. Nakao, H. Sato, S. Sakaki, *Dalton Trans.* **2010**, *39*, 3279-3289.
- [107] a) G. Ujaque, A. A. C. Braga, N. H. Morgon, A. Lledos, F. Maseras, *J. Organomet. Chem.* **2006**, *691*, 4459-4466; b) C. L. McMullin, J. Jover, J. N. Harvey, N. Fey, *Dalton Trans.* **2010**, *39*, 10833-10836; c) B. P. Carrow, J. F. Hartwig, *J. Am. Chem. Soc.* **2011**, *133*, 2116-2119; d) N. N. Nair, *J. Phys. Chem. B* **2011**, *115*, 2312-2321.
- [108] a) J. S. Temple, M. Riediker, J. Schwartz, *J. Am. Chem. Soc.* **1982**, *104*, 1310-1315; b) T. B. Marder, H. Zhang, X. C. Luo, K. Wongkhan, H. Duan, Q. Li, L. Z. Zhu, J. Wang, A. S. Batsanov, J. A. K. Howard, A. W. Lei, *Chem.-Eur. J.* **2009**, *15*, 3823-3829; c) M. Perez-Rodriguez, A. A. C. Braga, M. Garcia-Melchor, M. H. Perez-Temprano, J. A. Casares, G. Ujaque, A. R. de Lera, R. Alvarez, F. Maseras, P. Espinet, *J. Am. Chem. Soc.* **2009**, *131*, 3650-3657.

- [109] B. Milani, A. Anzilutti, L. Vicentini, A. S. O. Santi, E. Zangrando, S. Geremia, G. Mestroni, *Organometallics* **1997**, *16*, 5064-5075.
- [110] a) N. E. Carpenter, D. J. Kucera, L. E. Overman, *J. Org. Chem.* **1989**, *54*, 5846-5848; b) A. Demeijere, F. E. Meyer, *Angew Chem Int Edit* **1994**, *33*, 2379-2411; c) W. J. Drury, N. Zimmermann, M. Keenan, M. Hayashi, S. Kaiser, R. Goddard, A. Pfaltz, *Angew. Chem. Int. Ed.* **2004**, *43*, 70-74; d) X. L. Hou, W. Q. Wu, Q. Peng, D. X. Dong, Y. D. Wu, *J. Am. Chem. Soc.* **2008**, *130*, 9717-9725; e) O. Loiseleur, P. Meier, A. Pfaltz, *Angew. Chem. Int. Ed. Engl.* **1996**, *35*, 200-202; f) Y. Mata, M. Dieguez, O. Pamies, C. Claver, *Org. Lett.* **2005**, *7*, 5597-5599; g) Y. Sato, M. Sodeoka, M. Shibasaki, *J. Org. Chem.* **1989**, *54*, 4738-4739.
- [111] For some recent examples, see: a) M. Lautens, A. Rudolph, *Angew. Chem. Int. Ed.* **2009**, *48*, 2656-2670; b) E. Nakamura, N. Yoshikai, H. Matsuda, *J. Am. Chem. Soc.* **2009**, *131*, 9590-9599; c) M. Nakamura, T. Hatakeyama, S. Hashimoto, K. Ishizuka, *J. Am. Chem. Soc.* **2009**, *131*, 11949-11963; d) G. A. Molander, O. A. Argintaru, I. Aron, S. D. Dreher, *Org. Lett.* **2010**, *12*, 5783-5785; e) G. A. Molander, F. Beaumard, *Org. Lett.* **2010**, *12*, 4022-4025; f) M. Nakamura, K. Ishizuka, H. Seike, T. Hatakeyama, *J. Am. Chem. Soc.* **2010**, *132*, 13117-13119; g) L. Ackermann, R. Sandmann, W. F. Song, *Org. Lett.* **2011**, *13*, 1784-1786; h) M. R. Biscoe, A. Joshi-Pangu, M. Ganesh, *Org. Lett.* **2011**, *13*, 1218-1221; i) M. S. Sigman, R. Jana, T. P. Pathak, *Chem. Rev.* **2011**, *111*, 1417-1492; j) Z. X. Wang, L. G. Xie, *Angew. Chem. Int. Ed.* **2011**, *50*, 4901-4904.
- [112] For some recent examples, see: a) I. Koyama, T. Kurahashi, S. Matsubara, *J. Am. Chem. Soc.* **2009**, *131*, 1350-1351; b) F. Lopez, L. Saya, G. Bhargava, M. A. Navarro, M. Gulias, I. Fernandez, L. Castedo, J. L. Mascarenas, *Angew. Chem. Int. Ed.* **2010**, *49*, 9886-9890; c) T. Miura, M. Morimoto, M. Murakami, *J. Am. Chem. Soc.* **2010**, *132*, 15836-15838; d) S. Ogoshi, A. Nishimura, M. Ohashi, *Org. Lett.* **2010**, *12*, 3450-3452; e) Z. Z. Qiu, S. R. Wang, Z. W. Xie, *Angew. Chem. Int. Ed.* **2010**, *49*, 4649-4652; f) P. Kumar, D. M. Troast, R. Cella, J. Louie, *J. Am. Chem. Soc.* **2011**, *133*, 7719-7721.
- [113] For some recent examples, see: a) K. Namitharan, K. Pitchumani, *Eur. J. Org. Chem.* **2010**, 411-415; b) K. Ogata, Y. Atsuumi, S. Fukuzawa, *Org. Lett.* **2010**, *12*, 4536-4539; c) K. Ogata, J. Sugawara, Y. Atsuumi, S. Fukuzawa, *Org. Lett.* **2010**, *12*, 148-151; d) C. M. Yang, M. Jeganmohan, K. Parthasarathy, C. H. Cheng, *Org. Lett.* **2010**, *12*, 3610-3613.
- [114] a) N. K. Garg, B. M. Rosen, K. W. Quasdorf, D. A. Wilson, N. Zhang, A. M. Resmerita, V. Percec, *Chem. Rev.* **2011**, *111*, 1346-1416; b) Z. J. Shi, B. J. Li, D. G. Yu, C. L. Sun, *Chem.-Eur. J.* **2011**, *17*, 1728-1759.
- [115] a) A. C. Frisch, M. Beller, *Angew. Chem. Int. Ed.* **2005**, *44*, 674-688; b) G. C. Fu, N. A. Strotman, S. Sommer, *Angew. Chem. Int. Ed.* **2007**, *46*, 3556-3558; c) A. E. Jensen, P. Knochel, *J. Org. Chem.* **2002**, *67*, 79-85; d) J. Terao, A. Ikumi, H. Kuniyasu, N. Kambe, *J. Am. Chem. Soc.* **2003**, *125*, 5646-5647; e) J. Terao, H. Watanabe, A. Ikumi, H. Kuniyasu, N. Kambe, *J. Am. Chem. Soc.* **2002**, *124*, 4222-4223; f) J. Zhou, G. C. Fu, *J. Am. Chem. Soc.* **2004**, *126*, 1340-1341.
- [116] a) G. C. Fu, B. Saito, *J. Am. Chem. Soc.* **2008**, *130*, 6694-6695; b) G. C. Fu, S. W. Smith, *J. Am. Chem. Soc.* **2008**, *130*, 12645-12647; c) F. Glorius, *Angew. Chem. Int. Ed.* **2008**, *47*, 8347-8349; d) G. C. Fu, S. Lou, *J. Am. Chem. Soc.* **2010**, *132*, 5010-5011; e) G. C. Fu, N. A. Owston, *J. Am. Chem. Soc.* **2010**, *132*, 11908-11909; f) Z. Lu, A. Wilsily, G. C. Fu, *J. Am. Chem. Soc.* **2011**, *133*, 8154-8157.
- [117] B. L. Lin, L. Liu, Y. Fu, S. W. Luo, Q. Chen, Q. X. Guo, *Organometallics* **2004**, *23*, 2114-2123.
- [118] a) B. H. Bhanage, F. Y. Zhao, M. Shirai, M. Arai, *Catal. Lett.* **1998**, *54*, 195-198; b) C. H. Cheng, P. S. Lin, M. Jeganmohan, *Chem. -Asian J.* **2007**, *2*, 1409-1416; c) K. Inamoto, J. Kuroda, T. Danjo, T. Sakamoto, *Synlett* **2005**, 1624-1626; d) K. Inamoto, J. Kuroda, K. Hiroya, Y. Noda, M. Watanabe, T. Sakamoto, *Organometallics* **2006**, *25*, 3095-3098; e) S. Y. Ma, H. J. Wang, K. M. Gao, F. Y. Zhao, *J. Mol. Catal. A-Chem.* **2006**, *248*, 17-20; f) W. Pei, L. Sun, C.

- Shen, *J. Chem. Res. -S* **2006**, 388-389; g) Z. X. Wang, Z. Y. Chai, *Eur. J. Inorg. Chem.* **2007**, 4492-4499.
- [119] T. F. Jamison, R. Matsubara, *J. Am. Chem. Soc.* **2010**, *132*, 6880-6881.
- [120] a) A. Bengtson, M. Larhed, A. Hallberg, *J. Org. Chem.* **2002**, *67*, 5854-5856; b) A. L. Hansen, T. Skrydstrup, *J. Org. Chem.* **2005**, *70*, 5997-6003; c) T. Tu, X. L. Hou, L. X. Dai, *Org. Lett.* **2003**, *5*, 3651-3653; d) K. S. A. Vallin, Q. S. Zhang, M. Larhed, D. P. Curran, A. Hallberg, *J. Org. Chem.* **2003**, *68*, 6639-6645.
- [121] R. Matsubara, A. C. Gutierrez, T. F. Jamison, *J. Am. Chem. Soc.* **2011**, In press, DOI:10.1021/ja209235d.
- [122] a) M. Larhed, R. K. Arvela, S. Pasquini, *J. Org. Chem.* **2007**, *72*, 6390-6396; b) J. Mo, L. J. Xu, J. L. Xiao, *J. Am. Chem. Soc.* **2005**, *127*, 751-760; c) C. Sonesson, M. Larhed, C. Nyqvist, A. Hallberg, *J. Org. Chem.* **1996**, *61*, 4756-4763; d) K. S. A. Vallin, M. Larhed, K. Johansson, A. Hallberg, *J. Org. Chem.* **2000**, *65*, 4537-4542; e) J. L. Xiao, J. W. Ruan, J. A. Iggo, N. G. Berry, *J. Am. Chem. Soc.* **2010**, *132*, 16689-16699.
- [123] G. A. Lawrance, *Chem. Rev.* **1986**, *86*, 17-33.
- [124] a) K. Matos, J. A. Soderquist, *J. Org. Chem.* **1998**, *63*, 461-470; b) B. H. Ridgway, K. A. Woerpel, *J. Org. Chem.* **1998**, *63*, 458-460.
- [125] C. Amatore, A. Jutand in *Structural and mechanistic aspects of palladium-catalyzed cross-coupling*, Wiley-Interscience, New York, **2002**, pp. 943-972.
- [126] a) A. S. Guram, R. A. Rennels, S. L. Buchwald, *Angew. Chem. Int. Ed. Engl.* **1995**, *34*, 1348-1350; b) J. Louie, J. F. Hartwig, *Tetrahedron Lett.* **1995**, *36*, 3609-3612.
- [127] a) J. Hartwig, *Modern Amination Methods*, (Ed. A. Ricci) Wiley-VCH, Weinheim, **2000**; b) J. Hartwig, *Handbook of Organopalladium Chemistry for Organic Synthesis*, (Ed. E.-I. Negishi) Wiley-Interscience, New York, **2002**; c) J. Hartwig, *Modern Arene Chemistry*, (Ed. C. Astruc) Wiley-VCH, Weinheim, **2002**.
- [128] For some recent examples, see: M. A. Fernandez-Rodriguez, Q. L. Shen, J. F. Hartwig, *J. Am. Chem. Soc.* **2006**, *128*, 2180-2181.
- [129] For some recent examples, see: a) U. Schopfer, A. Schlapbach, *Tetrahedron* **2001**, *57*, 3069-3073; b) S. Cacchi, G. Fabrizi, A. Goggiamani, L. M. Parisi, *Org. Lett.* **2002**, *4*, 4719-4721.
- [130] For some recent examples, see: a) N. S. Gray, S. Ding, X. Wu, Q. Ding, P. G. Schultz, *J. Am. Chem. Soc.* **2002**, *124*, 1594-1596; b) X. P. Zhang, G. Y. Gao, A. J. Colvin, Y. Chen, *Org. Lett.* **2003**, *5*, 3261-3264; c) S. L. Buchwald, A. V. Vorogushin, X. H. Huang, *J. Am. Chem. Soc.* **2005**, *127*, 8146-8149.
- [131] H. Y. Chen, S. Schlecht, T. C. Semple, J. F. Hartwig, *Science* **2000**, *287*, 1995-1997.
- [132] a) M. S. Kharasch, E. K. Fields, *J. Am. Chem. Soc.* **1941**, *63*, 2316-2320; b) M. S. Kharasch, M. Kleiman, *J. Am. Chem. Soc.* **1943**, *65*, 491-493; c) M. S. Kharasch, P. O. Tawney, *J. Am. Chem. Soc.* **1941**, *63*, 2308-2315.
- [133] a) G. A. Molander, B. J. Rahn, D. C. Shubert, S. E. Bonde, *Tetrahedron Lett.* **1983**, *24*, 5449-5452; b) S. M. Neumann, J. K. Kochi, *J. Org. Chem.* **1975**, *40*, 599-606; c) R. S. Smith, J. K. Kochi, *J. Org. Chem.* **1976**, *41*, 502-509; d) M. Tamura, J. Kochi, *J. Organomet. Chem.* **1971**, *31*, 289-309; e) M. Tamura, J. K. Kochi, *J. Am. Chem. Soc.* **1971**, *93*, 1487-1489; f) M. Tamura, J. K. Kochi, *Bull. Chem. Soc. Jpn.* **1971**, *44*, 3063-3073.
- [134] G. Cahiez, H. Avedissian, *Synthesis* **1998**, 1199-1205.
- [135] J. Quintin, X. Franck, R. Hocquemiller, B. Figadere, *Tetrahedron Lett.* **2002**, *43*, 3547-3549.
- [136] a) J. W. Han, T. Hayashi, *Tetrahedron As.* **2002**, *13*, 325-331; b) N. Ostergaard, B. T. Pedersen, N. Skjaerbaek, P. Vedso, M. Begtrup, *Synlett* **2002**, 1889-1891.
- [137] A. Furstner, A. Leitner, *Angew. Chem. Int. Ed.* **2002**, *41*, 609-612.
- [138] A. Furstner, A. Leitner, M. Mendez, H. Krause, *J. Am. Chem. Soc.* **2002**, *124*, 13856-13863.
- [139] B. Scheiper, M. Bonnekessel, H. Krause, A. Furstner, *J. Org. Chem.* **2004**, *69*, 3943-3949.

- [140] a) R. B. Bedford, D. W. Bruce, R. M. Frost, J. W. Goodby, M. Hird, *Chem. Commun.* **2004**, 2822-2823; b) R. B. Bedford, D. W. Bruce, R. M. Frost, M. Hird, *Chem. Commun.* **2005**, 4161-4163; c) T. Nagano, T. Hayashi, *Org. Lett.* **2004**, *6*, 1297-1299.
- [141] K. G. Dongol, H. Koh, M. Sau, C. L. L. Chai, *Adv. Synth. Catal.* **2007**, *349*, 1015-1018.
- [142] M. Nakamura, K. Matsuo, S. Ito, E. Nakamura, *J. Am. Chem. Soc.* **2004**, *126*, 3686-3687.
- [143] H. Nagashima, D. Noda, Y. Sunada, T. Hatakeyama, M. Nakamura, *J. Am. Chem. Soc.* **2009**, *131*, 6078-6079.
- [144] a) R. B. Bedford, M. Betham, D. W. Bruce, A. A. Danopoulos, R. M. Frost, M. Hird, *J. Org. Chem.* **2006**, *71*, 1104-1110; b) R. R. Chowdhury, A. K. Crane, C. Fowler, P. Kwong, C. M. Kozak, *Chem. Commun.* **2008**, 94-96.
- [145] R. B. Bedford, M. Betham, D. W. Bruce, S. A. Davis, R. M. Frost, M. Hird, *Chem. Commun.* **2006**, 1398-1400.
- [146] K. Jonas, L. Schieferstein, C. Krueger, Y.-H. Tsay, *Angew. Chem.* **1979**, *91*, 590-591.
- [147] R. Martin, A. Fuerstner, *Angew. Chem. Int. Ed.* **2004**, *43*, 3955-3957.
- [148] A. Fuerstner, R. Martin, H. Krause, G. Seidel, R. Goddard, C. W. Lehmann, *J. Am. Chem. Soc.* **2008**, *130*, 8773-8787.
- [149] X. Xu, D. Cheng, W. Pei, *J. Org. Chem.* **2006**, *71*, 6637-6639.
- [150] C. C. Kofink, B. Blank, S. Pagano, N. Gotz, P. Knochel, *Chem. Commun.* **2007**, 1954-1956.
- [151] T. Hatakeyama, M. Nakamura, *J. Am. Chem. Soc.* **2007**, *129*, 9844-9845.
- [152] a) W. M. Czaplik, M. Mayer, A. Jacobi von Wangelin, *Angew. Chem. Int. Ed.* **2009**, *48*, 607-610; b) W. M. Czaplik, M. Mayer, S. Grupe, A. Jacobi von Wangelin, *Pure Appl. Chem.* **2010**, *82*, 1545-1553; c) A. Jacobi von Wangelin, M. Mayer, W. M. Czaplik, *Adv. Synth. Catal.* **2010**, *352*, 2147-2152.
- [153] A. Furstner, *Angew. Chem. Int. Ed.* **2009**, *48*, 1364-1367.
- [154] M. Nakamura, S. Ito, K. Matsuo, E. Nakamura, *Synlett* **2005**, 1794-1798.
- [155] R. B. Bedford, M. Huwe, M. C. Wilkinson, *Chem. Commun.* **2009**, 600-602.
- [156] M. Nakamura, S. Ito, Y. Fujiwara, E. Nakamura, *Org. Lett.* **2009**, *11*, 4306-4309.
- [157] a) A. Fuerstner, R. Martin, *Chem. Lett.* **2005**, *34*, 624-629; b) L. K. Ottesen, F. Ek, R. Olsson, *Org. Lett.* **2006**, *8*, 1771-1773; c) M. Seck, X. Franck, R. Hocquemiller, B. Figadere, J.-F. Peyrat, O. Provot, J.-D. Brion, M. Alami, *Tetrahedron* **2004**, *45*, 1881-1884; d) G. Seidel, D. Laurich, A. Fuerstner, *J. Org. Chem.* **2004**, *69*, 3950-3952.
- [158] B. Bogdanovic, M. Schwickardi, *Angew. Chem. Int. Ed.* **2000**, *39*, 4610-4612.
- [159] K. Weber, E.-M. Schnöckelborg, R. Wolf, *ChemCatChem* **2011**, *3*, 1572-1577.
- [160] a) P. J. Alonso, A. B. Arauzo, J. Fornies, M. A. Garcia-Monforte, A. Martin, J. I. Martinez, B. Menjon, C. Rillo, J. J. Saiz-Garitaonandia, *Angew. Chem., Int. Ed.* **2006**, *45*, 6707-6711; b) G. Cahiez, V. Habiak, C. Duplais, A. Moyeux, *Angew. Chem., Int. Ed.* **2007**, *46*, 4364-4366.
- [161] A. Guerinot, S. Reymond, J. Cossy, *Angew. Chem., Int. Ed.* **2007**, *46*, 6521-6524.
- [162] a) X. Creary, M. E. Mehrsheikhmohammadi, S. McDonald, *J. Org. Chem.* **1987**, *52*, 3254-3263; b) C. Hansch, A. Leo, R. W. Taft, *Chem. Rev.* **1991**, *91*, 165-195.
- [163] a) C. Amatore, A. Jutand, *Acc. Chem. Res.* **2000**, *33*, 314-321; b) M. Ahlquist, P. Fristrup, D. Tanner, P. O. Norrby, *Organometallics* **2006**, *25*, 2066-2073.
- [164] a) R. Alvarez, O. N. Faza, C. S. Lopez, A. R. de Lera, *Org. Lett.* **2006**, *8*, 35-38; b) A. Ariafard, Z. Y. Lin, I. J. S. Fairlamb, *Organometallics* **2006**, *25*, 5788-5794; c) A. Nova, G. Ujaque, F. Maseras, A. Lledos, P. Espinet, *J. Am. Chem. Soc.* **2006**, *128*, 14571-14578.

"I've got an idea - an idea so smart that my head would explode if I even began to know what I'm talking about"

Peter Griffin

